THE ROLE OF GLUTATHIONE SYNTHETASE IN TRYPANOTHIONE BIOSYNTHESIS IN *TRYPANOSOMA BRUCEI*

APPROVED BY SUPERVISORY COMMITTEE

Margaret A. Phillips, Ph. D.

Kim Orth, Ph. D.

Joel Goodman, Ph. D.

Larry Ruben, Ph. D.

DEDICATION

I would like to dedicate this work to my family and friends who have supported me through this endeavor. The love and encouragement they provided me proved invaluable through the years.

THE ROLE OF GLUTATHIONE SYNTHETASE IN TRYPANOTHIONE BIOSYNTHESIS IN *TRYPANOSOMA BRUCEI*

by

CHELSEA BRIANNE PRATT

DISSERTATION

Presented to the Faculty of the Graduate School of Biomedical Sciences

The University of Texas Southwestern Medical Center at Dallas

In Partial Fulfillment of the Requirements

For the Degree of

DOCTOR OF PHILOSOPHY

The University of Texas Southwestern Medical Center at Dallas

Dallas, TX

August 2013

THE ROLE OF GLUTATHIONE SYNTHETASE IN TRYPANOTHIONE BIOSYNTHESIS IN *TRYPANOSOMA BRUCEI*

Chelsea Brianne Pratt, Ph.D.

The University of Texas Southwestern Medical Center at Dallas, 2013

Supervising Professor: Margaret A. Phillips, PhD

Abstract

Trypanosoma brucei is the causative agent of Human African trypanosomiasis, commonly called sleeping sickness, which is a debilitating disease for which treatment is not currently ideal. Trypanosome parasites differ

from their human host by utilizing a novel cofactor termed trypanothione instead of glutathione for protection against reactive oxygen species. Trypanothione is formed by the conjugation of two molecules of glutathione to spermidine forming a link between the polyamine and thiol biosynthetic pathways. My work has investigated the enzyme annotated as glutathione synthetase (GS) in *T. brucei* to determine if it indeed catalyzes the synthesis of glutathione and if so, to define its kinetic parameters, decipher whether it has any role in the regulation of these pathways, and assess if it is essential for growth.

To determine whether the putative *Tb*GS gene was correctly identified through sequence homology, I cloned and expressed the *T. brucei* gene (*Tb*GS) in *Escherichia coli*, and purified the recombinant protein. Using an ATP-coupled spectrophotometric assay, I was able to measure *Tb*GS kinetic activity and determine that it was comparable to activities of other published GS homologs, indicating that this gene was correctly annotated.

To investigate the physiological role of *Tb*GS in *T. brucei*, I used genetic approaches to manipulate *Tb*GS levels, first by RNAi, and then by employing conditional knockout models. RNAi was used to decrease protein levels; however, even though *Tb*GS protein levels were depleted by more than eighty percent, there was no altered growth phenotype, and parasites did not have increased sensitivity to known inhibitors of the pathway. I then constructed a *Tb*GS conditional double knockout (cDKO) parasite cell line that contained a

tetracycline (tet) regulated episomal copy of *Tb*GS. By removing tet from the media and stopping *Tb*GS protein production, parasites entered growth arrest by day five, which correlated with depleted thiol pools. Parasites remained in growth arrest until day eight after which they resumed growth. This resumption of growth also correlated with the return of low levels of *Tb*GS and thiol pools indicating that loss of trypanothione caused growth arrest.

To evaluate if the loss of *Tb*GS had any regulatory effect, levels of biosynthetic pathway proteins were assessed by western blot analysis. A three-fold increase was seen in γ-GCS levels as well as a decrease in AdoMetDC prozyme and ODC levels. Thus our studies have shown that not only is *Tb*GS essential for parasite growth but have also uncovered cross regulation between the polyamine and thiol pathways.

TABLE OF CONTENTS

PRIOR PUBLICATIONS

Callaway, T. R., Carroll, J. A., Arthington, J. D., **Pratt, C.,** Edrington, T. S., Anderson, R. C., Galyean, M. L., Ricke, S. C., Crandall, P., and Nisbet, D. J. (2008) *Foodborne Pathog Dis* **5**, 621-627

LIST OF FIGURES

LIST OF TABLES

LIST OF ABBREVIATIONS

AdoMetDC	*S*-adenosyl methionine decarboxylase
AMP	ampicillin
BSO	buthionine sulfoximine
cDNA	complementary DNA
cDKO	conditional double knockout
CSA	camphorsulphonic acid
DKO	double knockout
DNA	deoxyribonucleic acid
DTPA	diethylene triaminepentaacetic acid
FBS	fetal bovine serum
FSC	forward scatter
γ-GC	γ-glutamyl cysteine
γ-GCS	γ-glutamyl cysteine synthetase
GGT	γ-glutamyl transferase
GR	glutathione reductase
Grx	glutaredoxin
GS	glutathione synthetase
GSH	glutathione
GspS	glutathionyl spermidine synthetase
GSSG	glutathione disulfide
HAT	Human African Trypanosomiasis
HEPPS	hydroxyethyl-1-piperazinyl propanesulfonic acid
HPLC	high pressure liquid chromatography
KAN	kanamycin
kDNA	kinetoplastid DNA
KO	knockout
mRNA	messenger RNA
MSA	methanesulphonic acid
NECT	nifurtimox-eflornithine combination therapy
OD	optical density
ODC	ornithine decarboxylase
PATTEC	Pan-African Tsetste and Trypanosomiasis Eradication Campaign
PBSG	PBS with glucose

PCR	polymerase chain reaction
PEP	phospho(enol)pyruvate
Prx	peroxiredoxin
Px	peroxidase
RBP	RNA binding protein
RISC	RNA induced silencing complex
RNA	ribonucleic acid
RNR	ribonucleotide reductase
ROS	reactive oxygen species
SKO	single knockout
Spd Syn	spermidine synthetase
SSC	side scatter
SSC buffer	saline sodium citrate buffer
*Tb*GS	*T. brucei* glutathione synthetase
TCA	trichloroacetic acid
TEA	triethylamine
Tet	tetracyclin
TR	trypanothione reductase
Trx	thioredoxin
TrxR	thioredoxin reductase
TryS	trypanothione synthetase
TSH	trypanothione
TXN	tryparedoxin
UPR	unfolded protein response
UTR	untranslated region
VSG	variant surface glycoprotein
WHO	World health Organization

CHATER ONE

INTRODUCTION

A. Trypanosomiasis

OVERVIEW

Human African trypanosomiasis (HAT) is the disease caused by infection with a subspecies of the parasite *Trypanosoma brucei*. This disease is a vector-borne illness currently endemic in 36 African countries [1]. The risk of infection is limited to the sub-Saharan region of Africa because transmission is dependent on the Tsetse fly (*Glossina* genus), which resides exclusively in rural sub-Saharan Africa [1]. Although control efforts have reduced the number of cases reported in recent years (under ten thousand in 2010 and 2011), HAT often goes unreported so the actual number of infected individuals is estimated to exceed reported cases by three- to ten-fold [2, 3]. The World Health Organization (WHO) estimates that there are approximately 30,000 people currently infected, while millions in the

region remain at risk of contracting the disease [1]. The disease occurs in two stages, the early or haemolymphatic phase and the late or neurological phase. Treatment of infected individuals in the latter stage of the disease is complex and requires medical facilities that are often unavailable or prohibitively expensive in regions most affected by the disease; however, without treatment, trypanosomiasis is fatal. Furthermore, the parasite is capable of infecting certain domesticated animals, resulting in animal trypanosomiasis. This capability provides host parasitic reservoirs in close proximity to human communities, impairing necessary agricultural development critically needed in these under-developed regions.

PARASITE

The parasite responsible for causing HAT is a member of the order *Kinetoplastida* and the family *Trypanosomatidia*. Trypanosomatids are unicellular, eukaryotic organisms that can only survive through a parasitic relationship with a diverse range of hosts. Humans can become infected by subspecies of *T. brucei*, *T. cruzi* (the causative agent of Chagas disease or South American

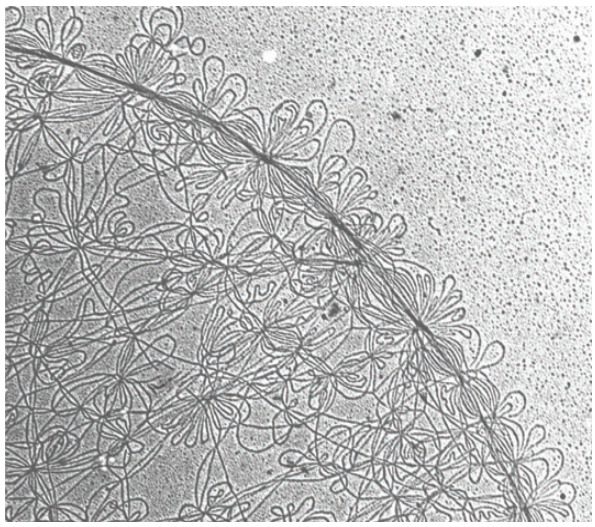

Figure 1. Electron Micrograph of Kinetoplast DNA. Taken from Jensen, 2012 [9] with permissions (Confirmation # 11044044)

sleeping sickness), and several species of *Leishmania* (responsible for the disease Leishmaniasis). However, trypanosomatids contain over fifty different species, some of which have the ability to infect livestock (cattle, horses, sheep, and pigs), fish, plants, amphibians, and insects [4, 5].

Trypanosomatids are considered one of the earliest branches in the eukaryotic lineages and, therefore, contain several unique features not found outside the Kinetoplastida class [6]. Notably, kinetoplasts contain a sophisticated network of DNA (called kDNA) located within the mitochondrion at the base of the flagella. The kDNA network contains DNA arranged as several thousand minicircles and a few dozen maxicircles, systematically linked and looped to form a very dense DNA-containing granule (Figure 1). Because of this complex DNA arrangement, replication of the kinetoplast is a time and energy-consuming task [7-9]. Loss of the kinetoplast results in lethality unless the parasite acquires a specific genomic mutation [10]. Speculation suggests kinetoplast replication is the target of ethidium bromide in the treatment of trypanosomiasis-infected cattle, but this has not been definitively proved [11].

In addition to the complex process of kinetoplast replication, gene transcription in kinetoplasts is also unique. Many mitochondrial genes require extensive messenger RNA (mRNA) editing, via the insertion or deletion of a specific number of uridylate residues [9]. The majority of the genes are located within the maxicircles, but are nonfunctional without proper editing. Minicircles

provide the guide RNAs that are necessary templates for uridylate insertion/deletion. Editing of mRNA is extensive, and in some transcripts, can account for half of the protein coding region [9]. Although the mechanism by which this process occurs has been extensively studied, the reason for developing such a precise transcription scheme remains to be elucidated.

Trypanosomatids do not regulate polymerase II transcription, which is a significant difference from most eukaryotic cells. Messenger RNAs are transcribed in a polycistronic fashion that are trans-spliced and capped with a 5'-splice leader sequence and post-transcriptionally regulated by the 3'-UTR [12-18]. Significant progress has been made in elucidating the mechanism by which certain 3'-UTRs regulate translation through RNA binding proteins (RBP) and mRNA degradation. Future studies are needed to elucidate how trypanosomatids have evolved to respond to environmental changes without altering their gene expression via transcriptional regulation [19].

Trypanosomatids do regulate polymerase I transcriptional although it is responsible for a subset of genes. The more well studied pol I regulation in trypanosomatids is the alteration of the variant surface glycoprotein (VSG). Trypanosomatids have an exterior surface that is coated with a single VSG protein. As the population expands, the parasites randomly alter the VSG gene copies being transcribed. As the host immune system responds to the parasitic infection and mounts an attack, parasites expressing a novel or different VSG

protein avoid detection, continue to replicate, and prolong the infection. Estimates of the number of different VSG genes expressed by trypanosomatids range from hundreds to thousands, as some pseudogenes have not been properly investigated; however, only one form of the VSG gene is expressed at a time [20-23]. The frequency a parasite within the population will change the form of VSG gene expressed is 1:100 [24]. Changing of the VSG coat has hampered attempts at vaccine development for trypanosomiasis, and the mechanism by which only one VSG gene is expressed, while other VSG genes remain silent, is not yet completely understood [25].

Since different species of trypanosomatids infect a variety of different organisms, their life cycles reflect the different environments the parasite encounters. *T. brucei*, the parasite on which this dissertation is based, has four different stages within its life cycle: procyclic, metacyclic (tsetse fly forms), long-slender bloodstream, and stumpy blood stream (mammalian forms) (Figure 2). When an infected tsetse fly bites a mammalian host, the metacyclic form of the parasite is injected into the bloodstream of the mammalian host. The metacyclic form transforms into the highly proliferative, long and slender blood stage form of the parasite, which replicates in the blood and lymph system of the host. Once the parasite population reaches a sufficient concentration in the blood stream, the parasite enters the quiescent stage of the blood stream form termed "stumpy", reflecting their change in morphology. This transformation is triggered by accumulation of the stumpy induction factor (SIF), a parasite-derived factor that currently has evaded identification [26, 27].

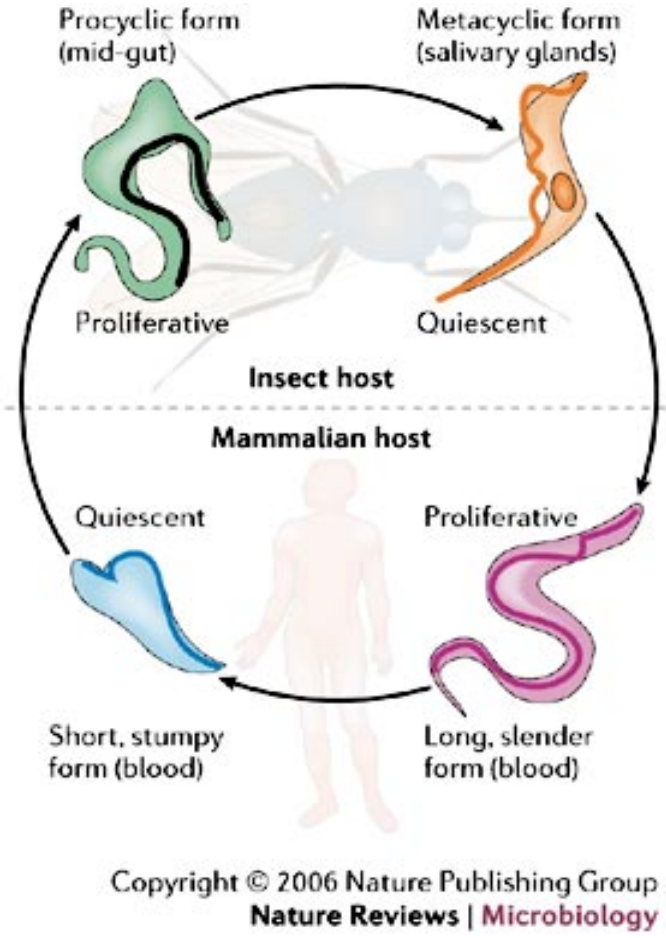

Figure 2. *T. brucei* Life Cycle. Taken from Pays, 2006 [34] with permissions (License #3024411025052)

To complete the life cycle, the stumpy form of the parasite is ingested by an uninfected tsetse fly during a blood meal and converted to the proliferative procyclic form; this form is responsible for replication in gut of the tsetse fly. As the parasite replicates, it traverses a complicated path through the insect in order to reach the salivary glands and be injected once again into a mammalian host [28]. Upon reaching the salivary glands, the parasite re-enters the metacyclic form, a quiescent stage, and waits for the next blood meal to restart the cycle. This complex life cycle is accompanied by changes in gene expression, protein levels, replication rates, and morphology of the parasite. Although a few of the proteins involved have been identified (i.e. TbMAPK, PAD1, etc.), the precise mechanisms of how the parasite regulates these changes in the absence of global transcriptional regulation remain unclear [23, 29-32].

As previously mentioned, there are several species of the *Trypanosoma* genus responsible for infecting different organisms; however, only the subspecies *T. brucei gambiense* (*T. b. gambiense*) and *T. brucei rhodesiense* (*T. b. rhodesiense*) cause HAT. *T. b. gambiense* is located primarily in western and central Africa and is responsible for over 95 percent of HAT infections. *T. b. rhodesiense* infections are observed in eastern and southern Africa, accounting for less than 5 percent of HAT [1]. The differences between these infections stem from their rates of progression (chronic *T. b. gambiense* versus acute *T. b. rhodesiense*), treatment options, and geographical localization. Although both

subspecies are capable of infecting livestock, *T. b. rhodesiense* is a zoonosis that uses nonhuman mammals as reservoirs between human infections, while *T. b. gambiense* is likely not [33]. This observation reveals an additional complication in eradicating trypanosomiasis, as success requires the screening of livestock.

DISEASE

HAT is transmitted through the bite of the tsetse fly, although the disease transmission can also occur from mother to child by crossing the placenta during pregnancy. Infections can also occur in research laboratory settings through contaminated needles or sharps. While this type of transmission is possible, the majority of laboratories uses the cattle variant *T. brucei brucei* strain, which lacks the serum-resistance associated (SRA) gene required to infect human hosts and reduces the risk of serious infection [34, 35]. The SRA gene is a truncated form of a VSG gene; however it is found in the endocytic pathway, differentiating it from other VSG genes. SRA works to alleviate the lysis that occurs to the parasite in human serum by associating with the trypanolytic factor (TLF) found in high-density lipoproteins (HDL) [35]. Lysis of the parasite is mediated through the TLF, which contains both the haptoglobin-related protein (Hpr) and the apolipoprotein (apoL1). Upon binding to the trypanosome hemoglobin receptor, the TLF is endocytosed and targeted to the lysosome. Upon entering the acidic compartment, the apoL1 protein undergoes a conformational change, inserts into

the lysosome membrane, and forms a pore resulting in the influx of chloride ions and water into the lysosome. This influx causes swelling of the lysosome and results in rupture of the cell. SRA is thought to inhibit this lysis by interaction with apoL1 and hindering pore formation [35].

Upon initial infection, trypanosomes replicate in the blood and lymph of the infected individual producing symptoms such as fever, headaches, joint pain, and itching [1]. This first stage of infection is referred to as the haemolymphatic phase. If the individual does not seek treatment within the first stage of the disease, it will eventually progress to the second stage (or neurological phase) of disease. The second stage of the disease begins once the parasite has crossed from the blood/lymph into the central nervous system. This results in more pronounced symptoms, including confusion, poor coordination, and insomnia occurring during the night while sleeping throughout the day [1]. Once the disease has progressed to the second stage, treatment options become more difficult.

Treatment of HAT during the first stage can be accomplished with either pentamidine or suramin. Pentamidine, used for *T. b. gambiense* infection, is generally well tolerated but can cause hypotensive reactions and damage to the liver, kidneys, and the pancreas [1, 33].

Figure 3. Exfoliative Dermatitis resulting from treatment with suramin (Fevre, 2008 [33]).

Suramin is used for early stage *T. b. rhodesiense* infection and produces severe reactions in less than five percent of patients. These reactions include fever, kidney damage, nausea, shock, delayed hypersensitivity reactions (e.g., exfoliative dermatitis, [Figure 3]), diarrhea, and jaundice [33]. Despite these side effects, treatment of HAT in the early stage is still preferential to treatment in the late stage.

Treatment of late-stage HAT is also dependent on the subspecies causing the infection. Late-stage *T. b. gambiense* treatment can be accomplished with the recently approved nifurtimox-eflornithine combination therapy (NECT). This therapy reduces the number of infusions of eflornithine required and shortens the administration treatment time from fourteen to seven days [36]. The side effects of NECT therapy include (in order of most common to least): fever, headache, weakness, cough, skin rash, injection site rash, chest pain, dehydration, urinary incontinence, urinary frequency/urgency, muscle pain, shortness of breath, respiratory distress, and nosebleed [36]. Treatment of late-stage *T. b. rhodesiense* requires the administration of melarsoprol, an arsenic-derived compound that has many undesirable effects with the most pronounced being fatal reactive encephalopathy in 3-10% of patients [1, 33]. Despite having such negative effects, melarsoprol is the last line of defense against *T. b. rhodesiense*, where death is certain without treatment.

The negative side effects and the difficulty in administration of these drugs underscore the need for developing new treatment options. Although the approval of NECT therapy is a marked improvement for the treatment of late stage *T. b. gambiense*, there is still a need for better treatment for *T. b. rhodesiense.* Furthermore, administration of NECT through intravaneous infusions is not ideal for a disease predominantly located in rural areas.

The burden of trypanosome infection is not only limited to the treatment of patients, but also causes economic strife in the treatment of livestock. Called *Nagana,* a Zulu term meaning "to be depressed", animal trypanosomiasis is a serious obstacle to the agricultural development and economic stability of the region [1]. It was estimated animal trypanosomiasis hindered livestock populations to 20% their potential [37]. Estimating the true cost/benefit of trypanosomiasis control is complicated. One study estimated that animal trypanosomiasis eradication would increase agricultural output by $700 million per year and encouraged further investigation because treatment of animal trypanosomiasis at the time was costing livestock owners over $1 billion annually [38]. Currently, eradication of the insect vector is being attempted in several countries through the Pan-African Tsetste and Trypanosomiasis Eradication Campaign (PATTEC) [39, 40].

The current state of HAT varies from country to country, though the number of reported cases has drastically declined in recent years. This is most

likely due to the WHO public-private partnership with Aventis Pharma and Bayer HealthCare providing drugs for treatment, an increase in mobile screening units, and efforts to eradicate the tsetse fly [1, 41]. There have been fewer than 10,000 cases reported for two consecutive years and, though this number is considered underreported, is a milestone that has not occurred since the 1960s [1].

The ideal solution for HAT would be to prevent disease onset with effective vaccine administration, rather than new therapeutics. While numerous research groups have attempted to develop a vaccine for HAT (summarized in [42]), none have produced an effective and persistent anti-trypanosome immune response that also gave promising results in a field setting. Both the lack of success in vaccine development and the inability of the immune system to clear the parasitic infection can be attributed to the parasite's ability to randomly express a different VSG protein coat. Effective vaccinations would be the gold standard in HAT prevention, but the parasite's ability to undergo antigenic variations suggests development of a vaccine is unlikely to be feasible. Therefore, efforts to develop new therapeutics as well as to eradicate the insect vector required for disease transmission must continue.

B. Host Redox System

OVERVIEW

In aerobic organisms, oxygen is used as the electron acceptor in a cascade of oxidative reactions that provide energy for the organism or cell. These processes produce reactive oxygen species (ROS) as byproducts. ROS are oxygen-generated free radicals, such as superoxide anions (O_2•−), hydroxyl radicals (HO•), peroxyl (RO_2•) species, alkoxyl (RO•) species, and O_2-derived non-radical species such as hydrogen peroxide (H_2O_2) [43]. These radicals can be produced during normal cell metabolism or through the addition of xenobiotics. Low physiological levels of ROS are not harmful, and play a role in in cell signaling and modulation of cellular function; however, high levels of ROS result in irreversible oxidative modifications to DNA, protein, and lipids, triggering apoptosis and are thought to be the cause of aging [44]. Cells protect against ROS-mediated damage by maintaining high concentrations of thiol-containing molecules and proteins, creating a redox network allowing the cell to buffer endogenously-produced ROS species and protect against xenobiotics/heavy metals. The mammalian redox system is composed of the molecule glutathione and proteins glutaredoxin (Grx), thioredoxin (Trx), and their corresponding reductases, catalase and peroxidase, each of which is reviewed in the following sections.

GLUTATHIONE/GLUTATHIONE REDUCTASE

Glutathione is the tripeptide γ-glutamyl-cysteine-glycine formed from the L-amino acids glutamate, cysteine, and glycine. Oxidation of glutathione (GSH) produces glutathione disulfide (GSSG). Glutathione is the most abundant thiol present in eukaryotic cells with greater than 90% of it in the reduced form [45]. Two separate enzymes synthesize glutathione: γ-glutamyl-cysteine synthetase (γ-GCS) (also known as glutamate cysteine ligase) and glutathione synthetase (GS) [46]. Biosynthesis provides the majority of glutathione, but mammalian cells can also transport glutathione into the cell via γ-glutamyltranspeptidase (GGT) to replenish levels of cysteine and, by proxy, glutathione. Upon import into the cell, GGT hydrolyzes the peptide bond, transferring the γ-glutamyl moiety to an amino acid, resulting in the formation of cysteinyl-glycine and an γ-glutamyl-amino acid. The most efficient amino acid substrate to receive the γ-glutamyl transfer is cysteine, forming γ-glutamylcysteine (γ-GC), and thus requiring only the addition of glycine by GS to reform glutathione [46].

Glutathione is responsible for detoxifying electrophiles, scavenging free radicals, maintaining the essential thiol status of proteins, providing a reservoir for cysteine, and modulating cellular functions [46]. Since glutathione plays many important roles in the cell, glutathione pools are compartmentalized in different organelles, allowing for the specific and targeted control of redox reactions [47]. Glutathione contained within the cytosol is highly reduced, maintaining a ratio of 100 to 1 GSH to GSSG [48]. The mitochondrial

glutathione pools are cell-type specific and are responsible for maintaining the integrity of proteins by protecting them from internally-generated ROS [44]. Low levels of glutathione are also found in the endoplasmic reticulum; however, they are maintained at a lower ratio (5 to 1 GSH to GSSG) than elsewhere in the cell [49, 50]. Glutathione within the endoplasmic reticulum helps facilitate proper protein folding while buffering against ROS as changes in the redox state trigger the unfolded protein response (UPR) and apoptosis [51]. Nuclear glutathione pools provide protection against DNA and protein damage induced by oxidative stress [52].

In order for glutathione to function properly in protecting the cell against oxidative stress, high levels must be maintained in the reduced state. Glutathione reductase (GR) is responsible for converting GSSG into two molecules of GSH. GR is a ubiquitously expressed flavoprotein disulfide oxidoreductase and is conserved from prokaryotes to eukaryotes [53].

GLUTAREDOXIN

Glutaredoxin (Grx) is a class of small, ubiquitous, thiol proteins that function within the redox cycle. There are three Grx genes in mammalian cells: Grx1, Grx2 and Grx5 [54]. Grx 1 and 2 are both dithiol (2-Cys-Grx) proteins and are localized in the cytosol and mitochondria, respectively. Grx5 is homologous to the yeast monothiol (1-Cys-Grx) Grx5, and is localized to the mitochondria

[55, 56]. The regeneration of reduced Grx is dependent on glutathione rather than a specific oxidoreductase enzyme and occurs nonenzymatically.

The active site of mammalian dithiol proteins is similar in Trx and Grx and contains a Cys–X–X–Cys motif [57]. The mechanism of reduction occurs by the N-terminal cysteine acting as a nucleophile and attacking a disulfide bond [58]. This forms a covalent disulfide intermediate between Trx/Grx and the substrate. The second cysteine residue acts to reduce this disulfide bond resulting in a disulfide bond in the active site of Trx/Grx and a dithiol in the substrate [54].

The mechanism of monothiol proteins is unique to Grx and is responsible for the reduction of protein-glutathione disulfides. The active site cysteine causes a nucleophillic attack on the disulfide bond resulting in a Grx-glutathione disulfide [59]. A second molecule of glutathione reduces this disulfide resulting in GSSG, reduced Grx, and removal of glutathione from the protein substrate [60].

Grx proteins have multiple functions within the cell with the most characterized being an electron donor for ribonucleotide reductase (RNR), the enzyme responsible for producing deoxynucleotides for DNA synthesis in cell division [61, 62]. Grx is involved in cellular differentiation, apoptosis, disulfide-dithiol exchanges, and protein de-glutathionylation [54]. Furthermore, Grx is considered a redox indicator within the cell, activating numerous transcription

factors upon sensing oxidative stress through the removal of inhibitory glutathione-protein modifications [63].

THIOREDOXIN/THIOREDOXIN REDUCTASE

Thioredoxin (Trx) is a small, dithiol protein ubiquitously expressed and conserved across all kingdoms of life. Trx, like Grx, is involved in the redox cycle and has several cellular functions. Grx and Trx have overlapping roles in many cases, but not all of their functions are redundant. While both Grx and Trx donate electrons to RNR and reduce inter-protein disulfides, only Trx can catalyze the reduction of intramolecular protein disulfide bonds and regenerate peroxiredoxins [64]. Furthermore, Trx must be reduced by thioredoxin reductase (TrxR) and cannot be regenerated by glutathione alone. TrxR, like GR is a flavoprotein disulfide oxidoreductase that uses NADPH and the cofactor FAD.

Mammals contain two Trx genes, Trx1 and Trx2, which are compartmentalized to the cytosol/nucleus or mitochondria, respectively [65, 66]. Similar to Grx, Trx1 serves as an oxidative indicator and upon oxidative stress it is transported to the nucleus.

PEROXIDASES/CATALASE

Peroxidases can be classified as glutathione peroxidases (Px) or peroxiredoxins (Prx). Both are responsible for the catalysis of hydroperoxides to

their corresponding alcohols; however, they differ in their active sites and mechanisms of regeneration.

Glutathione peroxidases (Px) contain a selenocysteine in their active site and use glutathione to regenerate after catalyzing the degradation of peroxides. There are six mammalian genes that encode glutathione peroxidases, although only Px1 (cytosolic localization) appears to play a role in maintaining oxidative balance. While the other Px genes are capable of reducing peroxides, they have additional roles in the cell, linking oxidative balance to inflammatory response and transcriptional regulation [67].

Prx is a non-seleno-thiol specific peroxidase that is responsible for the removal of organic peroxides and hydrogen peroxide. There are six mammalian Prx genes that are categorized as typical 2-Cys-Prx, atypical 2-Cys-Prx, or 1-Cys-Prx. Each has a specific subcellular localization, either in the cytoplasm, mitochondria, peroxisome, or extracellular space [44]. The Prx active site contains a peroxidatic cysteine that upon reaction with peroxide is oxidized to sulfenic acid [68, 69]. Prx is dependent upon the Trx/TrxR system to regenerate the active site, differentiating it from the glutathione peroxidases. Catalase is localized in the peroxisome, and is responsible for the catalysis of hydrogen peroxide to water and oxygen. It has one of the highest kinetic turnover rates, converting over a million molecules per second [70]. Although it does not have a

major role in the cell redox system, catalase serves to reduce levels of endogenously produced hydrogen peroxide.

C. Trypanosome Redox System

OVERVIEW

Two of the most prevalent molecules in any organism are polyamines, long chain cationic molecules, and thiols, sulfur-containing compounds or peptides. Both classes of compounds are involved in a variety of cellular functions and have proven to be essential across all kingdoms of life. Kinetoplastids have evolved to conjugate spermidine with glutathione to generate the novel a novel, conjugated cofactor, termed trypanothione [71]. This novel discovery has evoked research interest and opened windows of opportunity for discovering exploitable drug targets within the redox network.

TRYPANOSOME REDOX NETWORK

The trypanosome redox network is centered on the trypanothione cofactor and its protection against ROS generated either internally (by cofactors/drug metabolism) or externally (by the host's innate immune system) [72].

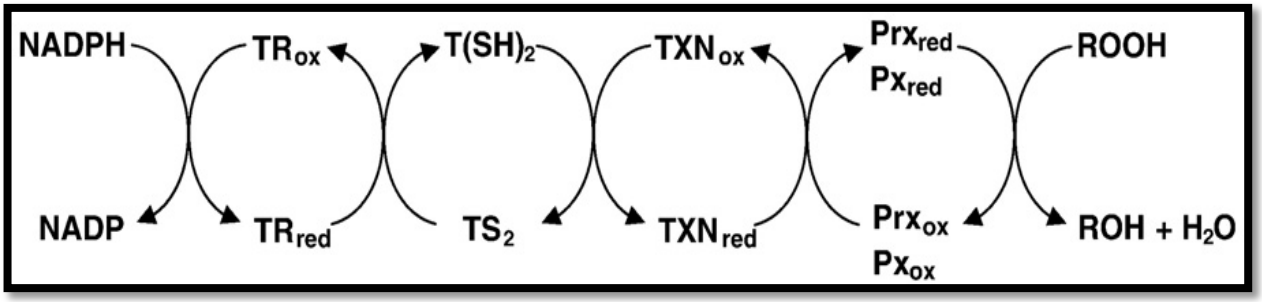

Figure 4. Trypanosome Thiol System. Taken from Krauth-Siegel, 2008 [80] with permissions License # 3024401442658) NADPH/NADP - nicotinamide adenine dinucleotide phosphate, TR - trypanothione reductase, $T(SH)_2/TS_2$ – trypanothione, TXN – tryparedoxin, Prx – peroxiredoxin, Px – peroxidase, ROOH – peroxides, ROH – Alcohol, H_2O - water

Trypanothione reductase (TR) is responsible for maintaining levels of reduced trypanothione and is upregulated in *T. brucei* upon the loss of trypanothione synthetase (TryS) and trypanothione [73, 74]. Tryparedoxin (TXN), an analog of the mammalian Trx, is a low molecular weight, dithiol protein responsible for donating electrons to RNR and peroxidases (Prx, Px), and aiding in the detoxification of hydroxides [75-77]. Because trypanosomes lack a conventional TrxR [20, 78, 79], it is believed that TXN is dependent solely on trypanothione for the maintenance of reduced TXN. Figure 4 shows a simplified schematic of the trypanosome redox network and its known components, each of which will be further discussed below [80].

TRYPANOTHIONE

Since trypanothione's discovery by Alan Fairlamb in 1985, it has been the subject of ongoing investigations into its biosynthesis, regulation, and metabolism [71]. The interest in trypanothione can be attributed to the uniqueness of the cofactor, the knowledge of the druggability of its biosynthetic pathway, and the desire to identify potential drug targets for the treatment of this fatal disease [81-89].

Trypanothione is a novel and almost exclusively trypanosomatid cofactor formed by the conjugation of two glutathione molecules to one molecule of spermidine. Thus, trypanothione provides a link between the polyamine and thiol biosynthetic pathways. Polyamines are required in eukaryotic and prokaryotic

organisms for growth and proliferation. While there are several forms of polyamines, the most common are putrescine, spermidine, and spermine. Trypanosomes utilize putrescine and spermidine, but lack the genetic components to synthesize spermine. Mammalian cells regulate the levels of polyamines by transcriptional, translational and protein turnover. While there is evidence of regulation of polyamine levels in trypanosomes, the mechanism has remained elusive.

Both the thiol and polyamine biosynthetic pathways are linked through trypanothione (Figure 5)). The first step in trypanothione biosynthesis in the thiol portion of the pathway is catalyzed by γ-GCS, an enzyme that has been kinetically characterized and shown to be essential in *T. brucei* [90-92]. The resulting product (γ-GC) is then conjugated to glycine by *Tb*GS (the subject of this dissertation) to form glutathione. Formation of *N*1-glutathionylspermidine occurs, as the name implies, through the conjugation of glutathione to the terminal amine group of spermidine [93]. A second glutathione molecule is then added to the opposing amine of *N*1-glutathionylspermidine, completing the formation of trypanothione [93]. Two separate enzymes in *Crithidia fasciculata* (glutathionylspermindine synthetase (GspS)) and TryS were initially suspected of catalyzing each of the final two steps of trypanothione synthesis individually [94]. Subsequent analysis, however, determined that TryS enzymes from *C. fasciculata, Leishmania major, L. donovoni, T. brucei,* and *T. cruzi* are capable of

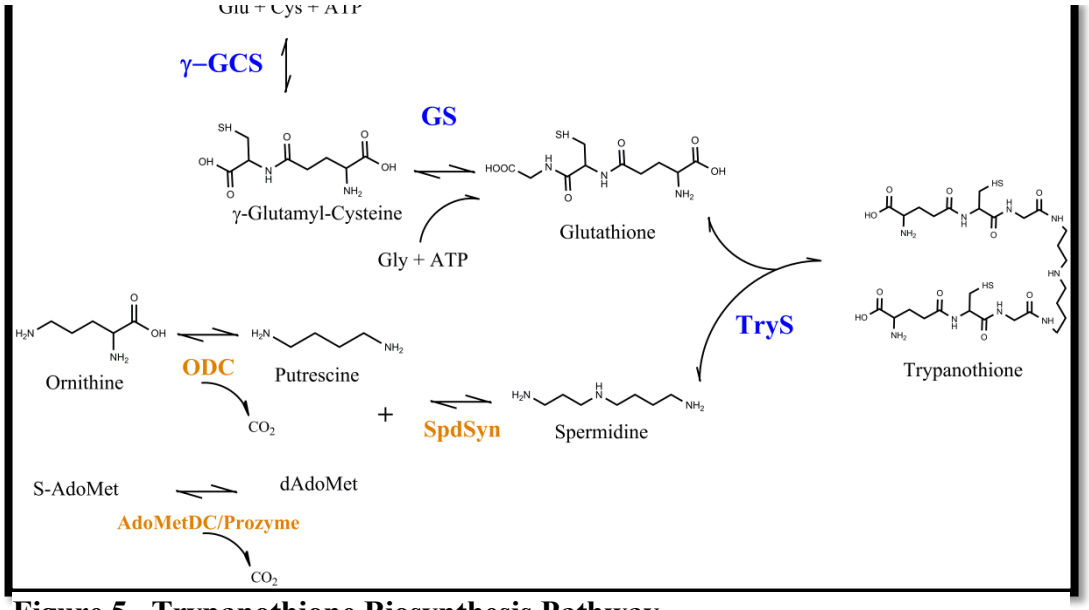

Figure 5. Trypanothione Biosynthesis Pathway

catalyzing both steps, synthesizing trypanothione from the substrates glutathione and spermidine, and thus bypassing the requirement for GspS [93, 95-98]. In *T. brucei*, GspS is absent and only the TryS gene is found in the genome.

The *C. fasciculata* and *T. cruzi* genomes both possess a functional GspS gene; and the corresponding *C. fasciculata* protein has been kinetically characterized as well as investigated for possible drug design [78, 99-101]. However, studying the role of GspS in these species has decreased in priority with the discovery of the ability of TryS to synthesize trypanothione from glutathione and spermidine. *L. major* also contains a GspS pseudogene, but it contains two separate frame shift mutations that cause two premature stop codons, resulting in a non-functional or absent protein *in vivo* [98].

Both GspS and TryS enzymes contain a second domain exhibiting amidase activity with its active site separate from the synthetic domain. The amidase domain is capable of hydrolyzing trypanothione and glutathionylspermindine back to glutathione and spermidine in the absence of

ATP, although it is less efficient than its synthetic counterpart [93, 96]. The amidase domain was shown to be inessential for viability, but parasites lacking the domain had reduced growth and infectivity, suggesting that while not required, it does play a role in the overall health of the parasite [87].

Of the biosynthetic enzymes producing trypanothione, only *Tb*GS has not been characterized by genetic methods to determine if it is essential and the enzymatic activity was uncharacterized when I began my studies. γ-GCS and TryS, along with the enzymes responsible for the synthesis of spermidine, (i.e. ornithine decarboxylase (ODC), *S*-adenosylmethionine decarboxylase (AdoMetDC), AdoMetDC prozyme, and spermidine synthase (SpdSyn)) are essential in *T. brucei*, as shown by RNAi methods and knockout strategies [74, 92, 102-104]. These genetic studies, coupled with studies using inhibitors, validate the need for further investigation into the regulation of this pathway [86, 89, 105-108].

TRYPANOTHIONE REDUCTASE

TR is an essential enzyme in trypanosomatids. In attempting to generate TR null strains of *L.donovoni* and *L. major*, partial trisomy occurred retaining the TR gene [109]. Furthermore, overexpression of a dominant mutant TR in *L. donovoni* resulted in a reduced ability to survive in activated macrophages [110]. In a controlled gene knockout line of *T. brucei*, reduced TR levels resulted in

growth arrest and increased sensitivity to exogenously added hydrogen peroxide [111]

Similar to glutathione relying on GR to maintain levels of reduced glutathione, trypanothione relies on TR to maintain high levels of reduced trypanothione. TR and GR are both flavoprotein disulfide oxidoreductases utilizing NADPH, but the activity of each is substrate-specific [73, 112, 113]. Secondary structure and domain organization is conserved between the two enzymes but the glutathione or trypanothione binding sites differ in their size and charge. The TR trypanothione binding site is larger and negatively charged, while the GR glutathione binding site lacks charge [114-119]. The negative charge facilitates binding of the positively charged spermidine backbone of trypanothione. GR can be engineered to have activity against trypanothione by mutating key amino acids that expand and impart negative charge to the active site. [120].

Due to the differences in the GR and TR substrate binding sites, TR has become a well studied potential drug target [115, 119, 121-124]. However, to date there has not been a successful drug candidate developed based on inhibiting TR activity [124]. To have an effect on growth of the parasite, TR activity must be reduced by greater than 95%, and no compounds have achieved that level of inhibition *in vivo* with adequate bioavailability [111]. However, since TR meets several of the requirements of a good drug target (i.e. assay feasibility,

genetic/chemical validation, druggability, potential for resistance, potential for toxicity, and protein structure information), it continues to be investigated for drug design [108].

TRYPAREDOXIN

Trypanosomes utilize the low molecular weight dithiol protein tryparedoxin (TXN), which has functional similarities to both Grx and Trx [80]. TXNs were initially discovered in *C. fasciculata*, but were then identified and characterized in *T. brucei, T. cruzi,* and *L. infantum* [76, 125-128]. TXN proteins are oxidoreductases that function similarly to both Grx and Trx in the host cell. For example, TXN is considered to be the primary electron donor in trypanosomes for RNR, due to the preferential affinity of RNR to TXN over Trx and trypanothione [75, 129]. Furthermore, the oxidized disulfide form of trypanothione is an inhibitor of RNR, a potential mechanism by which parasites might slow cell growth in instances of oxidative stress [75]. Although sequence homology is low between TXN and Trx, the active sites retain similarity and the overall core structure of the protein is similar [130, 131]. Additionally, TXN and Trx both serve as electron donors to regenerate peroxidases in trypanosomes [76, 77]. However, trypanosomatids do not encode a TrxR, and instead rely on trypanothione to regenerate TXN. This mechanism is similar to Grx and its

reduction by glutathione [76, 128]. Furthermore, both Grx and TXN are capable of reducing glutathione-protein mixed disulfides [132].

TXN is an abundant protein in both *C. fasciculata* and *T. brucei*, accounting for 5% of total soluble protein and reaching intracellular protein concentrations greater than 100 μM, respectively [76, 133, 134]. It was originally hypothesized that two separate TXN proteins were localized independently in the mitochondria or cytoplasm [135-139]. The cytoplasmic TXN genes are essential in *T. brucei* and *L. infantum*; however, reduction of the mitochondrial TXN gene by RNAi did not result in a growth phenotype [133, 138, 140, 141]. This led to debate in the field as to whether the mitochondrial TXN protein is only externally-associated with the mitochondria and not involved in redox maintenance within the organelle. Thus, further investigation is warranted to elucidate the functional differences between these two proteins in maintaining trypanosome redox state.

Although trypanosomes do not encode a TrxR or GR, *T. brucei, L. major,* and *T. cruzi* do encode Trx and Grx genes [20, 78, 79]. *T. brucei* Trx protein behaves similarly to previously reported Trx proteins except for its basic pI (8.5), rather than the typical acidic pI of most Trxs, and it lacks a conserved aspartate residue [129]. TrxR from other species can reduce *T. brucei* Trx, and the addition of Trx enhanced the activity of RNR and provided electrons for peroxidases. However, the latter two activities were less efficient than that of TXN, and the

reduction of Trx by trypanothione was 1000-fold less efficient than reduction of TXN by trypanothione [129]. Another study demonstrated that ectopic expression of *T. brucei* Trx remained undetectable, even when overexpressed in trypanosomes. Furthermore, both alleles of the Trx gene were capable of being removed without having a deleterious effect [142, 143]. These results indicate that the *T. brucei* Trx gene is not a major player in the trypanosome redox system.

Grxs are another form of small, redox protective proteins that are categorized into two different groups based on their active site—monothiol (1-Cys-Grx) and dithiol (2-Cys-Grx). Trypanosomatids encode two 2-Cys-Grx and three 1-Cys-Grx genes. The dithiol 2-Cys-Grx proteins are localized in different compartments, with Grx1 found in the cytosol and Grx2 found in the mitochondria [144]. Both proteins are constitutively expressed, capable of catalyzing the reduction of glutathione disulfide by trypanothione, and preferentially use trypanothione over glutathione to regenerate the reduced form of the active site. However, Grx1 is capable of increasing the activity of RNR, while Grx2 is not.

The three 1-Cys-Grx proteins are expressed in *T. brucei,* with 1-C-Grx1 occurring in the mitochondria, while 1-C-Grx2 and 1-C-Grx3 are predicted to be found in the mitochondria and cytoplasm, respectively [145, 146]. To date, only 1-C-Grx1 has been adequately characterized. The recombinant 1-C-Grx1 protein was purified as a homodimer and found to form an intramolecular disulfide upon

oxidation [146]. 1-C-Grx1 is essential for growth and proliferation of the parasites but could not be rescued by overexpression of 1-C-Grx2, which is predicted to also be localized in the mytochondria, indicating different functions for these two proteins [145]. Similar to the dithiol Grx proteins, 1-C-Grx proteins prefer trypanothione to glutathione; highlighting the role of trypanothione in maintaining trypanosome redox homeostasis [145, 146].

PEROXIDASE

Two classes of peroxidase enzymes, glutathione-peroxidase (Px) and 2-Cys-peroxiredoxin (Prx), have been identified in *C. fasciculata, T. brucei,* and *T. cruzi* [76, 77, 127, 135, 147, 148]. Trypanosomatids lack catalase enzymes, thus Px/Prx are responsible for metabolism of hydrogen peroxide produced either exogenously or endogenously.

In trypanosomes, Prx enzymes are multicopy, abundantly expressed, and localized in both the cytoplasm and mitochondria. The cytosolic Prx enzyme is critical for protection from hydrogen peroxide in the bloodstream form of trypanosomes, while mitochondrial Prx is not [140]. However, overexpression of either the mitochondrial or the cytosolic protein conferred higher resistance to hydrogen peroxide in *T. cruzi* and increased infectivity [149]. Therefore, it is unknown whether the different Prx enzymes have complimentary functions.

Trypanosomes encode three similar Px genes that are localized to either the cytosol or the mitochondria. Each was deemed essential using RNAi, demonstrating the non-redundant function of Px enzymes [140, 150]. Trypanosomatid Px enzymes differ from the host Px enzymes by having a cysteine residue in the active site, instead of the selenocysteine that is typically found. Trypanosomatid Px enzymes also exhibit low activity when using glutathione, and prefer the TXN/trypanothione system for regeneration of reduced enzymes [77].

DIFFERENCES BETWEEN HOST AND PARASITE

The major distinction between the mammalian and trypanosome redox

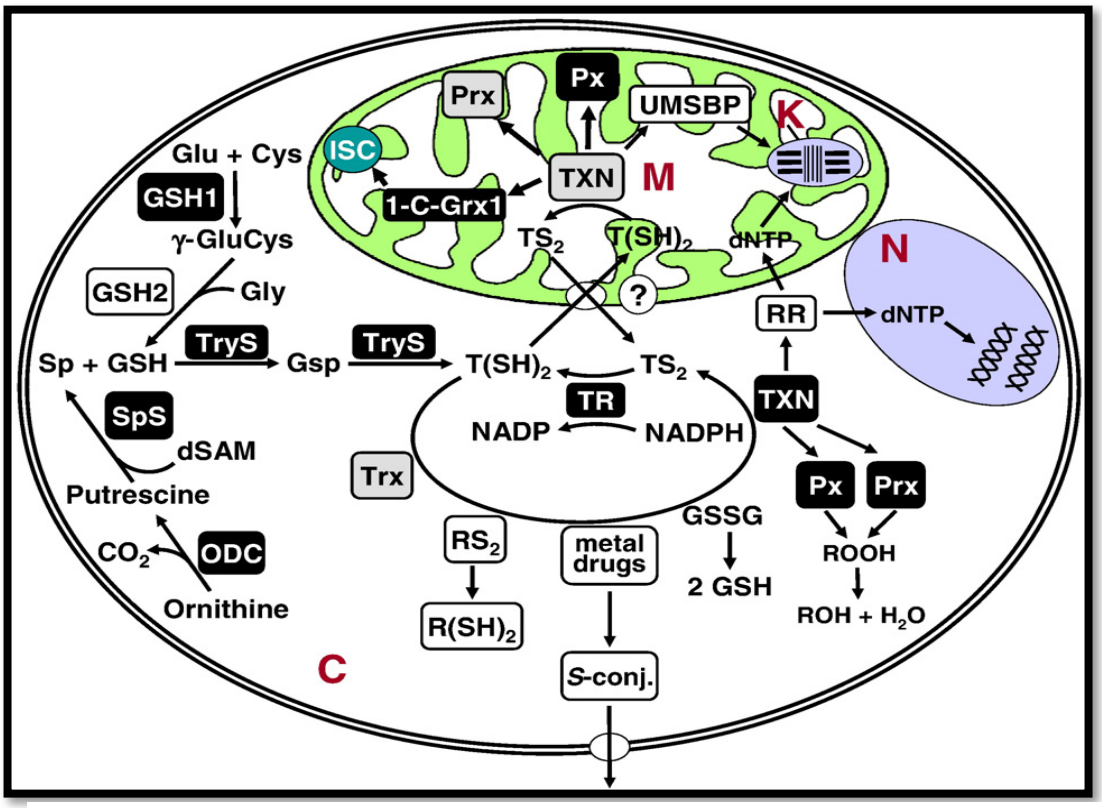

Figure 6. Trypanosome Redox Network. Taken from Krauth-Siegel, 2008 [80] with permission (License # 3024410128523)

systems are the reliance of the trypanosome parasite on trypanothione, rather than glutathione, in maintaining redox homeostasis. Mechanisms performed by individual proteins have not diverged significantly and homologs are present for each of the mammalian redox enzymes, with the exception of catalase. A recent study was performed to target the trypanosome redox system, rather than just an individual enzyme. Out of 80,000 compounds, 12 were found to inhibit the trypanothione redox system. The majority of these compounds were found to inhibit the TXN protein at levels under 1 μM, while needing over 83-fold higher levels to kill mammalian cells [151]. These findings further underscore the need to better understand differences between these redox cycles and how they are regulated.

D. Dissertation Scope

T. brucei is the causative agent of HAT and improved therapeutics are needed to treat the disease. The trypanosome redox system differs from that of the host and is an essential and targetable pathway. While regulation of this pathway has been observed, the mechanism by which trypanosomes regulate their redox system is unknown. *Tb*GS is a gene with only a putative functional identity that has yet to be characterized.

In this work, I focused on characterizing the *Tb*GS gene and elucidating its role in the trypanothione redox system. Initially, it appeared that the *Tb*GS gene was not essential and the enzyme had low kinetic activity in comparison to other

characterized homologs. However, I was able to optimize the expression of *Tb*GS, recapitulating activity similar to other homologs. I went on to generate a cell line with regulated expression of TbGS, and verify that *Tb*GS is an essential gene. This cell line also allowed a more in depth analysis of the mechanism of escape by flow cytometry. Furthermore, I also demonstrated that loss of GS and low levels of trypanothione induce changes of the protein levels of γ-GCS as well as ODC and prozyme. This indicates the parasites ability to detect its thiol levels and respond by modulating protein levels, although the mechanism for this has not been elucidated.

CHAPTER TWO

T. brucei GS Knockdown by RNA interference

A. Introduction

To investigate the role of the *Tb*GS protein in the trypanothione biosynthesis pathway, RNA interference (RNAi) was used to reduce *Tb*GS protein levels. RNAi is the process in which double-stranded RNA causes the reduction of homologous RNA through its recognition and degradation by the RNA-induced silencing complex (RISC). RNAi is initiated by introduction of a double stranded RNA stem-loop, which is processed into 21-23 nucleotide fragments. These fragments are loaded onto the RISC, which uses these fragments as template to recognize complementary mRNA. Once complementary mRNA is identified, mRNA is cleaved and degraded, resulting in the reduction of both mRNA and its corresponding protein [152].

In order to utilize RNAi, a tetracycline-regulatable *Tb*GS RNAi cell line was generated. Induction of RNAi resulted in reduction of the target *Tb*GS protein; however, this reduction did not cause a growth phenotype and suggested

that either the *Tb*GS protein was not necessary for the growth or RNAi was not sufficient to reduce protein levels so that a phenotype could be observed. Therefore, further research using different methods of perturbing the pathway had to be performed to elucidate the role of *Tb*GS in the *T. brucei* thiol biosynthetic pathway.

B. Materials and Methods

T. brucei cell culture

Bloodstream form *T. brucei* strain 90-13 was cultured in HMI-9 media at 37°C and 5% CO_2 with the appropriate antibiotics (G418 (2.5 μg/ml), hygromycin (5 μg/ml), phleomycin (2.5μg/ml)) [153]. Cells were split every 1-3 days to maintain healthy cultures in log phase (10^3-10^6 cells/ml) and cell densities were calculated with a hemocytometer (Fisher). Growth curves are represented as total cell number, which is a product of cell density and total dilution.

Cloning of TbGS RNAi Stem-loop Construct

The *Tb*GS RNAi stem-loop construct was generated according to previous methods described in [103] and was accomplished by Erin Willert, PhD at UT Southwestern. The pLEW100 and pJM326 vectors were used to generate the *Tb*GS RNAi stem-loop construct [154]. Using the sets of primers containing the appropriate restriction enzyme sites (Table 1), a portion of TbGS gene (nucleotides 1-440) was PCR-amplified from *T. brucei* 427 genomic DNA and subcloned into pLEW-100 in the forward direction (using XbaI and MluI) and

into pJM326 in the reverse direction (using HindIII and NheI). The *Tb*GS gene portion along with the stuffer region was excised from pJM326 using HindIII and XbaI and ligated into pLEW100 containing the first *Tb*GS RNAi section. The construct contained the two fragments of the *Tb*GS gene separated by the stuffer region in opposing directions under the transcriptional control of a tetracycline-regulated promoter (Figure 7). These elements were flanked by a ribosomal DNA sequence, allowing for homologous recombination into the multi-copy ribosomal locus of *T. brucei*. Sequencing confirmed the correct construct was obtained.

Transfection to generate GS RNAi cell line

To generate the *Tb*GS RNAi cell line, the pLEW100-*Tb*GS stem-loop RNAi construct was transfected by methods previously described and was accomplished by Dr. Willert [103]. The pLEW100-*Tb*GS stem-loop RNAi vector was linearized by EcoRV (80 μg) and transfected into log phase *T. brucei* 90-13 bloodstream form cells using the Amaxa Nucleofector and kit. Phleomycin-resistant cells that integrated the construct into rRNA locus were selected and clonal lines were obtained through limited dilution. To induce RNAi knockdown of the *Tb*GS gene, 1 μg/ml of tetracycline was added every 24 h during experiments.

Western Blot Analysis

Parasites (~10^8) were harvested by centrifugation (1000 X *g* for 10 m) and washed with cold (4°C) PBS (137 mM NaCl, 2.7 mM KCl, 10 mM Na_2HPO_4, 2.0

mM KH_2PO_4, pH 7.4) three times. Pellet was resuspended in protein lysis buffer (50 mM HEPES, pH 8.0, 100 mM NaCl, 5 mM β-mercaptoethanol, 2 mM PMSF, 1 μg/ml leupeptin, 2 μg/ml antipain, 10 μg/ml benzamidine, 1 μg/ml pepstatin, and 1 μg/ml chymostatin). Cells were lysed by three freeze/thaw cycles and clarified by high-speed centrifugation using a bench-top centrifuge. Protein concentration was determined by a colorimetric protein assay (BioRad).

Twenty μg of total protein was loaded per sample and separated by a 12% SDS-PAGE gel [155]. Protein was transferred from the gel to a polyvinylidene difloride (PVDF) membrane (Hybond-P, Amersham) using a wet transfer at 4°C for one hour using 100 V. Membranes were blocked in 5% non-fat dry milk in Tris-buffered saline (TBS) (20 mM Tris-HCl, 137 mM NaCl, pH 7.6) overnight at 4°C with gentle agitation prior to antibody incubations. Primary rabbit *Tb*GS polyclonal antibodies were made against His_6-*Tb*GS protein purified as described in Chapter 3 by Proteintech Group, Inc, Chicago, IL. α-*Tb*GS primary antibody incubations were performed in 5% nonfat milk in TBS-T (TBS containing 0.1% v/v Tween-20) at a 1:2500 dilution for 4 h with gentle agitation. The membrane was washed three times for 10 m with TBS-T. α-*Tb*DHODH, the protein loading control, primary antibody incubations were performed under similar conditions but with 1:10,000 dilution and 1 h incubation time. Secondary antibody incubations were done using 1:10,000 dilution in 5% milk in TBS-T for one hour using an anti-rabbit antibody conjugated to horseradish peroxidase

(ThermoFisher). Protein levels were visualized by chemiluminescence detected when incubating the membrane with ECL HRP substrate (ThermoFisher) and exposing to film (Fisher). In each experiment, a single membrane was developed for the *Tb*GS protein levels, stripped (using Restore Plus Western Blot Stripping Buffer (Thermo Fisher)), and re-probed for the DHODH protein levels. The *Tb*GS antibody only identified one protein at the correct size when probed against cell lysate, and this protein band decreased in intensity upon RNAi induction, indicating the antibody recognized the correct protein. The *Tb*GS antibody was also capable of detecting *Tb*GS purified protein at nM concentrations.

Intracellular Thiol Determination

Parasites (1×10^8) were harvested by centrifugation (1000 X *g* for 10 m) and washed with cold (4°C) PBS (137 mM NaCl, 2.7 mM KCl, 10 mM Na_2HPO_4, 2.0 mM KH_2PO_4 pH 7.4) three times. Cells were resuspended in 25 μl thiol lysis buffer (40 mM 3-[4-(2-Hydroxyethyl)-1-piperazinyl] propanesulfonic acid (HEPPS) buffer, 4 mM diethylene triaminepentaacetic acid (DTPA) pH 8.0, and 25 μl monobromobimine (10 mM dissolved in 100% ethanol). Cells were lysed using three freeze/thaw cycles and then heated to 70°C for 3 m. Proteins were precipitated by the addition of 50 μl of 4M, pH 1.6, methanesulphonic acid (MSA) and incubation on ice for 10 m. Proteins were pelleted by centrifugation in a bench-top centrifuge for 5 m at maximum speed and the supernatant was

removed and kept at 4°C until high-performance liquid chromatography (HPLC) analysis. Reagents were purchased from Sigma unless noted otherwise.

An HPLC system (System Gold Nouveau, Beckman Instruments) coupled to a DYNAMAX fluorescence detector (Rainin, model FL-1) was used to analyze derivatized thiol samples. Samples were separated on a Phenomonex Nucleosil C_{18} Column (30 x 4.6 mm) using gradient mixtures of eluent A (0.25% camphorsulphonic acid (CSA), pH 2.64) and eluent B (0.25% CSA and 25% 1-propanol, pH 2.64). The following linear gradient with a constant flow 1 ml/min at room temperature was used: 0% B to 20% B over 60 m followed by 20% B to 75% B over 40 m. The column was equilibrated between samples. Thiols were identified by retention time and quantified by reduced standard's peak area. Standards were purchased through Sigma (glutathione) or Bachem (trypanothione and glutathione-spermidine). Reagents were purchased from Sigma unless noted otherwise.

Buthionine sulfoximine EC_{50} determination

GS RNAi cell lines were grown in the presence of tetracycline (1 μg/ml) for 2 days prior to incubation with the γ-GCS inhibitor – buthionine sulfoximine. Parasites were quantified by a hemocytometer followed by dilution to 1 x 10^3 cells/ml and incubated for three days with varying concentrations of buthionine sulfoximine (0, 30, 60, 90, 120, and 150 μM). To maintain *Tb*GS knockdown, tetracycline was added daily. After 3 days, parasites were counted and plotted.

Data were analyzed using Graphpad Prism nonlinear regression (log (agonist) v. response (four parameter fit)).

C. Results

Knockdown of GS by RNAi does not produce a growth effect.

Upon addition of tetracycline to a final concentration of 1 μg/ml, the *Tb*GS RNAi stem-loop is transcribed and protein levels are reduced by 80 – 90% as determined by western blot (Figure 8 and Table 2). Because trypanothione is known to be essential in *T. brucei*, I expected that depletion of *Tb*GS would result in a growth defect. However, *Tb*GS RNAi cell lines grew at the same rate as wild-type cells and the intracellular thiol levels as measured by HPLC were similar to levels found in control cells (Figure 9).

Since the insertion of the *Tb*GS RNAi stem-loop was targeted to the repeat region of the ribosome locus, different levels of expression of the stem-loop can be found in different clonal lines. To investigate if an increased level of *Tb*GS knockdown could be obtained, different *Tb*GS RNAi clonal lines growth and protein knockdown were examined. All clones accessed were able to reduce *Tb*GS protein levels with the addition of tetracycline; however, none were capable of producing a growth phenotype even with reduction of protein levels by 80-90% (Figure 10, Figure 11, and Table 2).

Lack of a growth phenotype is not due to glutathione uptake from the media

The lab previously showed that addition of glutathione to the media was sufficient to rescue the RNAi knockdown of γ-GCS, suggesting that glutathione might be transported into the cells [92]. To elucidate if the lack of a phenotype in *Tb*GS RNAi cells was due to glutathione contamination, dialyzed serum was used to make HMI-9 media. However, even when grown in media containing dialyzed serum, cells continued to proliferate normally after reduction of *Tb*GS by RNAi. Media components were further analyzed by HPLC and no detectable glutathione was found to be in the media. Therefore, normal growth rates of *Tb*GS RNAi cell lines cannot be attributed to cells salvaging glutathione.

TbGS RNAi cells do not have increased sensitivity to pathway inhibitor

*Tb*GS RNAi cells were stressed using the glutathione synthesis inhibitor buthionine sulfoximine to observe if this might incite a difference between wild-type and RNAi cell lines (Figure 12). *Tb*GS protein levels were reduced prior to incubation with buthionine sulfoximine; however, cells with reduced levels of *Tb*GS protein did not display an increased sensitivity to buthionine sulfoximine (Figure 13). This result indicated that even though the *Tb*GS protein levels were reduced, the parasites thiol pathway was not under stress.

D. Conclusions

Previously, chemical inhibition and genetic manipulation have proven the trypanothione biosynthesis pathway is an essential and targetable pathway [74, 84, 85, 92, 102, 103, 156]. Here, I attempted to advance the understanding of the

T. brucei redox system and its regulation by genetic manipulation of the *Tb*GS gene using RNAi. By investigating this protein, I had hoped to gain insight into both the necessity of the gene and its role in possible regulation of the biosynthetic pathway.

In order to study the role that *Tb*GS plays in trypanothione biosynthesis, I generated a *Tb*GS RNAi cell line; however, it did not produce a phenotype in bloodstream form cells, even though protein levels were reduced by 80-90%. The lack of phenotype observed when using RNAi does not provide conclusive evidence for or against the requirement of *Tb*GS in trypanothione biosynthesis. Further attempts to perturb the pathway using the γ-GCS inhibitor buthionine sulfoximine did not elicit a phenotype in the *Tb*GS RNAi cell line, and thiol levels remained unchanged in comparison to control, indicating that RNAi of *Tb*GS was not having an effect on thiol pools along with parasite viability.

Due to lack of a growth phenotype, two opposing hypotheses were generated on what was occurring in the *Tb*GS RNAi cell line. The first hypothesis was the annotated *Tb*GS gene was not essential in parasites because another unidentified enzyme was capable of glutathione synthesis. This hypothesis was supported by the RNAi data that reduced *Tb*GS protein 80-90%, but did not affect thiol levels or increase sensitivity to pathway inhibitors. The second hypothesis was that 80-90% knockdown was simply insufficient to produce an effect. Therefore, to properly elucidate *Tb*GS function and its role in

T. brucei, a more effective method of eliminating or reducing *Tb*GS protein was needed. Consequently, a *Tb*GS double knockout (DKO) and *Tb*GS conditional double knockout (cDKO) studies were utilized to investigate the role of *Tb*GS in trypanothione biosynthesis.

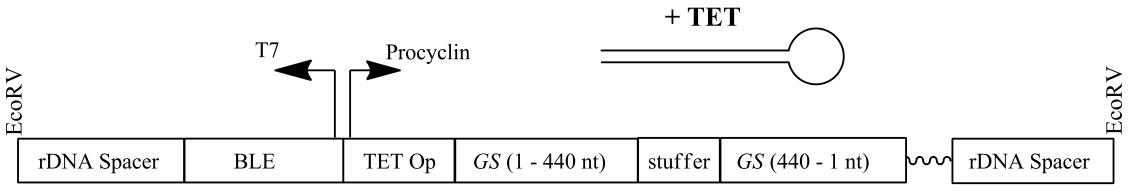

Figure 7. *Tb*GS RNAi Stem-loop Schematic. Construct contains two identical portions of *Tb*GS gene in opposing directions under the control of a Tet-regulated promoter. Addition of tetracycline allows transcription of stem-loop and initiation of RNAi. Construct is targeted for insertion into the ribosomal repeat sequences of the *T. brucei* genome.

Table 1. **Primer List**

Function	To generate	5'-3' Forward	5'-3' Reverse
Protein Expression	pET15b-GS	ATAAAGCTTGAATCACCCCTCTCTCCCGTGATTGTG	ATAAGATCTCCATCCACCCGGGGCATTGCAACTCAC
	pT7-*Tb*GS-flag-MAT	GCGAAGCTTGTGTTAAAATTGTTGCTGGAGCT	GCGGGTACCCGGTACAACCGCTAAGGAAT
	pE-SUMO-*Tb*GS	GGTCTCGAGGTATGGTGTTAAAATTGTTGCTGGA	TCTAGATTACGGTACAACCGCTAAGGAA
T. brucei RNAi	GS RNAi section 1	CCCAAGCTTATGGTGTTAAAATTGTTGCTGGAGC	CTAGCTAGCCCGGCGAAAGAGCAGCTGATGG
	GS RNAi section 2	CGACGCGTATGGTGTTAAAATTGTTGCTGGAGC	CTAGTCTAGACCGGCGAAAGAGCAGCTGATGG
T. brucei Allelic Replacement	GS 5' UTR	ATAGCGGCCGCGTGTTCCCAGTCGAGG	ATAACGCGTCTCGAGCAATCACGGGAGAGAGG
	GS 3' UTR	ATATCTAGAATTTAAATCCTCTCGTGTTGCGGTGGGCCC	ATAAGGCCTGCGGCCGCATGCGACAATAGTTTATAC
Ectopic v. endogenous	N/A	GCTATTATTAGAACAGTTTCTGTACTATATTGT	GCCGCTATGGAATGAGGC
T. brucei Ectopic expression	pLEW300-fGS	CCCAGGCTTATGGACTACAAAGACGATGACG	ATAAGATCTCCATCCACCCGGGGCATTGCAACTCAC
	pLEW100-fGS	CCCAGGCTTATGGACTACAAAGACGATGACG	ATAAGATCTCCATCCACCCGGGGCATTGCAACTCAC
	pLEW100v-GSf	GGAAGCTTATGGTGTTAAAATTGTTGC	GGGGATCCTTAAGCCTTGTCATCGTCGTC
	pLEW300-GSf	GGAAGCTTATGGTGTTAAAATTGTTGC	GGGGATCCTTAAGCCTTGTCATCGTCGTC

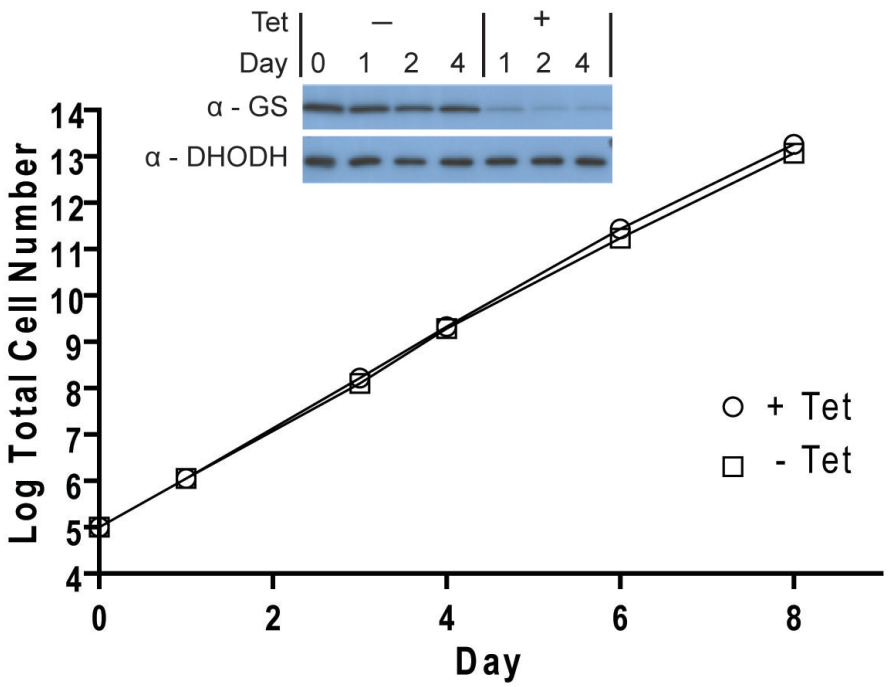

Figure 8. *Tb*GS RNAi Growth Curve. RNAi was induced using a Tet-inducible stem-loop vector. Tet was added every 24 h to maintain knockdown. Protein levels were evaluated by western with DHODH as a loading control. Growth is shown as total cell number, which is the product of cell density and total dilution. Each data point is the average of triplicate data. Error bars (SEM) are unseen because error was smaller than the symbols used to represent the data.

	- Tet				+ Tet		
Day	**0**	**1**	**2**	**4**	**1**	**2**	**4**
clone 1*	1	0.86	0.94	0.78	0.19	0.11	0.08
Day		**3**	**5**	**7**	**3**	**5**	**7**
clone 2		1	0.63	0.70	0.14	0.12	0.16
clone 3		1	1.13	1.32	0.16	0.23	0.20

Table 2. Relative *Tb*GS RNAi knockdown levels. Protein levels from three *Tb*GS RNAi clones were quantified upon knockdown induction. Each was compared to the loading control as well as the – Tet control to obtain the relative numbers shown.

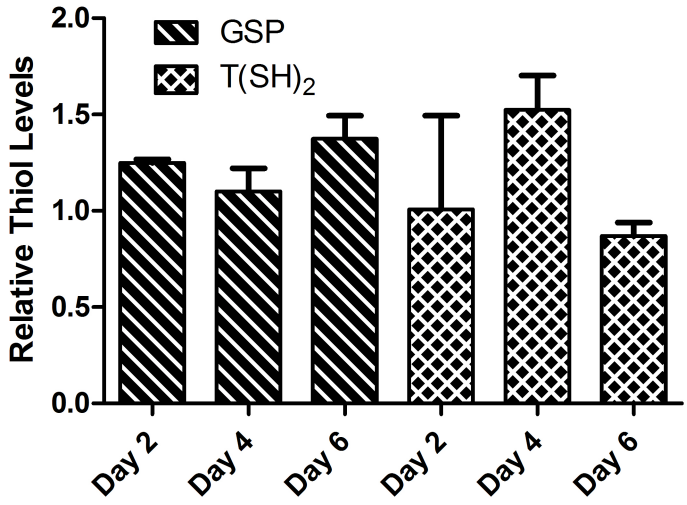

Figure 9. Relative *Tb*GS RNAi trypanothione and glutathionespermidine levels. Bar Graph representing the relative reduced trypanothione ($T(SH_2)$) and glutathionyl-spermidine (GSP) levels in cells with *Tb*GS RNAi knockdown cells (+ Tet) compared to control cells that do not have induced knockdown (- Tet). Error shown is SEM.

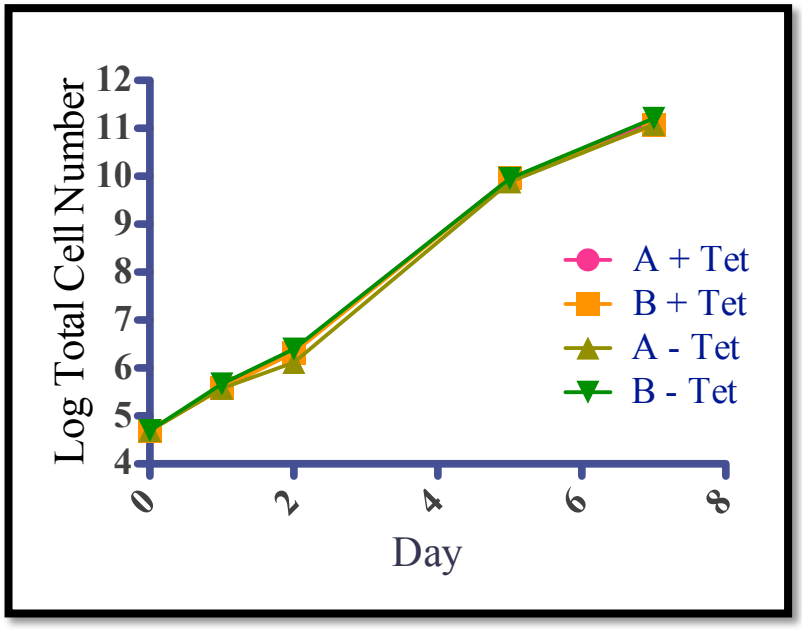

Figure 10. *Tb*GS RNAi growth curve of two different clonal lines. Two separate clonal lines of *Tb*GS RNAi cell line were compared for their ability to reduce *Tb*GS protein. RNAi was induced by the addition of tetracycline (1μg/ml) every 24 hours and growth was quantified on the days indicated. Cell number is represented by the product of cell density and total dilution. Each point is the average of triplicate data and error bars (SEM) were smaller than the symbol used to represent the data.

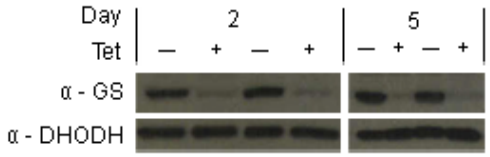

Figure 11. *Tb*GS RNAi western of two different clonal lines. Two separate *Tb*GS RNAi clonal cell lines were compared to determine *Tb*GS protein levels. Protein samples were taken on the days indicated and probed for *Tb*GS protein levels after induction of RNAi. DHODH protein levels served as loading controls.

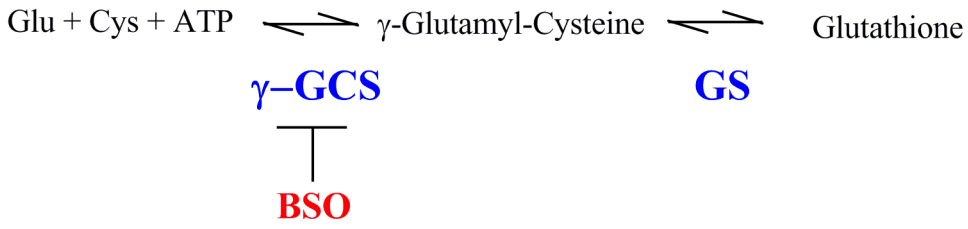

Figure 12. Schematic of Glutathione Synthesis (Figure 16)

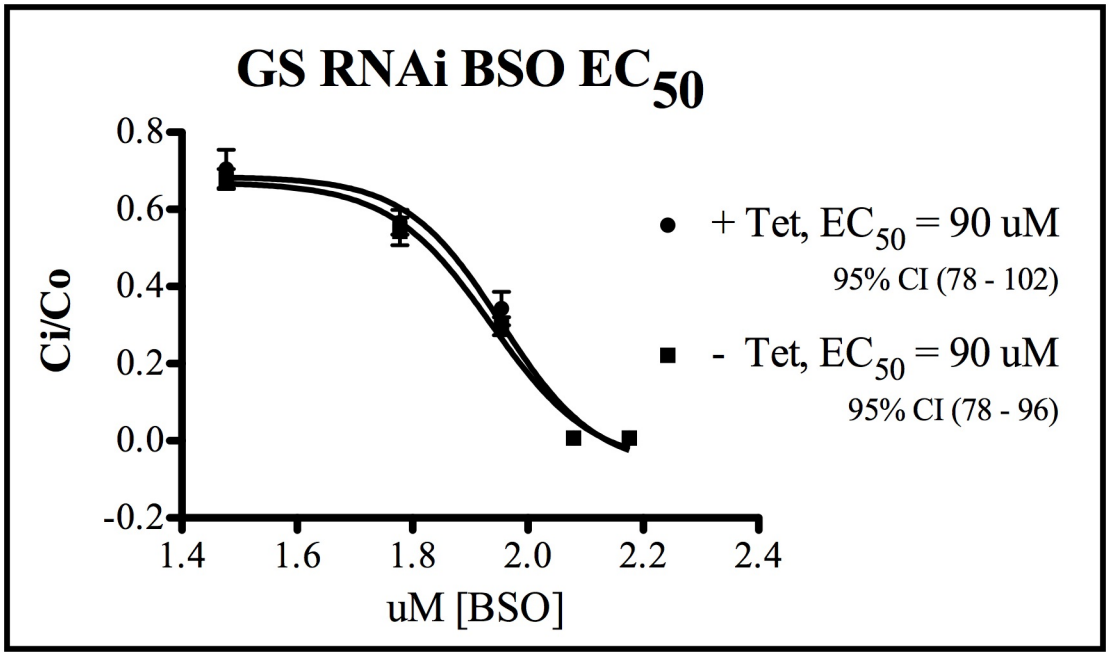

Figure 13. Stressing *Tb*GS RNAi with buthionine sulfoximine. *Tb*GS RNAi cell lines were grown in the presence of tetracycline for two days prior to incubation with buthionine sulfoximine (BSO). Parasites were quantified by hemocytometer after incubation with BSO for 72 hours. Ci is the concentration (or density) of parasites that have been treated with inhibitor. Co is the concentration of parasites that have been treated with vehicle and no drug. Ci/Co is the division of these concentrations. Each point is representative of triplicate data and error bars (SEM) that are not seen are smaller than the symbol used to represent the mean.

CHAPTER THREE

T. brucei GS Purification and Kinetic Activity

A. Introduction

The enzymatic reaction for glutathione synthesis occurs via two ATP dependent steps. The first is catalyzed by γ-glutamyl cysteine synthetase (γ-GCS), which forms a peptide bond between the amino group of L-cysteine (L-Cys) to the γ-carboxyl group of L-glutamate (L-glu) forming γ-glutamyl-cysteine (γ-GC) and is the rate-limiting step in the glutathione synthesis. The second reaction is performed by glutathione synthetase (GS) and is the conjugation of glycine (Gly) to the C-terminus of γ-GC resulting in the tripeptide glutathione. Both of these reaction mechanisms have been elucidated in multiple organisms [157-161].

In *T. brucei,* the GS identified by sequence homology shares 31% identity with the human enzyme. A low resolution (3.15 Å) crystal structure of *Tb*GS showed conservation in the overall fold and active site compared to the human enzyme [162]. However, despite the reported structural study, no kinetic data had

been published to show that the putative *Tb*GS has the capability to synthesize glutathione from γ-GC and Gly using ATP as the energy source. Therefore, one of the goals of my work was to express and purify *Tb*GS and to determine if it was capable of synthesizing glutathione.

Herein, I show that *Tb*GS is indeed capable of synthesizing glutathione and that it has kinetic parameters similar to those previously measured for its homologs. These findings support a role of this enzyme in the synthesis of glutathione *in vivo.*

B. Materials and Methods

Genomic DNA Purification

To clone expression vectors for *Tb*GS protein, genomic DNA was isolated from *T. brucei* parasites. Cells (1.0×10^8) were harvested by centrifugation (1000 X *g* for 10 m) and washed 3 times with PBS (137 mM NaCl, 2.7 mM KCl, 10 mM Na_2HPO_4, 2.0 mM H_2PO_4, pH 7.4). The pellet was resuspended in 500 µl DNA lysis buffer (100 mM Tris-HCl, pH 8.0, 5 mM EDTA, 200 mM NaCl, 0.2% SDS, 60 µg/ml RNase A), and allowed to incubate for 30 m at 37°C. Proteinase K (5 µl of 20 mg/ml) was added and the mixture was incubated at 55°C overnight. DNA was then extracted by phenol/chloroform and ethanol precipitation. DNA purity and concentration was determined using a spectrophotometer and diluted to 100 ng/µl using Tris-EDTA buffer, pH 8.0).

Cloning of Protein Expression Plasmids

A single copy of the *Tb*GS gene (Tb927.7.4000) was identified through sequence homology in the *T. brucei* genome. Erin Willert, PhD at UT Southwestern, cloned the pET15b-*Tb*GS protein expression construct. The *Tb*GS gene was PCR amplified from *T. brucei* 427 genomic DNA using primers containing the desired restriction enzymes (primers listed in Table 1) and cloned in to the pET15b (Novagen) construct linearized with NdeI and XhoI. The resulting construct allowed for expression of N-terminal His_6-tag *Tb*GS. The coding region of the pET15b-*Tb*GS expression plasmid was sequenced in its entirety and transformed into BL21 cells (Invitrogen).

To generate pE-SUMO-*Tb*GS, the *Tb*GS gene was amplified using pET15b-*Tb*GS as a template with the designated primers containing the appropriate restriction enzymes (Table 1). The resulting PCR product was ligated into TOPO-blunt vector (Invitrogen). TOPO-blunt-*Tb*GS was digested with BsaI/XbaI, gel purified, and cloned into BsaI linearized pE-SUMO. The resulting pE-SUMO-*Tb*GS construct contained an N-terminal His_6-SUMO fusion with *Tb*GS. The pE-SUMO-*Tb*GS was then transformed into Rosetta 2(DE3)pLysS competent cells (Novagen).

Dr. Willert produced the pET15b-*Tb*TryS by PCR amplifying *Tb*TryS gene and cloning the PCR product into pET15b using restriction sites NdeI and BamHI. pET15b-*Tb*TryS was then transformed into Rosetta 2(DE3)pLysS competent cells (Novagen).

The *Tb*γ-GCS pET-22b expression vector was cloned previously and was transformed into BL-21 cells containing the helper plasmid pRep-4 as described [91].

Purification of recombinant N-terminal His_6-tagged TbGS

An overnight culture inoculated from a single colony was used to seed 6 L of LB with ampicillin (100 μg/ml) that was grown at 37°C until optical density at 600 nm (OD_{600}) was 0.6-0.8. Protein expression was induced by adding isopropyl β-D-1-thiogalactopyranoside (IPTG) to a final concentration of 200 μM, followed by reduction of the temperature to 16°C, and expression was continued overnight. Cells were harvested the following day by centrifugation (1000 X *g* for 15 m) and resuspended in lysis buffer (50 mM NaH_2PO_4, pH 8.0, 300 mM NaCl, 10 mM imidazole, 1.0 % Triton X, 5 mM β-mercaptoethanol, 1 μg/ml leupeptin, 2 μg/ml antipain, 10 μg/ml benzamidine, 1 μg/ml pepstatin, 1 μg/ml chymostatin, 200 μM phenylmethanesulfonylfluoride (PMSF)). Cell lysis was performed by four brief bursts of sonication at 4°C for 30 s over 30 m. Cell debris was removed by centrifugation (10,000 X *g* for 45 m at 4°C). Soluble *Tb*GS protein was then purified over a Ni^{2+}-hand packed column and eluted using a step gradient of 10%, 50% and 100% buffer B to remove the protein. Buffer A contained 50 mM NaH_2PO_4, pH 8.0, 300 mM NaCl, 10 mM imidazole, 1.0 % triton X, and 1 mM DTT while buffer B contained 50 mM NaH_2PO_4, pH 8.0, 300 mM NaCl, 250 mM imidazole, 1.0 % Triton X, and 1 mM DTT. Elutate containing soluble protein

(detected by SDS-PAGE [155]) was concentrated using Amicon Ultracel – 30 kDa ultra centrifugal filters. *Tb*GS was further purified using a Mono Q column with a linear gradient to 100% buffer B over 10 column volumes with buffer A containing 50 mM NaH_2PO_4, pH 8.0, 50 mM NaCl, 0.1% Triton X, and 1mM DTT, and buffer B containing 50 mM NaH_2PO_4, 500 mM NaCl, 0.1% Triton X, and 1 mM DTT. These two purification steps yielded homogeneous protein, as assessed by SDS-PAGE.

Purification of γ-GCS protein

Purification of γ-GCs was performed as described by [91] with cell lysis occurring through an Avestin ElmulsiFlex-C5 cell disruptor. Purification resulted in 2 mg of homogeneous, soluble and active protein from 6 L of culture.

Purification of TryS protein

TryS protein purification was performed as described by [163], with slight modification. A single colony was used to inoculate 250 ml of terrific broth (TB) containing 50 μg/ml of carbenicillin, 12.5 μg/ml chloramphenicol and 100 μg/ml ampicillin and grown overnight. This was used to seed 6 L of TB containing the same antibiotics. Cells were allowed to grow at 37°C until OD_{600} was approximately 0.6. IPTG was added to a final concentration of 500 μM, temperature was reduced to 22°C, and cells were allowed to grow overnight. Cells were harvested by centrifugation (3600 rpm for 15 m) and resuspended in lysis buffer/buffer A for Ni^{2+} purification (50 mM Tris-HCl, pH 8.0, 300 mM

NaCl, 10 mM imidazole, 2 mM β-mercaptoethanol, 1 μg/ml leupeptin, 2 μg/ml antipain, 10 μg/ml benzamidine, 1 μg/ml pepstatin, 1 μg/ml chymostatin, 200 μM PMSF) and lysed using a Avestin ElmulsiFlex-C5 cell disruptor and all subsequent steps were performed at 4°C. Cell debris was removed by centrifugation (10,000 X *g*) for 30 m. The supernatant was pooled and passed over a GE HiTRAP Chelating HP 5 ml column using Amersham Biosciences AKTA FPLC with Unicorn 4.12 software. Buffer B contained 800 mM imidazole along with the same components of buffer A. After washing the column with 10% buffer B for 5 column volumes, the TryS protein was eluted using a gradient from 10% buffer B to 50% buffer B over 10 column volumes. Fractions were evaluated by SDS-PAGE [155] and fractions containing TryS protein were pooled and concentrated using Amicon Ultracel – 30 kDa ultra centrifugal filters. TryS protein was further purified using anion exchange with buffer A containing 20 mM bis-Tris propane, pH 7.4, 1 mM EDTA, and 1 mM DTT and buffer B containing 500 mM NaCl, 20 mM bis-Tris propane, pH 7.4, 1 mM EDTA, and 1 mM DTT. Over 10 mg of homogeneous, soluble and active TryS protein was obtained.

Purification of Ulp1

Phage-resistant BL21 cells containing pET28b-Ulp1 (a gift from Kim Orth, UT Southwestern Medical Center, Department of Microbiology) were used to inoculate a 10 ml culture. The cultures were grown overnight at 37°C and used

to seed a 2L flask of LB containing kanamycin (50 μg/ml). The culture was grown at 37°C until OD_{600} reached 0.6-0.8 and then induced by addition of 200 μM IPTG. The temperature was reduced to 30°C, and allowed to grow for 4-6 h. Cells were pelleted and resuspended in lysis buffer/buffer A (50 mM Tris-HCl, pH 7.5, 350 mM NaCl, 1 mM β-mercaptoethanol, 10 mM imidazole 0.2% IGEPAL, 20% glycerol, 200 μM PMSF). Cells were lysed using an Avestin ElmulsiFlex-C5 cell disruptor and all subsequent steps were performed at 4°C. Cell debris was removed by centrifugation (10,000 X *g*) for 30 m. The supernatant was then pooled and passed over a GE HiTRAP Chelating HP 5 ml column using Amersham Biosciences AKTA FPLC with Unicorn 4.12 software. Buffer B contained 800 mM imidazole along with the same components of buffer A. After elution, fractions were pooled and exchanged into storage buffer (50 mM Tris-HCl, 50 mM NaCl, 1 mM DTT/TCEP, 20% glycerol). Ulp1 was then aliquotted, frozen using liquid N_2 and stored at -80°C. From 2 L of culture, over 40 mg of protein was obtained.

Expression and purification of SUMO-TbGS from E. coli.

An overnight 200 ml culture inoculated with a single colony of Rosetta BL21 cells containing pE-SUMO-*Tb*GS was used to seed six 1.5 L flasks of LB with kanamycin (50 μg/ml). Upon cultures reaching an OD_{600} of 0.6-0.8, expression was induced by the addition of IPTG to a final concentration of 200 μM, and the temperature was reduced from 37°C to 16°C. The cultures were

allowed to grow overnight (~16 h) and harvested by centrifugation (3600 rpm for 15 m). Cell pellets were resuspended in 60 ml lysis buffer/buffer A (25 mM Hepes pH 8.0, 500 mM NaCl, 1 mM $MgCl_2$, 10 mM imidazole, 1 μg/ml leupeptin, 2 μg/ml antipain, 10 μg/ml benzamidine, 1 μg/ml pepstatin, 1 μg/ml chymostatin, 200 μM PMSF (all protease inhibitors were purchased from Sigma)) and lysed using a Avestin ElmulsiFlex-C5 cell disruptor. All purification steps were done at 4°C. After cell lysis, cell debris was removed by centrifugation (10,000 X *g*) for 1 h.

The supernatant was pooled and passed over a GE HiTRAP Chelating HP 5ml column using Amersham Biosciences AKTA FPLC with Unicorn 4.12 software and SUMO-*Tb*GS protein was eluted using an imidazole gradient. Buffer B contained 600 mM imidazole along with the same components of buffer A. After washing the column with 10% buffer B for 3 column volumes, the SUMO-*Tb*GS protein eluted using a gradient from 10% buffer B to 50% buffer B over 4 column volumes. Fractions were evaluated by SDS-PAGE [155] and fractions containing SUMO-*Tb*GS protein were pooled and concentrated using Amicon Ultracel – 30 kDa ultra centrifugal filters. From 9 L prep, approximately 70 mgs of SUMO-*Tb*GS was obtained. To remove the N-terminal SUMO domain, the SUMO-*Tb*GS protein was buffer exchanged into 25 mM Hepes, pH 8.0, 50 mM NaCl, 1mM $MgCl_2$, 10 mM imidazole, and incubated with Ulp1 at a

20 mg to 1 mg ratio at 4°C for 4 h. Cleavage was confirmed by SDS-PAGE [155].

*Tb*GS protein was further purified using a HiTRAP chelating column with a step gradient of 0, 10, 50, and 100% buffer B with each step consisting of 2 column volumes. Cleaved *Tb*GS protein eluted in the flow-through containing 0% B while uncleaved protein and impurities were retained on the column. Fractions containing cleaved *Tb*GS protein (determined by SDS-PAGE[155]) were pooled, concentrated, and buffer exchanged into storage buffer (25 mM Hepes pH 8.0, 150 mM NaCl, 1 mM $MgCl_2$, 1mM DTT). *Tb*GS protein was aliquotted and stored at -80°C. Protein concentration was determined by absorbance at 280 nm using an extinction coefficient of 59985 $M^{-1}cm^{-1}$ (estimated by the ExPASy ProtParam program available online). A total of 15 mgs of pure *Tb*GS protein from 9 L of bacterial culture was obtained (Figure 14).

ATP-NADH Coupled assay

The hydrolysis of ATP to ADP was monitored by the decrease in absorbance of NADH at 340 nm as it is oxidized to NAD^+ (which does not absorb at 340 nm) [164]. ADP production was coupled to the oxidation of NADH by the enzymes pyruvate kinase and lactate dehydrogenase. ADP along with phospho(enol)pyruvate (PEP) was converted by pyruvate kinase to produce ATP and pyruvate. Lactate dehydrogenase subsequently converted pyruvate to lactate, oxidizing NADH to NAD^+. Components of this assay were added in excess such

that ATP hydrolysis was the rate-limiting step. To verify this, the enzyme of interest was titrated to confirm that the rates of the reaction were linear. Once linearity is lost, ATP hydrolysis is no longer the rate-limiting step and the assay is not valid.

Kinetic assay/ATP coupled spectrophotometric assay – Spectrophotometer

The following assay is based off [165]. *Tb*GS enzyme activity was analyzed using a Beckman Du650 spectrophotometer. Total reaction volume was 500 μl, containing 200 μM NADH, 2 mM PEP, 10 U LDH, 5 U PK, 100 mM Tris-HCl, pH 7.5, 150 mM NaCl, 20 mM $MgCl_2$, 3 mM γ-GC, 30 mM Gly, and 10 mM ATP. The assay was shown to be in the linear range prior to substrate titrations. Individual substrate titrations were performed in the presence of 3 mM γ-GC (from Bachem), 30 mM Gly, or 10 mM ATP. Graphpad Prism was used to analyze data and determine the K_m and k_{cat} values. *Tb*GS protein concentration was determined by absorbance at 280nm using an extinction coefficient of 59985 $M^{-1}cm^{-1}$. Reagents were purchased from Sigma unless otherwise noted.

Kinetic assay/ATP coupled spectrophotometric assay – Plate Reader

The following assay is based off [161]. The ATP-coupled assay was performed at 37°C on a BioTek Synergy H1 Hybrid reader using Griener UV Star 96-well plates. Total reaction volume was 100 μl, contained 250 μM NADH, 5 mM PEP, 10 U LDH, 10 U PK, 100 mM Tris-HCl, pH 8.2, 50 mM KCl, 20 mM $MgCl_2$, 3 mM γ-GC, 30 mM Gly, and 10 mM ATP. Assay was tested to be in the

linear range before substrate titrations. Individual substrate titrations were performed in the presence of 3 mM γ-GC (from Bachem), 30 mM Gly, or 10 mM ATP. Graphpad prism was used to analyze data and determine the k_{cat} and apparent K_m values using Michaelis-Menten nonlinear regression enzyme kinetics. *Tb*GS protein concentration was determined by absorbance at 280 nm using the molecular coefficient 59985 $M^{-1}cm^{-1}$. Reagents were purchased from Sigma unless otherwise noted.

C. Results

TbGS activity with N-terminal affinity tag

Glutathione is synthesized from three amino acid precursors (Gly, L-Glu and L-Cys) in two ATP-dependent reactions by the γ-GCS and GS enzymes. The first reaction catalyzes the formation of γ-glutamylcysteine (γ-GC), and the responsible enzyme (γ-GCS) has also been well characterized [90, 91, 166, 167]. The second reaction to form glutathione is performed by GS and in *T. brucei,* this enzyme had not been characterized. Therefore, in order to kinetically characterize *Tb*GS, I developed an *E. coli* recombinant expression method and obtained homogeneous, purified enzyme.

The *Tb*GS protein was expressed and purified using an N-terminal non-cleavable His_6-tag. *Tb*GS protein was soluble, and its activity was analyzed by steady-state kinetic using an ATP-NADH coupled assay. The apparent K_m values for ATP, Gly and γ-GC were 610 ± 100 μM, 1.9 ± 0.4 mM, and 150 ± 40 μM,

respectively, and the k_{cat} values ranged between 0.3 – 0.5 s^{-1} (summarized in Table 3). Although the K_m values for *Tb*GS were relatively similar to values observed for other GS enzymes, the k_{cat} values were 20-40 fold lower than other published values and, thus, the overall efficiency of *Tb*GS was poor. These kinetic results along with the data obtained by RNAi analysis led to the hypothesis that another unidentified enzyme in *T. brucei* might be responsible for the synthesis of glutathione.

Glutathione Synthesis Activity by TryS and γ-GCS

To investigate the hypothesis that a different enzyme was responsible for glutathione synthesis, I elicited the help of Lisa Kinch (Nick Grishin's laboratory, UT Southwestern Medical Center, Department of Biophysics) to perform a bioinformatics search of the *T. brucei* genome for alternative genes that might have GS activity. Using the ATP grasp domain, which is conserved across the eukaryotic GS family, as the search parameter, no other potential genes with likely glutathione synthesis activity were identified. However, Dr. Kinch observed that the most likely alternative enzymes that might catalyze this reaction were TryS and γ-GCS, the enzymes directly before and after *Tb*GS in the trypanothione biosynthetic pathway (Figure 5). Since both of these expression plasmids were already present in the lab, the GS activity of each of these enzymes was tested.

γ-GCS and TryS were both expressed and, utilizing the ATP-NADH coupled assay, the enzymes were assayed for activity using both GS substrates and their native substrates. Both enzymes were active when their known substrates were used; however, no ATPase activity above background was detected when substrates for the GS reaction were used (Figure 15 and Figure 16), indicating that neither γ-GCS nor TryS was capable of catalyzing glutathione synthesis.

TbGS activity

During our attempts to elucidate the low activity of *Tb*GS, another group published the *Tb*GS X-ray crystal structure [162]. While their study did not provide any kinetic analysis, the structure of the enzyme provided a hypothesis for the low activity of our enzyme. The *Tb*GS structure contained an α-helix in close proximity to the N-terminus and located along the dimer interface (Figure 17). Since an N-terminal tag was used for purification, we hypothesized the tag caused disruption of this α-helix and dimer formation resulting in a protein with reduced activity. In order to test this hypothesis, *Tb*GS expression constructs were generated containing N-terminal His_6-tag that had a TEV cleavage site or C-terminal His_6-tag. However, the C-terminal expression constructs produced insoluble protein, and the N-terminal His_6-tag containing the TEV cleavage site produced scarce amounts of *Tb*GS protein. Additionally, TEV cleavage of the N-terminal tag was inadequate, and untagged protein could not be obtained.

Therefore, a different method of expression and purification was needed to produce untagged *Tb*GS protein.

Another graduate student in the lab, Nahir Velez, had recently achieved success with a new expression system – pE-SUMO (small ubiquitin-like modifier). This expression system fuses the Yeast Smt3 domain with the N-terminus of the protein of interest. The Smt3 domain enhances protein expression and promotes solubility by attracting chaperons that facilitate the proper protein folding [168, 169]. Using the SUMO expression system, soluble *Tb*GS protein was greatly enhanced (over 70 mg from the first purification step) (Figure 14). The SUMO domain was removed using SUMO protease, Ulp1, which recognizes the SUMO domain and cleaves at a specific site between the SUMO domain and the protein of interest. The purified *Tb*GS protein was then used for kinetic analysis.

Kinetic results from the untagged protein yielded apparent K_m values of 490 ± 180 μM, 2.4 ± 1.2 mM, and 41 ± 10 μM for ATP, Gly, and γ-GC, respectively, and the k_{cat} was between 7.7 – 8.7 s^{-1} (summarized in Table 3). While the apparent K_m values did not significantly change for ATP and Gly when compared to the values obtained with the N-terminally His_6-tagged enzyme, the K_m for γ-GC decreased from 150 μM to 41 μM in the untagged enzymes and the k_{cat} for untagged *Tb*GS was 20-fold faster than for the N-terminal tagged protein.

Thus, the N-terminal tag had a detrimental effect on the *Tb*GS activity by largely reducing the enzyme turnover.

D. Conclusions

Trypanothione and its biosynthetic enzymes are required for the growth and proliferation of *T. brucei* [74, 92, 102, 103]. These enzymes have previously been characterized with the exception of *Tb*GS. Here, we were able to express and purify *Tb*GS protein and define the kinetic parameters of the enzymes (Table 3).

In the process of defining the kinetic parameters of the enzyme, we discovered that the turnover of the enzyme (k_{cat}) was significantly affected if an N-terminal His_6-tag was present. While currently unproven, this change in activity might be a result of the tag disrupting an N-terminal α-helix that is located on the dimer interface, resulting in the active dimer not being able to form (Figure 17). After purifying a tagless enzyme, *Tb*GS k_{cat} values increased 20-fold (k_{cat} 7.7 – 8.7 s^{-1}) to a value that was similar to those published on other eukaryotic GS enzymes (Table 3). Furthermore, the removal of the tag reduced the γ-GC K_m from 150 μM to 41 μM. Although this was a modest reduction, it demonstrated the significant impact of the tag on enzyme kinetics.

In comparing the kinetic parameters of *Tb*GS to *A. thaliana* GS enzymes, the apparent K_m values for γ-GC and Gly were relatively similar (41 μM versus 39 μM, 2.4 mM versus 1.5 mM, respectively). However, the ATP apparent K_m was 10-fold higher in *Tb*GS enzymes than in *At*GS, *Hs*GS, and *T. cruzi* (490 μM versus 57 μM and 70 μM, and 30 μM, respectively). Since apparent K_m values

are condition-dependent the higher value for ATP may simply reflect the different reaction conditions, including different concentrations of γ–GC, Gly and Mg^{+2} in our assay. However, it is possible this difference in ATP is the result of differences in the *T. brucei* enzyme. In the crystal structure of the *Tb*GS, one of the coordinating lysine residues (K428) in the ATP-grasp fold of the *Tb*GS enzyme points away from the active site [162]. Because the structure was not solved with substrates and mutational kinetic analyses have not been performed, we cannot conclusively determine whether this is the reason for a difference in substrate binding. However, it provides a plausible hypothesis for further investigation.

Since the trypanothione biosynthetic pathway is targetable and essential, it is important to understand the control points within the pathway. This knowledge provides a better understanding of the similarities and differences between the host and parasite thiol network. By kinetically characterizing *Tb*GS, we show that this enzyme has similar kinetic activity to other homologous GS enzymes (including the human host) and confirm this enzyme is capable of glutathione synthesis and is correctly annotated in the genome.

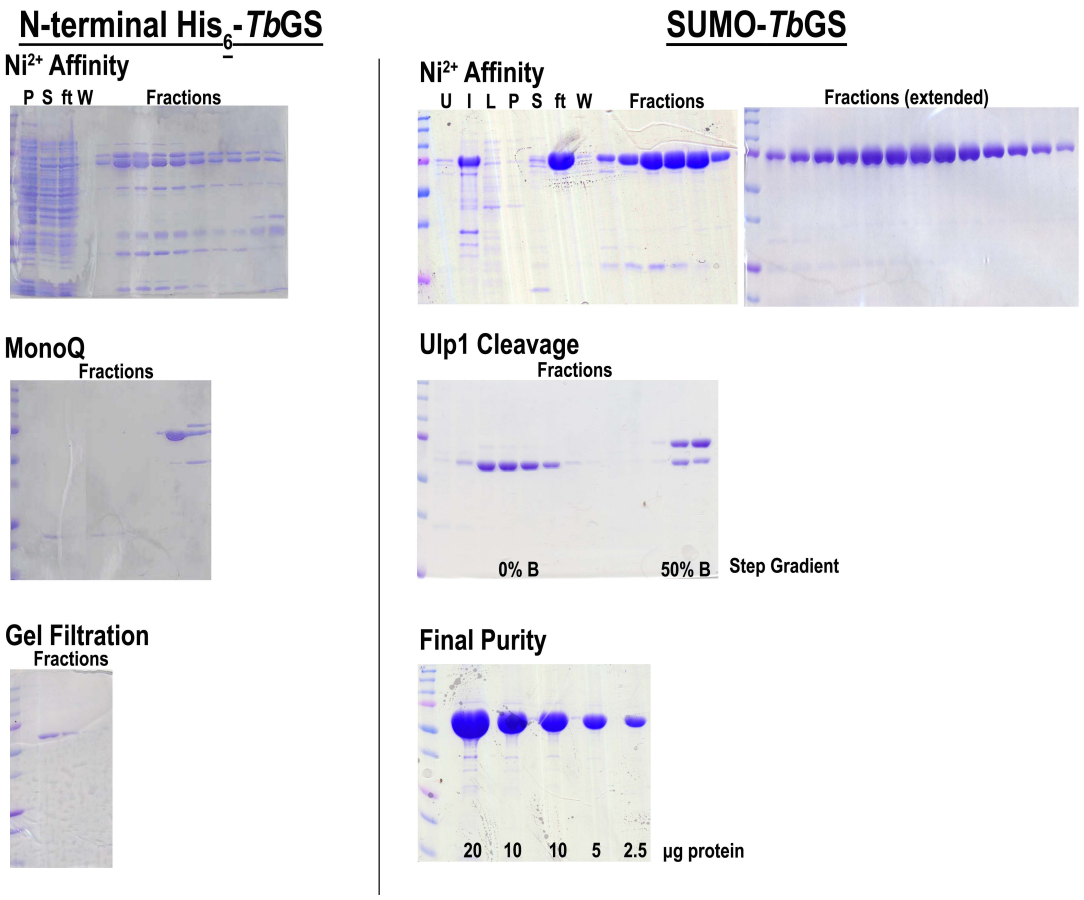

Figure 14. *Tb*GS Protein Purification. U - uninduced, I – induced, L – lysate, P – pellet, S – Supernatant, ft – flow through, W – wash. Different contrasts between gels is due to some being scanned after drying and some being scanned while still wet. SUMO expressed and purified *Tb*GS protein yielded >15 mg of protein from 9 L of culture.

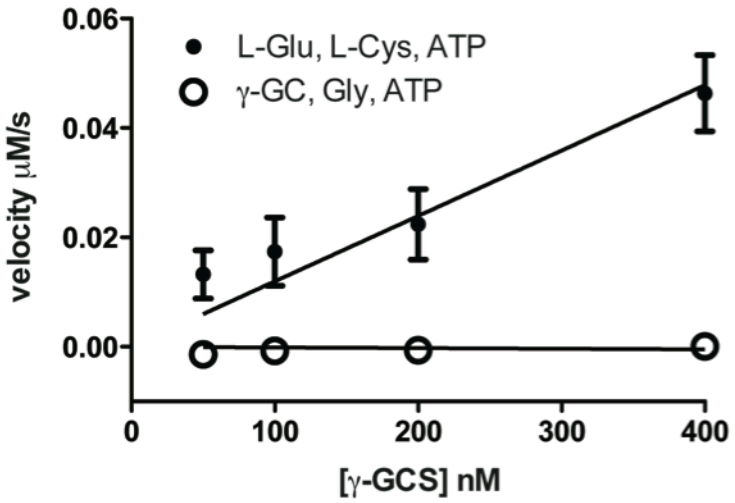

Figure 15. γ-GCS Activity. Velocity of the reaction (μM per s) versus the amount of enzyme (nM). Closed circle indicates rates when the native substrates of γ-GCS – glutamate, cysteine, and ATP – are used to measure activity. Open circle indicates the rates when substrates for glutathione synthesis are used (i.e. Gly, γ-GC and ATP). Error bars (SEM) when not shown are smaller than their respective symbol.

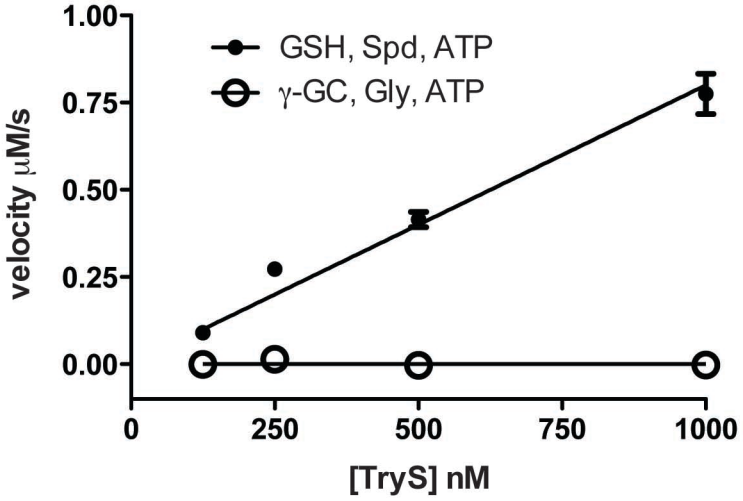

Figure 16. TryS Activity. (Figure 9) Velocity of the reaction (μM per s) versus the amount of enzyme (nM) is shown. Closed circle indicates rates when the native substrates of TryS – glutathione (GSH), spermidine (Spd), and ATP – are used to measure activity. Open circle indicates the rates when substrates for glutathione synthesis are used (i.e. Gly, γ-GC and ATP). Error bars (SEM) when not shown are smaller than their respective symbol

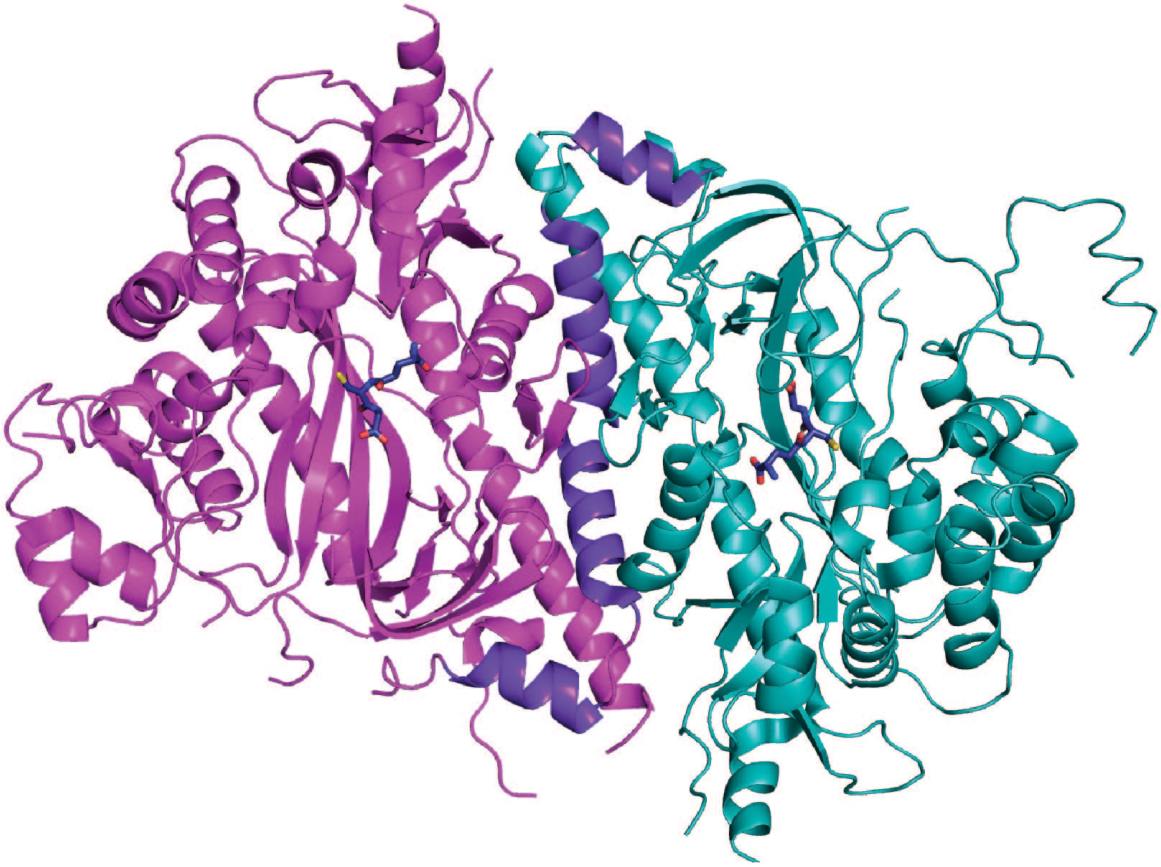

Figure 17. Structure of *Tb*GS. As solved by Fyfe et. al, 2010, the *Tb*GS protein was crystalized in a dimer [162]. Turquoise and pink indicate the individual proteins while the region highlighted in purple is the N-terminus forming the α-helical domains thought to be required for dimerization and optimal kinetic activity. The ball and stick figure within each protein is glutathione.

			T. brucei N-term Tag	*T. brucei*	*T. cruzi**	*A. thaliana***	*H. sapiens****
ATP	k_{cat}	s^{-1}	0.35 ± 0.03	8.7 ± 2.2	4.25	12.1 ± 0.5	6.5
	K_m^{app}	mM	0.61 ± 0.1	0.49 ± 0.18	0.03 ± 0.01	0.057	0.07 ± 0.01
	k_{cat}/K_m^{app}	$M^{-1} s^{-1}$	5.7×10^2	1.8×10^4	1.4×10^5	2.1×10^5	9.3×10^4
Gly	k_{cat}	s^{-1}	0.45 ± 0.04	7.8 ± 1.5	4.25	12.6 ± 0.33	6.5
	K_m^{app}	mM	1.9 ± 0.4	2.4 ± 1.2	1.2 ± 0.3	1.51 ± 0.09	1.75 ± 0.1
	k_{cat}/K_m^{app}	$M^{-1} s^{-1}$	2.4×10^2	3.3×10^3	3.5×10^3	8.3×10^3	3.7×10^3
γ-GC	k_{cat}	s^{-1}	0.31 ± 0.02	7.7 ± 2.0	4.25	12.2 ± 0.3	6.5
	K_m^{app}	mM	0.15 ± 0.04	0.041 ± 0.10	0.04 ± 0.01	.039 ± 0.005	0.66 ± 0.10
	k_{cat}/K_m^{app}	$M^{-1} s^{-1}$	2.1×10^3	1.9×10^5	1.1×10^5	3.1×10^5	9.8×10^3

Table 3. GS Enzyme Kinetics. Kinetic parameters of *Tb*GS obtained through ATP-NADH coupled assay compared to human and *A. thaliana* obtained values.

* numbers obtained from Olin-Sadoval et. al 2012 [89]
** numbers obtained from Herrera et. al 2007[160]
*** numbers obtained from Dinescu et. al 2004[158]

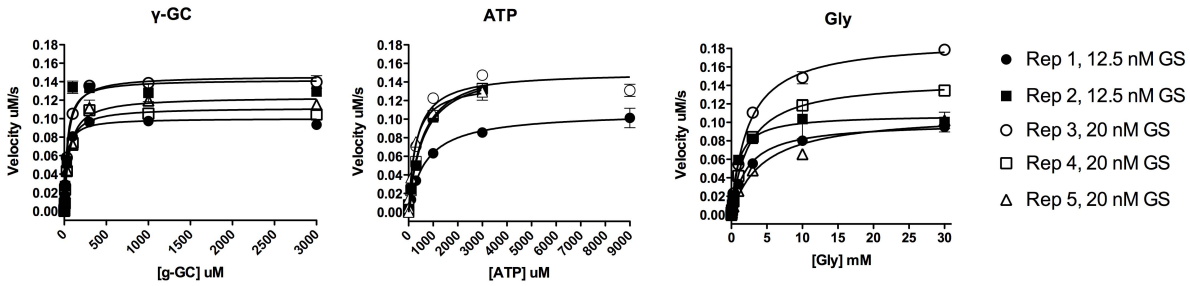

Figure 18. Substrate Titrations. Kinetic parameters were obtained by substrate titration in the presence of excess secondary and tertiary substrate. Each curve is the result of triplicate data analyzed individually. Either 12.5 nM or 20 nM of untagged *Tb*GS enzyme was used as indicated. Each titration was done at a minimum of five times. Error bars (SEM) when not shown are smaller than their respective symbol.

CHAPTER FOUR

T. brucei GS conditional double knockout indicates that it is an essential protein in the trypanothione biosynthesis pathway

A. Introduction

In trypanosomatids, trypanothione is required for the maintenance of cellular redox balance and the regeneration of Txn, Gxn, and Px/Prx, each of which has various roles in maintaining cell homeostasis and proliferation [80]. By being formed by the conjugation of glutathione to the spermidine, trypanothione links the polyamine and thiol biosynthetic pathways. While mammalian cells have multiple layers of regulation to control polyamine levels, using transcriptional, translational and protein turnover, the mechanism of regulation of polyamines in *T. brucei* is not completely understood. Currently, the only identified regulation in the *T. brucei* polyamine biosynthetic pathway is the modulation of AdoMetDC prozyme levels in response to either chemical or genetic loss of AdoMetDC activity, with the data supporting a translational control mechanism [103, 170]. Prior to this work, there was no known regulation of the trypanothione biosynthetic enzymes. The goals of the studies outlined in

this chapter were to determine if *Tb*GS is essential for proliferation of *T. brucei* and to assess if it plays a role in the regulation of the trypanothione and/or polyamine biosynthetic pathways.

Initially, the role of *Tb*GS was investigated using RNAi; however, lack of a growth phenotype when *Tb*GS levels were reduced suggested either *Tb*GS was not essential or *Tb*GS levels may not have been sufficiently reduced by RNAi to elicit a growth phenotype. Therefore, in order to investigate the role of *Tb*GS in the trypanothione biosynthetic pathway, a different and more tightly controlled approach was required. Therefore, I opted to use regulated knockout strategies to examine the role of *Tb*GS. Although *Tb*GS is a single copy allele in the parasite, *T. brucei* is a diploid organism; consequently, both alleles had to be removed to obtain the desired cell line. By utilizing a regulated double knockout cell line, *Tb*GS levels were depleted leading to growth arrest and loss of measureable reduced trypanothione levels. This effect was not rescued by exogenously added glutathione, suggesting that glutathione is imported into the parasite by a transpeptidase system, similar to mammalian cells, rather than being transported intact, as in yeast. Reduced expression of *Tb*GS also resulted in increased levels of the upstream glutathione biosynthetic enzyme and suppressed expression of polyamine biosynthetic enzymes, thus providing a novel insight into the regulatory mechanisms used by the parasite to maintain spermidine and trypanothione homeostasis.

While analysis of the *Tb*GS knockout cell line provided clear evidence that GS was required for growth, depletion of GS did not lead to complete cell death and after several days in growth arrest, parasites recommenced growth at rates comparable to control cells. The exit from growth arrest coincided with low levels of expression of *Tb*GS protein and by reinstated levels of trypanothione. *T. brucei* has previously been shown to escape Tet-regulation of the ectopic copy either by a mutation within the promoter region or by loss of the Tet repressor gene; however, our data does not support this method of escape from regulation [171-173]. Flow cytometry analysis of the knockout cell line indicated that while a significant portion of the population underwent cell death, a small subset remained healthy suggesting that stochastic or epigenetic variability in *Tb*GS expression levels that allowed this population of cells to up regulate sufficient *Tb*GS for growth. Thus our data show that *Tb*GS is an essential gene in *T. brucei* and further underscores the importance of trypanothione for growth and proliferation.

B. Materials and Methods

Gene ID numbers

The TriTrypDB gene ID numbers are as follows: *GS* (Tb927.7.4000), γ-GCS (Tb927.10.12370), TryS (Tb927.2.4370), TR (Tb927.10.10390), ODC (Tb927.11.13730), AdoMetDC (Tb927.6.4410 and Tb927.6.4460), AdoMetDC prozyme (Tb927.6.4470), SpdSyn (Tb927.9.7770) and DHODH (Tb427.05.3830)

Cloning of GS allelic replacement constructs

Methods for gene disruption and regulated gene expression are well established in *T. brucei* and the vectors and approaches used to generate *Tb*GS knockout cell lines followed these established procedures [103, 174, 175]. Briefly, two approximately 300 bp segments of the *Tb*GS 5' and 3' UTR (corresponding to nucleotide -387 to -61 and 1745 to 2135, respectively where base 1 represents the ATG start codon and base 1668 represents the TAA stop codon) were PCR amplified using primer sets containing the appropriate restriction enzymes (Table 1) and the resultant PCR fragment was cloned into TOPO-Blunt (Life Technologies). The UTRs were sequentially subcloned into the pLEW13 vector first by introducing the 5' UTR region using NotI/MluI followed by the 3' UTR region using XbaI/StuI. The resulting pLEW13-*Tb*GS knockout construct A (KO-A) contained the T7 polymerase and neomycin cassette sandwiched between the *Tb*GS UTRs. To generate the pLEW90-*Tb*GS knockout construct B (KO-B), the *Tb*GS KO-A vector was digested with XhoI/SwaI to remove to T7 polymerase and neomycin cassette, and the pLEW90 vector was digested with XhoI/StuI to liberate the Tet repressor and Hygromycin cassette (SwaI/StuI are blunt end endonucleases). The TetR and hygromycin cassette were ligated into the pLEW13-*Tb*GS KO-A forming the pLEW90-*Tb*GS KO-B vector (Figure 19).

Cloning TbGS Tet-regulatable constructs

The first Tet-regulatable construct developed was pLEW300-fGS. It was generated from the pLEW300-FLAG-prozyme used to investigate the role of prozyme in AdoMetDC regulation [103]. The *Tb*GS gene was PCR amplified using primers with the designated restriction enzymes (Table 1) and inserted into TOPO-Blunt. Quick change mutagenesis was used to remove a BamHI site from inside the *Tb*GS gene and subsequently ligated into the pLEW300-FLAG using NdeI/BamHI creating an N-terminal FLAG-tag on the ectopic *Tb*GS gene. The pLEW100-fGS construct was generated by digestion of the pLEW300-fGS and pLEW100-luciferase construct with HindIII/BamHI. The FLAG-GS insert was then ligated into pLEW100 resulting in the second N-terminal FLAG-tag ectopic expression vector.

To generate the C-terminal FLAG-tag ectopic, the *Tb*GS gene was PCR amplified using primers with appropriate restriction enzymes (Table 1), digested with HindIII/KpnI, and ligated into HindIII/KpnI linearized pT7-FLAG-MAT to generate the pT7-GS-FLAG-MAT bacterial expression vector. The GS-FLAG was moved from the pT7 vector by PCR amplification and digestion with BamHI/HindIII to the pLEW300 and the pLEW100v vectors, creating the C-terminal FLAG-tag ectopic expression vectors (Figure 19). The coding regions of all ectopic expression vectors were sequenced in entirety after completion.

T. brucei Cell Culture

Bloodstream form *T. brucei* strain 427 were cultured in HMI-11 media at 37°C and 5% CO_2 [153] with the appropriate antibiotics (G418 (2.5 μg/ml), hygromycin (5 μg/ml), phleomycin (2.5μg/ml)). Parasites were split every 1 – 3 days to maintain healthy cultures in log phase (10^3-10^6 cells/ml). Cell densities were calculated with a hemocytometer (Fisher). Growth curves are represented as total cell number, which is the product of cell density and total dilution.

Generating the TbGS DKO/cDKO cell lines

The transfection protocol used to generate the *Tb*GS SKO, *Tb*GS DKO and the *Tb*GS cDKO cell lines is the same as described in Chapter 3 using the Amaxa Nucleofector and kit. Cells were transfected with NotI linearized vectors and transfectants were selected using the antibiotic corresponding to the resistance gene inserted.

To generate the *Tb*GS DKO cell line, log phase bloodstream 427 cell lines were transfected with the NotI linearized pLEW13-*Tb*GS KO-A vector. After establishing a *Tb*GS SKO cell line with neomycin/G418, glutathione (80 μM) was added to the media and parasites were transfected with the NotI linearized pLEW90-*Tb*GS KO-B vector. The resulting transfectants were established in media containing glutathione, neomycin, and hygromycin.

To generate the *Tb*GS cDKO cell line, *Tb*GS SKO cells were transfected with Tet-regulated *Tb*GS ectopic expression vector and selected in the presence of either blasticidin or phleomycin. The resulting cell lines, single knockout with

inducible *Tb*GS (SKO+iGS), were investigated for expression of a FLAG-tagged *Tb*GS protein. After expression of the ectopic copy of *Tb*GS had been established, parasites were transfected with the pLEW90-*Tb*GS KO-B vector in the presence of Tet to generate the *Tb*GS cDKO cell line. Limited dilution was used to obtain clonal lines and parasites were maintained in media that contained Tet, hygromycin, neomycin, and phleomycin.

Evaluation of TbGS cDKO Growth Rates

*Tb*GS cDKO growth rates were evaluated by first washing cells twice with Tet-free media followed by plating into fresh media at a density of 1-5 x 10^4 cells/ml with and without Tet. Cells were counted on the days indicated and split into fresh media every 24-48 h, depending on growth. Growth curves are represented as log total cell number verses time. Total cell number is the level of parasites measured by the hemocytometer multiplied by the dilution factor.

Southern Blot Analysis

The genotype of *Tb*GS DKO cell lines was evaluated by Southern blot. Genomic DNA was isolated from cells using methods mentioned in Chapter 2, digested with BanI, separated on a 1% agarose gel, and transferred to a positively charged membrane (Ambion Bright Star) by vacuum in 10x saline sodium citrate (SSC) buffer (1.5 M NaCl, 150 mM trisodium citrate, pH 7.0). The membrane was UV-crosslinked, prehybridized with UltraHyb solution for 1 h at 42°C and hybridized with biotinylated probe overnight at 42°C.

The membrane was visualized using the BrightStar BioDetect Kit from Ambion following methods outlined in the protocol. Membrane was washed twice with 10 ml of low stringency buffer for 15 m each at room temperature followed by two more washes using 10 ml of high stringency buffer for 15 m each at 42°C. The membrane was washed twice for five m in 1X wash buffer, incubated in blocking buffer twice for five m and once for 30 m, incubated in blocking buffer containing Strep-Alkaline Phosphatase for 30 m, incubated in blocking buffer once for 10 m, washed three times for 5 m each with 1X wash buffer, incubated twice for 2 m each in 1X assay buffer and incubated for 5 m in CDP star followed by exposure to film. Unless otherwise noted, all reagents were purchased from Ambion. The probe was a 611 bp region upstream of the *Tb*GS coding region starting at -1215.

Elucidation of Ectopic Transcription

RNA from *Tb*GS cDKO or SKO+iGS cell lines was harvested from cells (~10^8) by centrifugation (1000 X *g* for 10 m), washed in PBS (137 mM NaCl, 2.7 mM KCl, 10 mM $Na_2HPO_4(2\ H_2O)$, 2.0 mM KH_2PO_4, pH 7.4) twice, and the pellet resuspended in 1 ml Trizol (Life Technologies). RNA was purified using the RNeasy kit from Qiagen and quantity/quality of RNA was determined by A_{260}/A_{280}. Samples were DNase treated to remove genomic DNA contamination (Life Technologies) and cDNA synthesis was done using Life Technologies SuperScriptIII RT kit. Samples were then amplified using the splice-leader

sequence and a reverse primer 200 bp inside the *Tb*GS gene (Table 1). PCR products were ran on 1.25% agarose gel and visualized with UV.

Western Blot Analysis.

Protein was isolated from lysed cells collected and prepared as described in Chapter 3. Antibodies against trypanothione biosynthesis pathway were used as previously described [74, 92, 103, 167, 176]. Dilutions for each primary antibody in 5% Milk in TBS-T were: α-*Tb*GS – 1:2,500, α-*Tb*DHODH – 1:10,000, α-FLAG – 1:1,000 (Sigma), α-*Tb*AdoMetDC – 1:2,500, α-*Tb*prozyme – 1:5,000, α-*Tb*ODC – 1:10,000, α-*Ld*SpdSyn – 1:1,000, α-*Tb*TryS – 1:1,000, and α-*Tb*γ-GCS – 1:10,000. Secondary antibodies (anti-rabbit, anti-rat (TryS), and anti-mouse (FLAG)) were used at 1:10,000 dilutions in 5% nonfat milk in TBS-T. To measure the levels of each trypanothione biosynthesis protein on the days indicated, parallel gels were loaded with 20-40 μg total protein per well, transferred, and each membrane was sectioned and probed with a different antibody. Therefore, each membrane was used to assess protein levels of two biosynthesis pathway proteins along with the DHODH loading control.

Primary and secondary antibodies were incubated with membranes at the indicated dilutions for 1 h, followed by three 10 m washes in TBS-T. Secondary antibodies were commercially conjugated to horseradish peroxidase so proteins could be visualized by chemiluminescence after membrane incubation with ECL substrate and exposure to film.

Intracellular Polyamine Determination

Analysis of polyamines was done as previously described by Willert et al. 2008, [103]. For analysis of intracellular polyamines, 1 x 10^7 cells were harvested by centrifugation (1000 X g. for 10 m), washed twice with 1 ml of PBS (137 mM NaCl, 2.7 mM KCl, 10 mM Na_2HPO_4 (2 H_2O), 2.0 mM KH_2PO_4, pH 7.4) and then resuspended in 25 µl polyamine lysis buffer (100 mM MOPS, pH 8.0, 50 mM NaCl, 20 mM $MgCl_2$). Cells were lysed by 3 freeze/thaw cycles followed by acid precipitation of proteins by addition of 7.5 µl of 40% trichloroacetic acid (TCA) and incubation on ice for 10–15 m. Cell debris was removed by centrifugation at maximum speed on a bench top centrifuge. Supernatant was fluorescently labeled using AccQ-Fluor reagent (6-aminoquinolyl-n-hydroxysuccinimidyl, Waters) by incubating 5 µl of sample supernatant with 20 µl labeling reagent and 75 µl borate buffer at 55°C for 10 m. Polyamines were separated by HPLC using a Waters' AccQtag (3.9x150mm) column run on a Beckman System Gold HPLC with a Rainin Dynamax Fluorescent detector. Peaks were separated by using the linear gradient previously described with eluent A containing 450 mM sodium acetate, 17 mM triethylamine (TEA), 0.01% sodium azide, pH 4.95 and eluent B containing 60% acetonitrile and 0.01% acetone [102, 103, 166]. The gradient was as follows: stay at 0% B for 5 m, go to 20% B over 45 m, go to 50% B over 5 m, go to 100% B over 2 m, stay at 100% B for 1 m, go to 0% B over 1 m, stay at 0% B for 10 m. Polyamines were

identified by retention time and quantified by peak area in comparison to standards run under the same conditions.

Intracellular Thiol determination

Reduced intracellular thiols were determined by the following optimized protocol, which was based off methods previously described [156, 177, 178]. Cells (1 x 10^8) were harvested by centrifugation (1000 X g, 10 m room temperature) and washed twice with pre-warmed HMI-9 media lacking fetal bovine serum (FBS), β-mercaptoethanol, and L-cysteine. A final wash was done with cold (4°C) PBS, (137 mM NaCl, 2.7 mM KCl, 10 mM Na_2HPO_4 (2 H_2O), 2.0 mM KH_2PO_4, pH 7.4) and cells were pelleted by centrifugation (1000 X *g* for 5 m). PBS was removed, and cells were immediately acid precipitated by resuspension in 150 µl of ice cold 5% TCA in 10 mM HCl and allowed to incubate on ice for 5-10 m. Denatured proteins and cell debris was removed by maximum speed centrifugation in a bench-top centrifuge at 4°C. The supernatant was extracted four times with 450 µl ice-cold diethyl ether to remove excess TCA and 345 µl of 40 mM HEPPS containing 4 mM DTPA was added to the extractant.

To derivatize thiols in the extracted supernatant, 5 µl of 200 mM monobromobimane was added for a final concentration of 2 mM and vortexed. Samples were incubated at room temperature for 10 – 15 m in the dark. To stop

the labeling reaction and prevent oxidation of samples, 2.5 µl of 5 M MSA was added. Samples were stored at -80°C until analyzed by HPLC.

HPLC analysis used a Phenomenex Kinetex 2.6µ C_{18} column with a constant flow rate of 1.25 ml/min at room temperature of eluent A, 0.25 % CSA and eluent B, 0.25 % CSA and 25% 1-propanol both at pH 2.64. The timed program was as follows: 0% eluent B for 1 m, gradient from 0% to 5% eluent B over 0.5 m, constant 5% eluent B for 4.5 m, gradient from 5% to 12.5% eluent B over 29 m, gradient from 12.5% to 35% eluent B over 12 m, gradient from 35% to 60% eluent B over 2 m, constant 60% eluent B for 4 m, then gradient from 60% eluent B to 0% eluent B over 1 m. Column was re-equilibrated for 20 m between samples using the same flow rate and 0% eluent B. Thiols were identified by retention time and quantified by reduced standard's peak area.

Evaluation of the anti-trypanosomal activity of BSO

To measure the BSO EC_{50} in *Tb*GS cDKO cell lines, parasites were grown with or without Tet for the days indicated, quantified, and diluted to 1 x 10^3 cells/ml. Parasites were plated into 96 well plates (Greiner) with 200 µl/well. BSO concentrations were varied from 0 to 3 mM using 10 different concentrations and incubated with parasites for 72 h. Cell viability was then measured using cell titer glow (Promega), an ATP/luminescence assay. BioTek Synergy H1 Hybrid reader measured cell viability in the form of luminescence and these values were plotted in Graphpad Prism. EC_{50} curves were generated for

BSO using the nonlinear regression (log (agonist) v. response (four parameter fit)).

Hydrogen peroxide (H_2O_2) 24 h stress test

*Tb*GS cDKO cell lines were analyzed for their ability to withstand external H_2O_2 stress by incubating cells (with or without Tet for the number of days indicated) with varying concentrations of H_2O_2 (0, 10, 30 or 100 μM). After 24 h, cell viability was measured using cell titer glow (Promega).

Flow cytometry analysis/Live/Dead cell assay

This protocol was based on previously published methods and optimized for *Tb*GS cDKO cell lines [179]. Cells (~10^6) were harvested by centrifugation (1000 X *g* for 10 m) and washed using pre-warmed (37°C) PBS containing glucose (PBSG) (137 mM NaCl, 2.7 mM KCl, 10 mM Na_2HPO_4 (2 H2O), 2.0 mM KH_2PO_4, 10 mM glucose, pH 7.4). Cells were then resuspended in 500 μl PBSG and calcein and ethidium bromide were added to final concentrations of 50 nM (Life Technologies). Cells were incubated for 15-20 m at 37°C and then analyzed immediately by flow cytometry. Samples were analyzed on a Beckman Coulter Calibur flow cytometer using a 530/40 filter (calcein) and 692/40 filter (ethidium). Data were analyzed using FlowJo software with single-stained cells used for compensation of spectral overlap within the software. Cells treated with eflornithine (DFMO) (200 μM) determined gating for unhealthy populations while proliferating cells determined gating for healthy populations.

C. Results

Generation of TbGS DKO cell line was the result of trisomy.

*Tb*GS knock out strategies were used to generate a more tightly regulated *TbGS* gene that would allow examination of its role in trypanothione biosynthesis. *T. brucei* is a diploid organism and required both endogenous alleles be removed. Initially, elimination of both alleles was attempted presence of exogenously added glutathione (80 μM). Glutathione was previously shown to restore growth of RNAi knockdown of γ-GCS, the enzyme immediately prior to *Tb*GS in trypanothione biosynthesis (Figure 5) [92]. Cell lines (*Tb*GS DKO) were obtained that conveyed resistance to both selectable markers targeted to replace the *Tb*GS gene (neomycin and hygromycin); however, Southern blot confirmed that the cells had obtained a partial trisomy to retain the *Tb*GS gene along with the 2 resistance genes (Figure 20). This occurrence has been previously described in trypanosomatids for other genes and is indicative of an essential gene [180, 181]. Furthermore, the inability of glutathione to replace the requirement of *Tb*GS suggests glutathione is not imported in to the cell whole (like in yeast) but rather is likely taken up through a transpeptidase mechanism similar to GGT in mammalian cells [46, 182]. Therefore, in order to probe the role of *Tb*GS in the trypanothione biosynthetic pathway, a regulated or conditional DKO (cDKO) cell line was needed.

Generation of TbGS cDKO cell line established using C-terminal FLAG-tag

To generate the necessary *Tb*GS cDKO cell line, both endogenous alleles were removed and a Tet-regulatable ectopic copy of the gene was inserted into the ribosomal repeat locus of the genome (Figure 19). In order to differentiate between the endogenous and ectopic allele, a FLAG-tag was placed on the N-terminus of *Tb*GS gene to allow for verification of expression of the ectopic gene prior to removal of the second endogenous *Tb*GS allele. The decision to place the tag on the N-terminus of the protein preceded the publication of *Tb*GS X-ray crystal structure and my findings of the effects of an N-terminal tag on kinetic efficiency. Subsequently, transfections using two separate ectopic constructs with the Tet-regulatable *FLAG-TbGS* gene failed to produce any detectable levels of FLAG-*Tb*GS protein observed by western blot using an anti-FLAG antibody. To determine if the lack of expression was occurring at transcription or translation, PCR primers to the 5' UTR were designed to distinguish between the native and the ectopic *Tb*GS cDNA (Table 1). Analysis of the cDNA obtained from cell lines containing the ectopic FLAG-*TbGS* gene proved the ectopic gene was indeed transcribed although FLAG-*Tb*GS protein was not detected. Therefore the lack of detectable protein suggested the message was either poorly translated or the expressed protein was unstable (Figure 20).

While investigating this dilemma, another group solved the *Tb*GS X-ray crystal structure [162] and I observed that N-terminus of the protein formed an α-helix that is located along the dimer interface of the protein (Figure 17). Since the

ectopic copy of *Tb*GS was not being expressed even though it was being transcribed, I hypothesized that the N-terminal FLAG-tag was prohibiting the formation of a functional enzyme and therefore limiting its kinetic ability, similar to the N-terminal His_6-tag used for kinetic studies. Therefore, to generate a functional *Tb*GS ectopic expression plasmid, the FLAG-tag was moved to the C-terminus of the protein. This instigated the generation of the pLEW100v-*Tb*GS-FLAG construct and resulted in SKO+iGS-FLAG cell line. Expression of the ectopic *Tb*GS protein was observed using an anti-FLAG antibody (Figure 22). Subsequently, the second endogenous allele was removed, generating a *Tb*GS cDKO cell line that was used to elucidate the role of *Tb*GS in the trypanothione biosynthetic pathway.

Loss of TbGS led to cell growth arrest.

Since the *Tb*GS cDKO cell line relied on a Tet-on system, Tet was required to maintain expression of *Tb*GS protein once the endogenous alleles were removed. To deplete *Tb*GS, parasites were washed with Tet free media and their growth was monitored over 10 days. Initially, trypanosomes grew at identical rates with and without Tet; however, after 4 – 5 days, parasite in media lacking Tet entered a period of growth arrest where little to no growth was seen (Figure 23A). This period of growth arrest was not due to overgrowth because trypanosomes were maintained within the appropriate range of optimal density that still allowed for quantitation by hemocytometer. Furthermore, control

parasites continued to grow at normal rates. Growth arrest was accompanied by an observation of increased "stumpy" or non-proliferating bloodstream form parasites along with an increased amount of visibly dead cells in comparison to control. However, even though "stumpy" and dead cells were observed during growth arrest, long, slender proliferating parasites were still observed, albeit at a lower density than control cells. Once a trypanosome has transitioned to the "stumpy" form, it is arrested in the G1 phase of the cell cycle and cannot resume proliferation unless it enters the tsetse mid-gut through a blood meal [183]. This observed growth arrest lasted 3 – 4 days after which parasites resumed growth at rates similar to that of control cells. The addition of glutathione did not rescue the growth defect that occurred upon *Tb*GS depletion (Figure 23A), again suggesting the hypothesis that glutathione is not transported into cells intact. The timing of growth arrest coincided with depletion of *Tb*GS protein as evaluated by western analysis. *Tb*GS protein levels were decreased to less than 3-4 % of control levels by day 2 and were undetectable by day 4 (Figure 23B and Figure 24). However, low levels of *Tb*GS expression (3-4% of control) could be detected starting on day 8, correlating to the point where cell growth resumed. These data suggest that cells escaped Tet regulated control of *Tb*GS expression 7-8 days after Tet removal leading to re-expression of the gene.

The loss of TbGS affected intracellular thiol pools but not polyamine pools.

Intracellular reduced trypanothione and polyamine levels were measured over the course of growth analysis (Figure 23C-D). Polyamine levels remained relatively unchanged compared to controls. In contrast, trypanothione levels were depleted by day 4, corresponding to the point where growth arrest was observed. Moreover, trypanothione levels returned to control levels by day 8, again corresponding to the point were growth resumed along with low levels of *Tb*GS protein. Thus, the observed growth arrest coincides with both the loss *Tb*GS protein and depletion of reduced trypanothione, indicating *Tb*GS is an essential enzyme for parasite growth and is involved in trypanothione biosynthesis. The intracellular thiol levels were measured using a modified protocol that reduced the impact of the secondary amidase activity of TryS thus giving a more accurate view of the intracellular thiol pools [178]. This resulted in the majority of reduced thiol pools being found in the form of trypanothione along with low levels of glutathionespermidine rather than glutathione, contrary to previous publications where glutathione was abundant and trypanothione and glutathionespermidine levels were low [92, 102, 103].

Loss of TbGS altered expression of a subset of polyamine and trypanothione biosynthetic enzymes.

To investigate if loss of *Tb*GS had an effect on the levels of other polyamine and trypanothione biosynthetic pathway proteins, each of the pathway proteins were monitored by western blot on days leading up to the growth arrest.

While no changes were observed in SpdSyn, TryS or AdoMetDC protein levels, γ-GCS protein levels were increased (2-3-fold) and AdoMetDC prozyme and ODC levels were reduced (2-3 fold for prozyme and 1.5 fold for ODC) on days 4 and 5. Changes in protein levels not only correlated with the time point where trypanothione levels were most reduced but also occurred in proteins that have previously been shown to have a regulatory effects on polyamine and thiol levels (Figure 23B and Figure 24) [102, 103, 170].

TbGS cDKO cells have increased sensitivity to a pathway inhibitor.

Sensitivity to the γ-GCS inhibitor buthionine sulfoximine (BSO) was tested on *Tb*GS cDKO cells. Cells were grown without Tet for 2 days followed by incubation with various levels of BSO. The EC_{50} for BSO was increased 3-fold in the absence of Tet (EC_{50} = 270 ± 24 μM) relative to the control *Tb*GS cDKO cells (EC_{50} = 88 ± 43 μM). These were the findings of three independent experiments of three replicates each (Figure 25). After resumption of growth, cells displayed similar EC_{50} values to control cells.

TbGS cDKO cells did not have increased sensitivity to oxidative stress by H_2O_2.

Since trypanothione is important for the maintenance of proteins that protect against ROS (Txn, Grx, Px, and Prx), *Tb*GS cDKO cells were evaluated for increased sensitive to H_2O_2. Cell lines were cultured with and without Tet and then stressed for 24 hours with various levels of H_2O_2. No change in sensitivity to

H_2O_2 was observed in comparison to control cell regardless of the length of time cells were cultured in the absence of Tet (Figure 26).

Escape from cell death in the TbGS cDKO cell lines was not the result of an acquired genetic mutation

In some cases, *T. brucei* has been shown to escape Tet-regulated control, and in some instances the mechanism of escape was an inheritable genetic mutation [172]. In contrast for the TR knockout, genetic changes were not seen and it was hypothesized that epigenetic differences in the cell populations allowed for regrowth of the parasite [111]. To determine if parasites had acquired a genetic mutation reducing or eliminating Tet regulation, *Tb*GS cDKO parasites capable of growing 10 days in the absence of Tet that displayed low levels of re-expression of *Tb*GS protein were used to generate clonal lines using limited dilution. Recloned parasite were then grown in the presense of Tet for three days, washed with Tet-free media, and their growth observed for 8 days. Parasites still entered a phase of growth arrest 3-4 days after removal of Tet, indicating the mechanism escape from Tet-regulation was not through an inheritable genetic mutation (Figure 27). Instead, the data suggests epigenetic differences between subpopulations result in different expression of *Tb*GS allowing for escape from Tet regulation.

Population analysis of cell viability after TbGS knockdown.

Since the *Tb*GS cDKO cells went through a period where growth stalled for several days and was followed by resumption of growth, the question arose if parasites were actively entering growth arrest or if there were subpopulations of cells with differing responses to Tet withdraw. To investigate this possibility, a previously described live/dead cell flow cytometry assay was used to evaluate the *Tb*GS DKO cell line for mixed populations [179]. The live/dead cell assay contains ethidium and calcein staining for analysis. Ethidium enters cells with compromised membranes and becomes fluorescent upon binding to nucleic acid, indicating dead or dying cells. Calcein is a cell permeable nonfluorescent compound that is cleaved by nonspecific esterase upon crossing the cell membrane. Once cleaved, it becomes fluorescent and is retained within the cell. Cells that are positive for calcein contain esterase activity and therefore calcein is considered to be a live cell marker. As stated earlier, increases of stumpy and dead cells were seen during the period of growth arrest and flow cytometry analysis using forward scatter (FSC) and side scatter (SSC) allowed observation of changes in cell shape, size, and complexity. FSC and SSC are non-fluorescent methods to measure a cell by its scattering of light either in line with the source (FSC) or perpendicular to the source (SSC). FSC measures a cell's size and shape while SSC measures the complexity of a cell's surface.

Flow cytometry was used to analyze *Tb*GS cDKO cells using FSC and SSC as well as calcein and ethidium fluorescence in the FL1 and FL3 channels,

respectively. Control cells (+ Tet) maintained high levels of calcein only positive cells (~94%) and low levels of ethidium positive cells (~5%) throughout the growth curve, consistent with a healthy, growing population (Figure 28 and 29A). To generate a control population of unhealthy cells, *Tb*GS cDKO (+ Tet) were treated with the anti-trypanosomal drug eflornithine (DFMO) (200 μM) for 24 hours prior to flow cytometry analysis. Treatment of DFMO resulted in higher levels of ethidium positive staining as well as higher levels of SSC, both of which are indicative of cells being either dead or in the process of dying (Figure 29A). These drug-treated cells were used to determine the gating regions between the healthy and unhealthy populations of cells.

In order to analyze and compare the GS cDKO cells by flow cytometry at different time points after Tet withdraw, three growth curves were staggered by 24 hour intervals, allowing up to three different time points to be analyzed together on the same day by flow cytometry. The growth curves obtained were identical with growth arrest occurring 3 days after Tet withdraw (Figure 30). As the *Tb*GS cDKO cells progressed into growth arrest (days 3 – 6 after Tet withdraw), a new population of cells was observed on the FSC v. SSC plot (quadrant marked as unhealthy). This new population fell within the same region as control drug-treated unhealthy parasite cells treated with eflornithine that stained positive for ethidium. When the two populations were analyzed for ethidium and calcein staining (gated populations) the unhealthy population

showed a mixture of cells that were either ethidum positive alone (dead) or stained positive for both ethidium and calcein, suggesting cells with damaged membranes that still contained esterase activity (Figure 29C). The percentages of ethidium or dual ethidium/calcein cells increased on day 3 and peaked on days 4 and 5 after Tet withdraw, again correlating the when trypanothione levels were at their lowest. On days 4 and 5, approximately 75% of the cells were in the dead or dying population (Figure 23D). These data confirm that that *Tb*GS protein is essential for parasite survival. However, while a majority of the population was experiencing cell death, 25% of the cells remained healthy (calcein positive alone and cell shape and size not distorted) by this analysis (Figure 29B), and the data suggest that this healthy population grew out and took over the culture by day 8 and possibly never lost expression of *Tb*GS to greater than 97% of control cells.

Tet withdrawal from the GS cDKO cells results in at least two cell populations, one that is dead/dying and the other that is healthy. Since cells did not obtain heritable genetic mutations to escape tet-regulation, these data suggest that expression of *Tb*GS varies between cells. Parasites that remain healthy and proliferative may have slightly less regulation and thereby low levels of expression of *Tb*GS resulting in escape from cell death. During flow cytometry, it was not possible to collect different populations of gated cells to confirm this by western analysis.

D. Conclusions

The trypanothione and polyamine biosynthetic enzymes constitute a fundamental pathway for the proliferation of the *T. brucei* [107]. Genetic methods have been used to show that loss of any of the pathway proteins results in growth arrest that proceeds to cell death. Furthermore, inhibitors of this pathway have anti-trypanosidal effects, the more notable being the ODC suicide inhibitor, DFMO, in its current use for treatment of late stage *T. brucei gambiense.* The polyamine and glutathione pathways are highly regulated in eukaryotic cells; however, the regulatory mechanisms that have been observed in other eukaryotes do not seem to be present in *T. brucei*. Instead, polyamine biosynthesis is uniquely regulated by prozyme, the novel regulatory subunit of AdoMetDC responsible for activating the enzyme and appears to be translationally regulated [103, 170, 184]. Less is known about how the trypanothione biosynthetic pathway is regulated. By investigating the *Tb*GS enzyme, it was discovered that the protein was not only essential for proliferation, but also loss of the protein instigated compensatory effects on the expression levels of both the polyamine and trypanothione biosynthetic enzymes.

To elucidate the role of *Tb*GS, a *Tb*GS cDKO was generated in bloodstream form parasites by knocking out both alleles after insertion of a Tet regulated copy of the gene. Generation of this cell line was dependent on the epitope tag being placed on the C-terminus of the protein rather than the N-

terminus, which results in an enzyme with significantly reduced kinetic activity. Upon loss of expression of *Tb*GS by withdrawal of Tet, parasites entered growth arrest coinciding with loss of greater than 97% of *Tb*GS protein and depletion of trypanothione pools. These data indicate that *Tb*GS, similar to the other pathway enzymes, is essential for parasite proliferation and further underscores the importance of trypanothione as a cofactor in the cell. Furthermore, *Tb*GS cDKO cells exhibit an increase in sensitivity to the γ-GCS inhibitor BSO; however, *Tb*GS cDKO did not have increased sensitivity to exogenously added H_2O_2. This discrepancy could be due to an up-regulation of other redox protective proteins such as Trx, Grx, Prx, or Px, which mediate stress by H_2O_2 but could not alleviate the additional stress caused by BSO, though this hypothesis remains untested.

Loss of *Tb*GS led to an initial stalling of growth but eventually parasites were able to escape the selective pressure leading to re-expression of *Tb*GS and restoration of growth, as was also observed in knockouts of TR [111]. This phenotype has been previously observed in *T. brucei* for other genes and is indicative of an essential gene [172]. Flow cytometry analysis of the parasite population after loss of *Tb*GS expression resulted in two distinct populations. One population included 75% of the parasites, which appeared to be either dead or in the process of dying, and a second population that contained the other 25% that still appeared healthy. Taken together with the data showing that parasites that were resistant to cell death did not appear to contain any genomic mutations,

these data suggest the levels of *Tb*GS expression may vary between the populations. In this situation, it seems small variations in expression levels between cells could lead to the different subpopulations, those with >97% *Tb*GS reduced expression proceed to cell death, and those with less survive and escape the selective pressure. Altogether, these data provide strong evidence for the requirement of TbGS in the proliferation of trypanosomes.

In previous studies, it was demonstrated that the first enzyme in the glutathione biosynthetic pathway, γ-GCS, was essential for parasite growth [92]. In these studies, exogenously added glutathione was able to rescue the cell growth arrest that occurred after γ-GCS knockdown by RNAi. The inability of glutathione to similarly rescue the *Tb*GS double knockout and the growth arrest of the cDKO suggests that unlike in yeast [46, 182], glutathione is not taken up into the parasite intact but rather is imported through a trasnpeptidase mechanism that results in the cleavage of glutathione to cysteinyl-glycine and γ-glutamyl with conjugation of the γ-glutamyl moiety to an amino acid with uptake of both products of the reaction [46, 182]. A glutathione transporter has not been identified in *T. brucei* and no obvious homologs were identified using simple bioinformatics searches; however, our data suggest that *T. brucei* contains this transporter since glutathione is able to rescue the loss of γ-GCS but not GS.

The only known mechanism of regulation within the *T. brucei* polyamine biosynthetic pathway relies on the AdoMetDC subunit, prozyme and to a lesser

extent, ODC. Currently, the regulation of prozyme is considered to respond to dcAdoMet depletion, which upregulates prozyme protein production through a (hypothetically) translationally controlled mechanism [103, 170]. The mechanism of regulation of ODC is currently unknown. Remarkably, loss of *Tb*GS lead to decreases in prozyme and ODC protein and to an increase in γ-GCS protein. Taken together, these data suggest that parasites detect and respond to either glutathione or, more likely, trypanothione depletion using a classic feedback mechanism by increasing levels of the first enzyme required for glutathione synthesis. Spermidine levels remain unaffected after loss of *Tb*GS; therefore the simultaneous decrease in levels of the two key polyamine biosynthetic enzymes appears to be a cell mediated response. This response could be to maintain polyamine intermediate levels since spermidine can no longer be used to make trypanothione. In a previous study, AdoMetDC prozyme protein levels were inversely proportional to dcAdoMet levels, suggesting that dcAdoMet could be a trigger for a regulatory response [170]. Crystallographic studies have shown both spermidine and methylthioadenosine bind SpdSyn [187] Methylthioadenosine is a reaction product of SpdSyn chemistry and has been shown to feedback inhibit SpdSyn from human and *Plasmodium* [185, 186]. Therefore, current hypothesis that accounts for all the data is when spermidine is no longer being used to form trypanothione, it feedback inhibits SpdSyn, resulting in an increase of dcAdoMet

levels, which in turn down regulates prozyme translation. Still, more work would be required to evaluate this working model.

In summary, *Tb*GS is an essential protein for growth of the BSF *T. brucei* and >97% inhibition of the protein is required to lead to cell growth arrest. Loss of *Tb*GS also results in an increased sensitivity to the pathway inhibitor, BSO. Additionally, depletion of *Tb*GS results in regulatory responses of both the thiol and polyamine biosynthetic pathways. Reduction of *Tb*GS leads to an increase in γ-GCS, suggesting that γ-GCS maybe the key regulatory control point for glutathione biosynthesis as is seen in other organisms. Moreover, prozyme and ODC levels decrease, providing additional evidence that control of this pathway is dependent on AdoMetDC activity. Taken together, these data are the first evidence of crosstalk between the polyamine and thiol biosynthetic pathways.

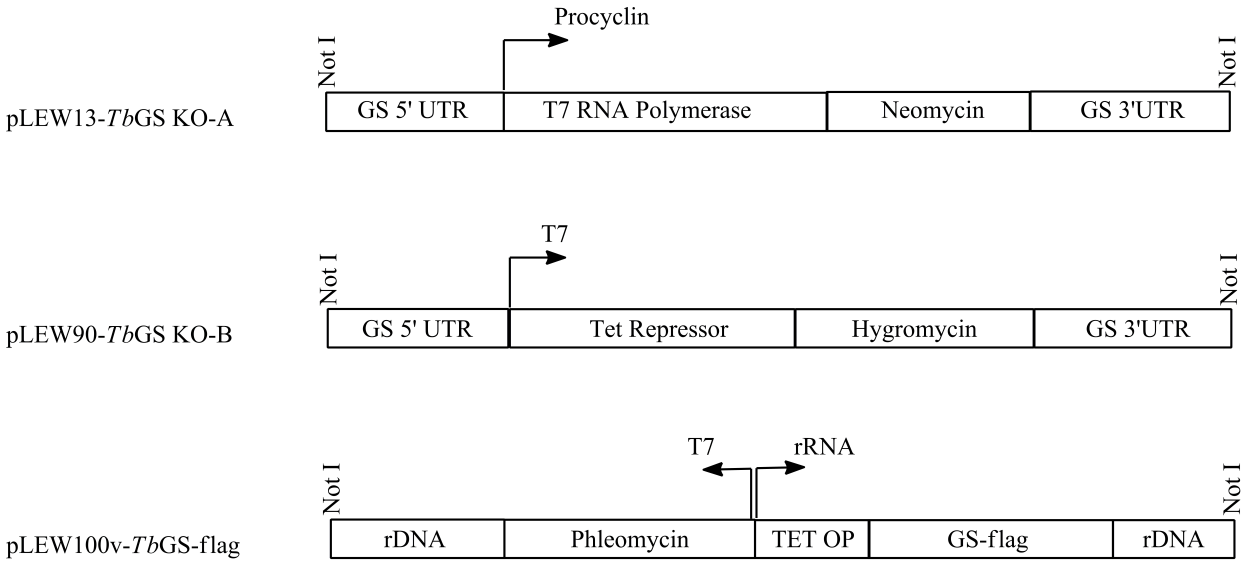

Figure 19. Schematic of *Tb*GS DKO/cDKO Vectors. These constructs were created to genetically manipulate the WT BSF 427 cell line and generate the *Tb*GS DKO and cDKO cell lines

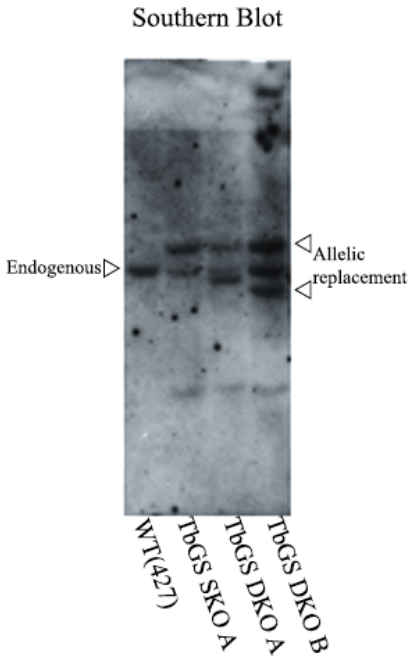

Figure 20. *Tb*GS DKO cell lines result in trisomy. Genomic DNA from *Tb*GS knockout cell lines was analyzed using a probe to a region upstream of the recombination area. Correct DKO would result in an absence of the endogenous band.

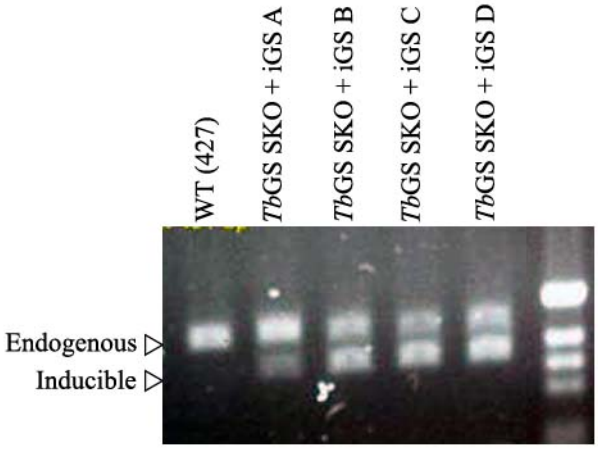

Figure 21. Endogenous and inducible *Tb*GS genes transcribed. cDNA was generated from RNA from WT and *Tb*GS SKO containing the inducible FLAG-GS ectopic construct cell lines. Using a splice leader sequence designed forward primer and a reverse primer located within the *TbGS gene*, cDNA produced the PCR products shown above. The endogenous 5'UTR is 50 bp longer than the inducible 5'UTR, shown by the difference in size.

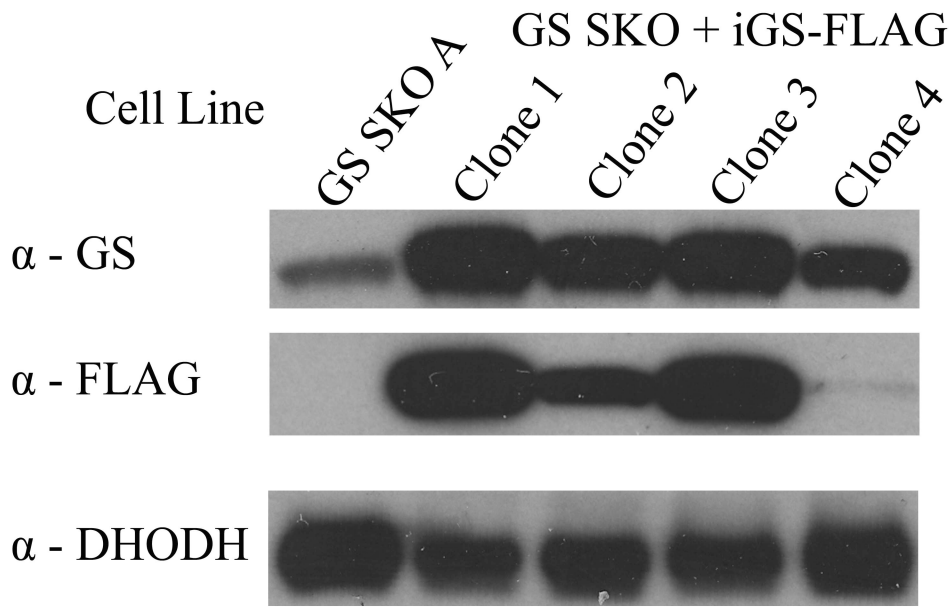

Figure 22 C-terminal FLAG construct protein expression. SKO cell line generated with KO-A construct were transfected with a *Tb*GS-FLAG expression construct targeted to the ribosomal RNA repeat sequences. Clones 1-3 were generated with a phleomycin resistance construct and clone 4 was generated with a blasticidin resistance construct. Clone 1 was used to generate the GS cDKO cell line used in subsequent studies.

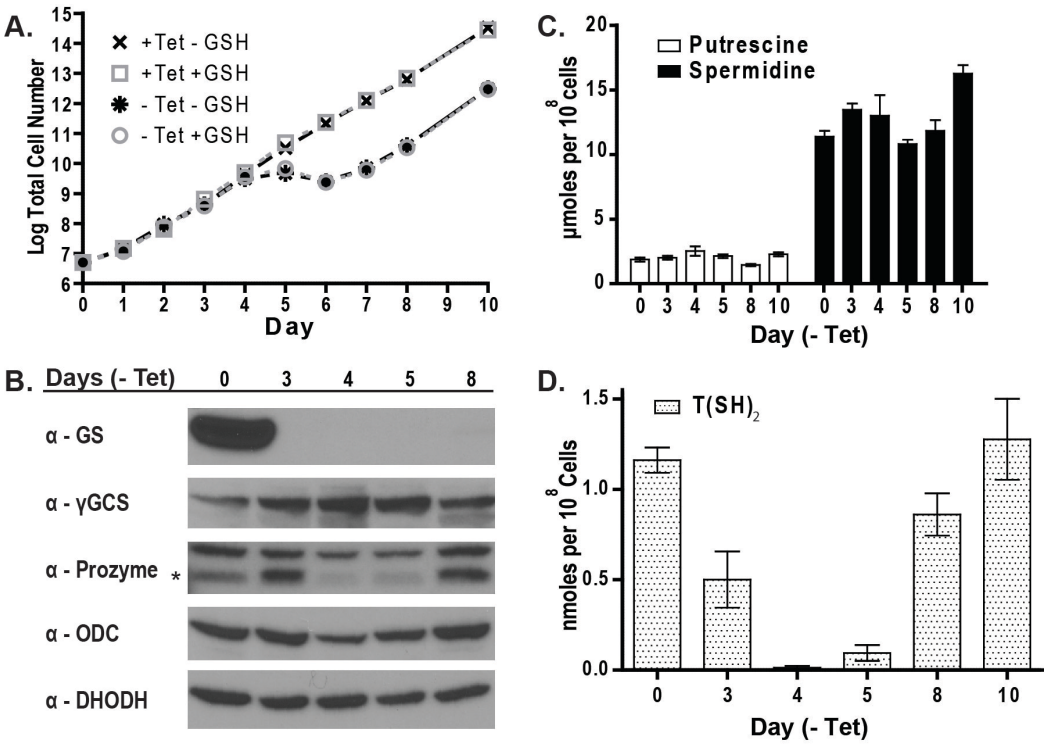

Figure 23. Analysis of *Tb*GS cDKO Cell Line. All results shown are representative of biological triplicate data. **A.** Growth curve of the *Tb*GS cDKO cell line in the presence and absence of Tet. Tet was added daily to maintain expression of the ectopic copy of *Tb*GS protein and cell number is represented as the product of cell density and total dilution. **B.** Western blots of select polyamine and glutathione biosynthetic enzymes. DHODH was used as a loading control. **C.** Intracellular polyamine levels measured by HPLC. **D.** Intracellular reduced trypanothione levels measured by HPLC. When not shown, error bars (SEM) are smaller than their respective symbol.

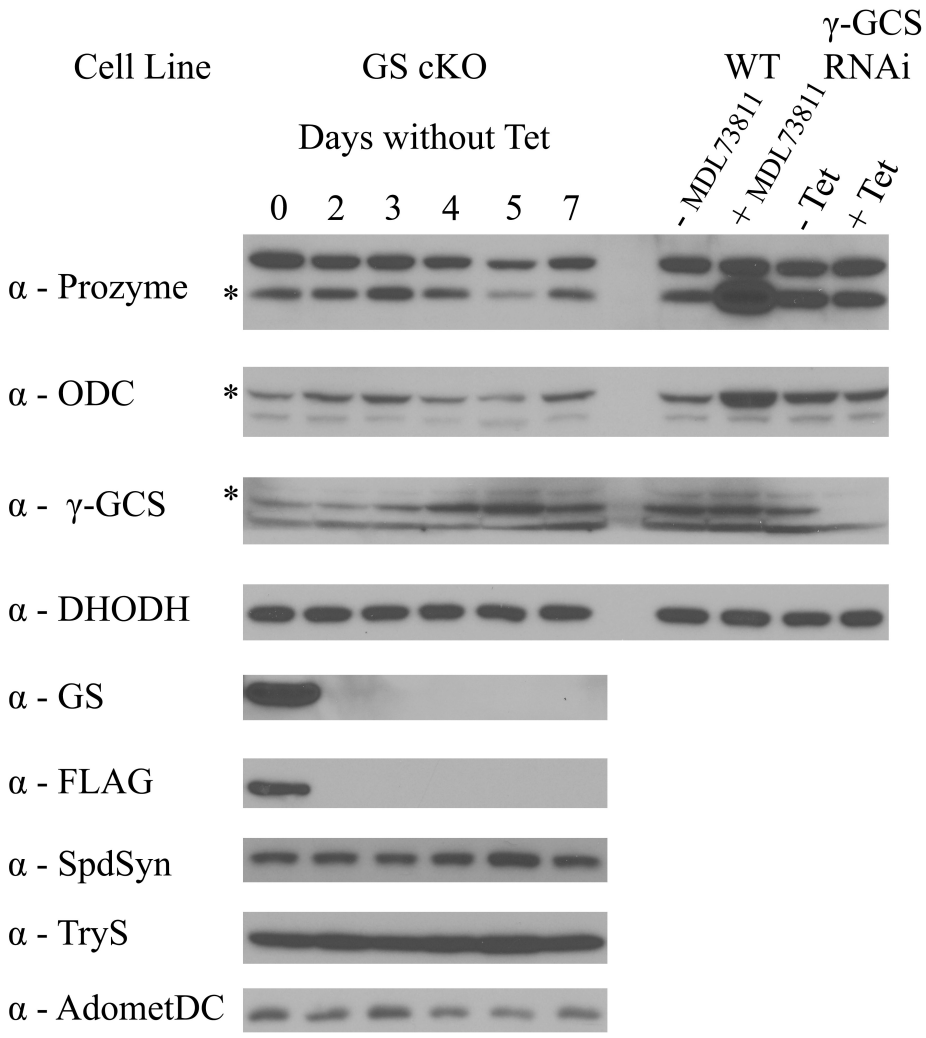

Figure 24. Western blot of Pathway Proteins. Western blot of biosynthetic pathway proteins with controls to prozyme, ODC, and γ-GCS showing variation in protein levels in the mentioned proteins.

	Day	0	2	3	4	5	8
Antibody	GS	1.00	0.04	0.00	0.01	0.01	0.01
		1.00		0.04	0.00	0.00	0.04
		1.00		0.01	0.01	0.01	0.03
	γ-GCS	1.00	0.80	1.96	2.21	3.62	1.55
		1.00		1.34	2.41	2.31	1.37
		1.00		0.86	1.64	2.71	0.48
	ODC	1.00	1.62	1.17	0.70	1.16	1.37
		1.00		1.89	1.11	0.84	1.80
		1.00		1.02	0.89	0.71	0.14
	AdoMetDC Prozyme	1.00	1.05	1.69	0.29	0.50	1.97
		1.00		1.35	1.03	0.40	0.89
		1.00		0.49	1.14	0.75	0.01

Table 4. Relative Changes in Pathway Protein. Westerns from three independent growth curves were analyzed for their changes in protein levels. Changes were seen in γ-GCS, ODC, and AdoMetDC prozyme upon loss of *Tb*GS. These changes were quantified compared to the loading control and are shown here.

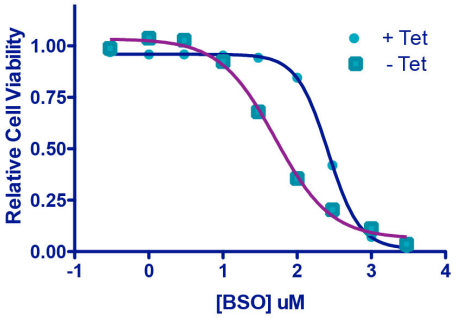

GS cKO	EC_{50} (μM)	95% CI
+ Tet	270	240 - 300
- Tet	88	70 - 130

Figure 25. *Tb*GS cDKO stressed with BSO. Parasites were grown with or without Tet for the number of days indicated followed by incubation with BSO for 72 hours. Cell viability was measured using cell titer glow (Promega), an ATP based luminescence assay. When not shown, error bars (SEM) are smaller than their respective symbol.

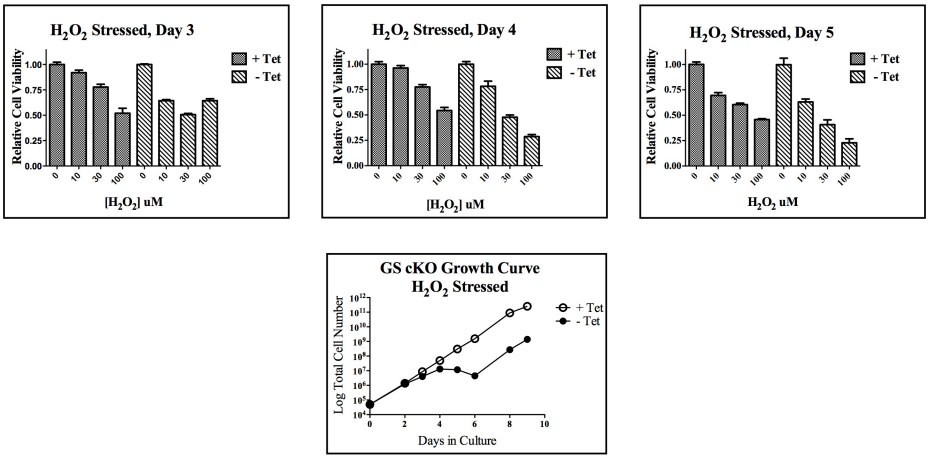

Figure 26. *Tb*GS cDKO stressed with H_2O_2. Parasites were grown in the presence or absence of Tet for the number of days indicated and stressed with H_2O_2 for 24 hours. Cell viability was measured following stress using cell titer glow (Promega). When measuring growth, each line is the average of three flasks grown in the conditions indicated. When not shown, error bars (SEM) are smaller than their respective symbol

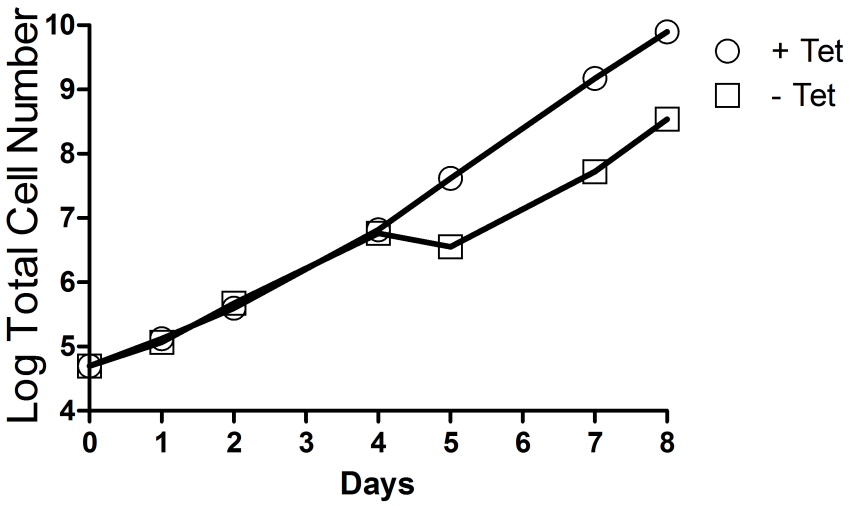

Figure 27. Growth Curve after escape from Tet control. *Tb*GS cKO growth curve after parasites had escaped stagnant growth and were grown for three days in the presence of tet prior to the start of the experiment. During the experiment, tet was added every day and growth was monitored on the days indicated. Growth is plotted as total cell number, which is the product of cell density and total dilution. When not shown, error bars (SEM) are smaller than their respective symbol

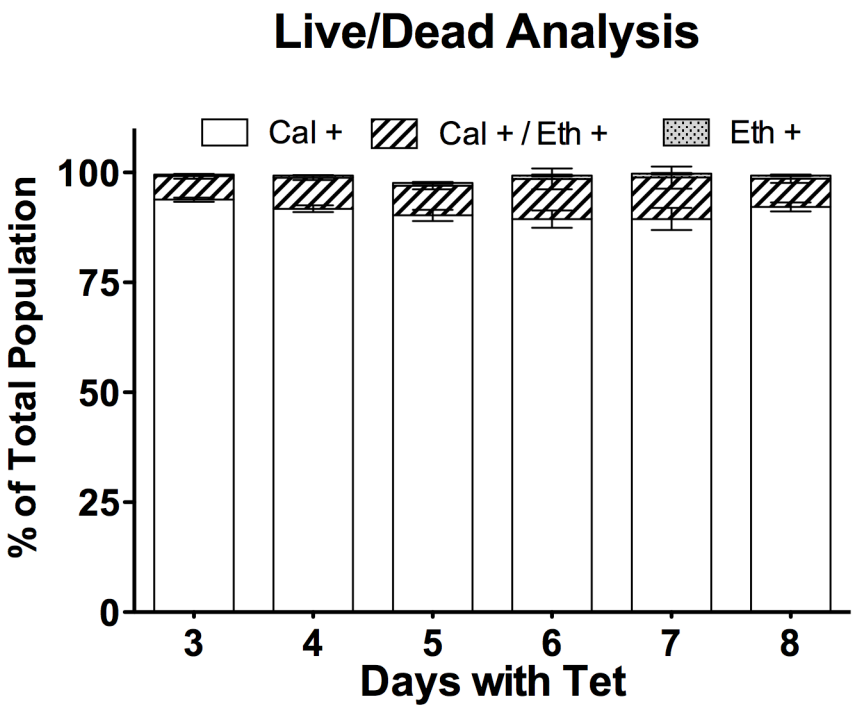

Figure 28. Flow cytometry analysis of Control Cells. Bar Graph representing the percentage of cells that are either calcein positive, ethidium positive or calcein and ethidium double positive in cells grown in the presence of tet and *Tb*GS protein expression. These numbers were obtained from ungated fluorescent populations where unstained cells set quadrants.

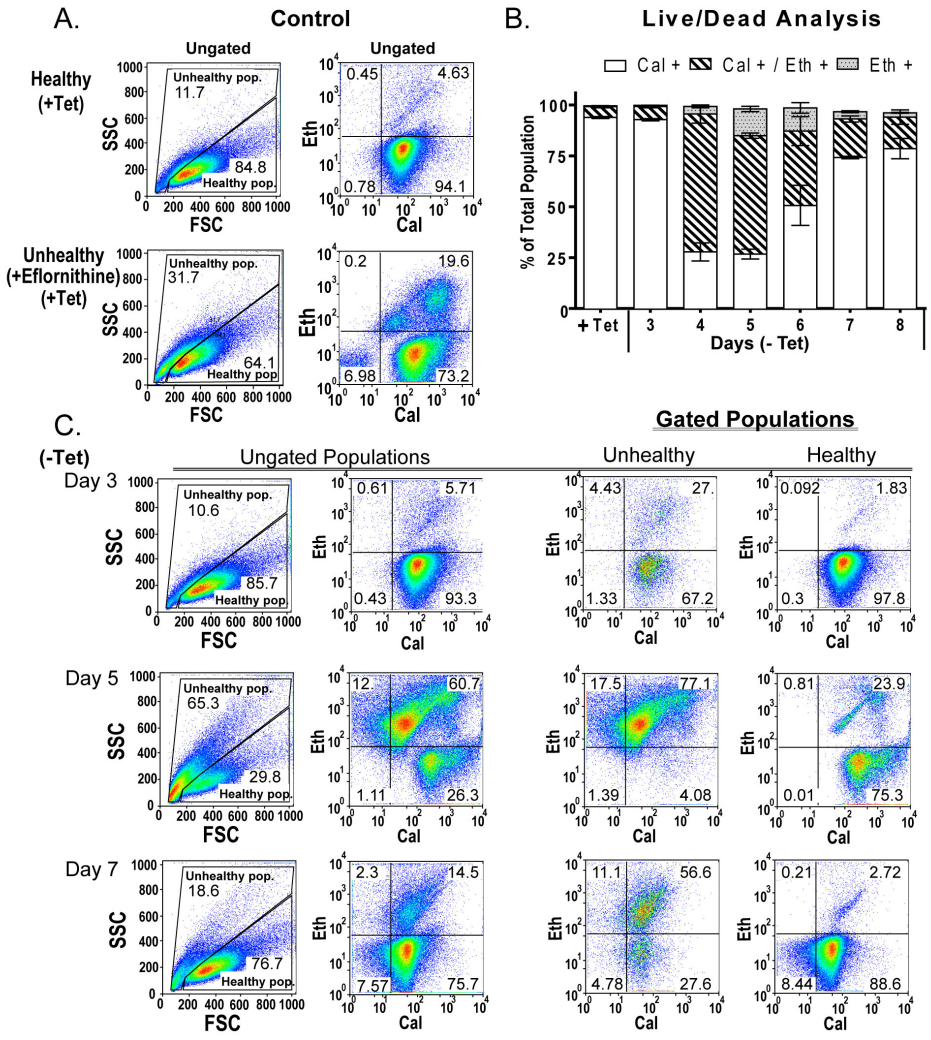

Figure 29. Flow cytometry Analysis of *Tb*GS Cell Line. A. Analysis of Control *Tb*GS cDKO cells (+Tet) parasites ± eflornithine using forward scatter v. side scatter to observe cell shape and morphology and FL1 v. FL3 channels to observe calcein or ethidium positive cells, respectively. **B.** Bar Graph summarizing the effects of *Tb*GS knockdown (-Tet) on the percentage of cells that are either calcein positive, ethidium positive or calcein and ethidium double

positive. Numbers were obtained from ungated fluorescent populations where unstained cells set quadrants. Data represent the average and standard deviation of the mean for n=3 independent experiments **C.** Representative samples of flow cytometry data obtained from *Tb*GS cDKO cells on days 3, 5 and 7 minus Tet. Ungated populations forward v. side scatter plots are shown on the left while the ungated fluorescent populations are shown in left center plots. Within the fluorescent population plots, the upper left quadrant represents cells staining with ethidium only, the lower right quadrant represents cells staining with calcein only, and the upper right quadrant represents cells that stain with both ethidium and calcein. The populations that were gated by their forward versus side scatter plot (gates shown in first plot) are shown in the two right columns. The health/unhealthy gates were determined by healthy proliferating cells and cells that had been treated with drug (eflornithine) for 24 h where the majority of cells were dead (stained with ethidium only).

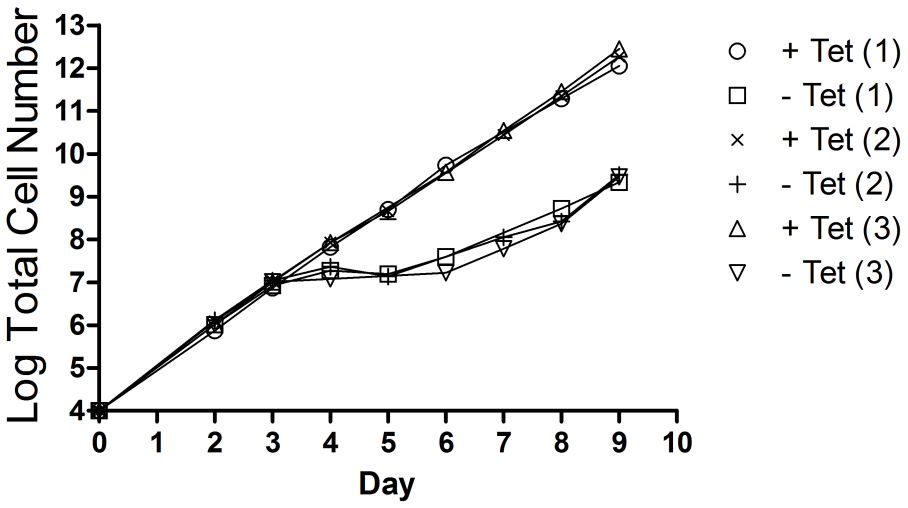

Figure 30. *Tb*GS growth curves obtained during flow cytometry analysis.

Growth is represented as the product of cell density and total dilution. When not shown, error bars (SEM) are smaller than their respective symbol

CHAPTER FIVE

Perspectives

HAT is a debilitating disease that takes its toll not only on the patients, but also has an effect on the agricultural development of the endemic region. Advancements in treatment are necessary to accomplish eradication of this disease and these advancements are dependent on a more complete understanding of the parasite. The work accomplished in this dissertation has lead to more knowledge of the regulation within the parasites polyamine and trypanothione biosynthetic pathway. Furthermore, it has lead to interesting questions that remain to be answered. Each of which is discussed and hypothesized about below.

How is γ-GCS up regulated?

In studying the effects of loss of *Tb*GS, we found levels of γ-GCS increase by 2-3 fold. While being the first known occurrence of regulation in the thiol portion of the trypanothione pathway, it is similar to what occurs in eukaryotic cells that use glutathione rather than trypanothione for redox homeostasis. In

order to understand the regulation seen in trypanosomes, it is important to first understand how regulation occurs in mammalian cells.

In the majority of eukaryotic cells, glutathione is the main line of defense against ROS and is involved in maintenance of the cellular redox state. Studies have gone on to show that the redox state of a cell is closely linked with cell cycle progression and the levels of glutathione are tightly regulated with inadequate levels of glutathione resulting in cell cycle arrest [44, 188-191]. Regulation of glutathione occurs at multiple levels in mammalian cells. Oxidative stress has been shown to increase glutathione production by increasing transcription, increasing transport of glutathione into the cell via by the γ-glutamyltranspeptidase (GGT), and, to a lesser extent, stabilizing mRNA, and the phosphorylation state of γ-GCS [46, 189, 192].

In mammalian cells, the main control point of glutathione synthesis is through regulation of γ-GCS, the initial step of biosynthesis [46, 188]. Mammalian γ-GCS is regulated both through the expression of synthetic protein and by enhancement of its enzymatic activity through interaction with a protein modulator, termed γ-GC modulator (γ-GCM). γ-GCS is feedback inhibited by glutathione and γ-GCM enhances the activity of γ-GCS by reducing the inhibition of glutathione and decreasing the K_m for glutamate [193]. Furthermore, both of these genes are transcriptionally up regulated by the activation of signal transduction pathways by oxidant species and electrophiles. This regulation

occurs through cis elements in the 5'UTR regions of the promoters of both γ-GCS and γ-GCM [194]. The two most well characterized elements in the up regulation of γ-GCS are the AP-1 binding site (also called TRE element) and EpRE (electrophile response element). TRE binds members of the Jun and Fos families of transcription factors while EpRE binds protein members in the Nrf, Jun, or small Maf families [192]. Although these cis elements have been identified, less is known about the signaling pathways that lead to activation of transcription. Additionally, import of glutathione through GGT is increased when cells encounter oxidative stress [195]. This is due to increased levels of GGT through similar signal transduction pathways as γ-GCS and γ-GCM.

While mammalian cells have multiple mechanisms to regulate glutathione levels, *T. brucei* relies on trypanothione rather than glutathione to maintain cellular redox and protect against xenobiotics. Furthermore, *T. brucei* lacks the components of regulation seen in mammalian cells. Transcriptional regulation through signal transduction pathways to transcription factors is lacking in *T. brucei*. Also, a γ-GCM protein has not been identified in the genome to enhance the γ-GCS activity. Therefore, *T. brucei* must regulate its levels of trypanothione through a different mechanism than seen in mammalian cells. Regulation does occur in *T. brucei* since loss of *Tb*GS resulted in an increase of γ-GCS levels in the parasite. Since transcriptional regulation is absent, this regulation is likely to

be done through increasing protein half-life, stabilizing the γ-GCS mRNA, or increasing the translation efficiency.

While this is the first evidence that the thiol portion of the trypanothione biosynthetic pathway is regulated, it is not surprising since trypanothione has a central role in maintaining the reduced state of the redox protective proteins. The mechanism of this regulation poses an interesting question moving forward and are likely different than regulation seen in mammalian cells, possibly leading to new targets for drug design.

How are prozyme and ODC down regulated?

In this study, we discovered that prozyme and ODC levels are responsive to loss of *Tb*GS and subsequently trypanothione. These two enzymes were known to be key regulatory points within the pathway but had responded to trypanothione loss previously [103, 170, 184]. Since the polyamine pathway is the known target of eflornithine, one of the drugs used to treat HAT, it is important to understand the differences in regulation of these pathways between mammalian and trypanosome cells.

Mammalians cells also have high coordinated regulation of the biosynthesis, degradation and efflux of polyamines [196-201]. This occurs both through modulating activity as well as controlling the amount of available enzyme. Of the polyamine biosynthetic enzyme, the ones that are known for their regulating effects are ODC, AdoMetDC and *N*1-spermine/spermidine

acetyltransferase (SSAT, not discussed at length here since *T. brucei* do not use spermine). In mammalian cells, ODC is regulated translationally through mRNA synthesis, mRNA stability, and through protein turnover[200, 202]. ODC has a short protein half-life that undergoes enhanced degradation when bound to the ODC regulatory – antizyme [203]. Antizyme increases protein degradation through an ubiquitin dependent manner when polyamine levels are high. When polyamine levels are low, the protein aptly named antizyme inhibitor is expressed, binding and sequestering antizyme away from ODC, allowing ODC to replenish polyamine pools [203, 204]. AdoMetDC is both transcriptionally and translationally regulated in mammalian cells. The AdoMetDC gene has a small upstream open reading frame that, in conditions of high polyamines, causes the ribosome to stall and results in the decrease of synthesis of polyamines [205-208]. Furthermore, it also has a short protein half-life with degradation occurring through polyubiquitination [107].

Similar to *T. brucei* lacking γ-GCM, it also lacks genes encoding for antizyme protein and antizyme inhibitor protein. Furthermore, both proteins in *T. brucei* have long half-lives[103, 209]. These differences indicate that the regulation of the pathway must occur through a different mechanism than what is seen in mammalian cells. In *T. brucei*, AdoMetDC is regulated by a catalytically dead homolog that originated through a gene duplication event [103, 167]. This protein, termed prozyme, activates AdoMetDC and its expression is induced upon

chemical inhibition or genetic down regulation of AdoMetDC. Prozyme levels are limiting in comparison to AdoMetDC in the parasite, which would allow for induction of prozyme to increase the kinetic activity of AdoMetDC [103]. The induction of prozyme is currently thought to occur through a translation mechanism detecting decarboxylated AdoMet levels, however, this has not been fully elucidated [170]. ODC levels are also induced upon inhibition of AdoMetDC, but the mechanism of this regulation has not been elucidated.

By investigating the role of *Tb*GS in the polyamine biosynthetic pathway, we found that both prozyme and ODC levels were reduced, maintaining these proteins as key regulators of the *T. brucei* polyamine pathway. While both the mammalian and *T. brucei* polyamine pathways use these proteins as regulatory control points in the pathway, they use different methods to accomplish regulation. It was previously shown that perturbing the pathway by inhibition of AdoMetDC resulted in an increase of ODC and prozyme. We show here that the loss of *Tb*GS results in a decrease of ODC and prozyme, hypothetically to stabilize polyamine levels rather than allow the build up of spermidine. The decrease in prozyme protein may occur through a similar mechanism of translational sensing levels of decarboxylated AdoMet; however, it is still possible that the decrease in protein occurs through a different mechanism, such as increased degradation or decreased protein stability. The mechanism of ODC

regulation has not been elucidated but both of these questions pose interesting hypotheses going forward.

Are there kinetic differences between TbGS and other homologous GS enzymes?

The kinetics of the *Tb*GS enzyme was similar to that described for the human, plant and *T. cruzi* GS enzyme with the exception of the apparent K_m for ATP, which was 10 fold higher in *Tb*GS. This difference could simply be due to experimental differences, including different concentrations of Mg^{+2}, γ-GC, and Gly in our assay. However, it is also possible that this difference in ATP occurs in *T. brucei* while not in other organisms. When the *T. brucei* GS enzyme was crystalized, co-crystalization with ATP or ATP analogs did not yield crystals with ATP bound in the active site [162]. Furthermore, ATP coordinating residues were oriented away from the active site in these same studies, which is in conflict of what was seen in the human GS crystal structure. The authors speculated that this difference was due to two insertions surrounding the ATP binding loop. However, in a recent paper investigating the *T. cruzi* GS enzyme, which also contains these insertions surrounding the ATP binding loop, the authors did not see a difference in apparent K_m values for ATP [89]. Therefore, if *T. brucei* does have a difference in the kinetic parameters of ATP, it is unique to this species. To resolve this issue, more kinetic experiments would need to be performed using different concentrations of secondary and tertiary substrates to verify the K_m value obtained.

Does loss of trypanothione instigate transformation from the proliferative (long, slender) stage to the non-proliferative (stumpy) stage?

While observing the parasites during the period of growth arrest seen on days 4-7, I noticed the morphology of a significant number of parasites had changed from the long, slender morphology of the proliferating parasite. While this change in morphology was not investigated at the time, the observed phenotype does postulate a question of if it was simply parasites proceeding to cell death or if it was a transformation to the stumpy stage of the parasite.

The transformation to stumpy from the long, slender form of the parasite is required for transitioning to the next stage of the life cycle in the tsetse fly mid-gut. This transformation is instigated by a parasite-derived factor termed the stumpy induction factor (SIF). SIF remains unidentified but is thought to act through cAMP signaling pathways [30, 31]. Upon activation of these pathways, parasites enter cell cycle arrest, increase mitochondrial activity, lose VSG expression and gain expression of the procyclic extracellular protein coat - procyclin, undergo cytoskeleton remodeling, reposition the kinetoplast, and irreversible commit to the next stage of life [30]. These changes allow the parasite to withstand the environment encountered in the tsetse fly mid-gut.

Currently, there are not markers for the slender to stumpy transition. Parasites are thought to be entering the stumpy form when cell cycle arrest occurs and is coupled enhanced transmission to procyclic form of the parasite when

activated by citrate/*cis*-aconitate measured by the expression of the procyclin [31]. The observation of morphological changes coupled with the growth arrest seen in *Tb*GS cDKO cells warrants the question of if these cells are transforming to the non-proliferative stumpy form. While it is likely that these cells are simply proceeding to cell death and the morphology phenotype is a byproduct, if loss of trypanothione did induce the transformation to the stumpy stage of the life cycle, then it would be a major advancement toward elucidating how the parasite regulate this transition.

In conclusion, *Tb*GS is an essential protein for the growth of *T. brucei* that is involved in the production of trypanothione. These experiments suggests more than 97% of the protein must be eliminated for it to have an effect on cell growth, which could not be accomplished by RNAi. Furthermore, upon loss of *Tb*GS and subsequently trypanothione, cross-regulation was observed between the two biosynthetic pathways, indicated that they work in a coordinated manner. The mechanism for this regulation has yet to be elucidated but has the potential to be a viable area for drug target development since the regulation mechanisms between mammalian and parasite cells differ drastically.

References

1. Organization, W.H. *Human African Trypanosomiasis*. 2012 January 2012 [cited 2012; Fact sheet N'259]. Available from: http://www.who.int/mediacentre/factsheets/fs259/en/index.html.
2. Odiit, M., et al., *Quantifying the level of under-detection of Trypanosoma brucei rhodesiense sleeping sickness cases.* Tropical medicine & international health : TM & IH, 2005. **10**(9): p. 840-9.
3. Simarro, P.P., et al., *The human African trypanosomiasis control and surveillance programme of the World Health Organization 2000-2009: the way forward.* PLoS neglected tropical diseases, 2011. **5**(2): p. e1007.
4. Simpson, A.G., J.R. Stevens, and J. Lukes, *The evolution and diversity of kinetoplastid flagellates.* Trends Parasitol, 2006. **22**(4): p. 168-74.
5. Stevens, J.R. and W.C. Gibson, *The evolution of pathogenic trypanosomes.* Cadernos de saude publica / Ministerio da Saude, Fundacao Oswaldo Cruz, Escola Nacional de Saude Publica, 1999. **15**(4): p. 673-84.
6. Hausler, T., et al., *Conservation of mitochondrial targeting sequence function in mitochondrial and hydrogenosomal proteins from the early-branching eukaryotes Crithidia, Trypanosoma and Trichomonas.* Eur J Cell Biol, 1997. **73**(3): p. 240-51.
7. Hannaert, V., et al., *Evolution of energy metabolism and its compartmentation in Kinetoplastida.* Kinetoplastid Biol Dis, 2003. **2**(1): p. 11.
8. Liu, B., et al., *Fellowship of the rings: the replication of kinetoplast DNA.* Trends Parasitol, 2005. **21**(8): p. 363-9.
9. Jensen, R.E. and P.T. Englund, *Network news: the replication of kinetoplast DNA.* Annu Rev Microbiol, 2012. **66**: p. 473-91.
10. Schnaufer, A., G.J. Domingo, and K. Stuart, *Natural and induced dyskinetoplastic trypanosomatids: how to live without mitochondrial DNA.* International journal for parasitology, 2002. **32**(9): p. 1071-84.
11. Roy Chowdhury, A., et al., *The killing of African trypanosomes by ethidium bromide.* PLoS pathogens, 2010. **6**(12): p. e1001226.
12. Parsons, M., et al., *Trypanosome mRNAs share a common 5' spliced leader sequence.* Cell, 1984. **38**(1): p. 309-16.
13. Bartholomeu, D.C., et al., *Trypanosoma cruzi: RNA structure and post-transcriptional control of tubulin gene expression.* Exp Parasitol, 2002. **102**(3-4): p. 123-33.

14. Clayton, C. and M. Shapira, *Post-transcriptional regulation of gene expression in trypanosomes and leishmanias.* Mol Biochem Parasitol, 2007. **156**(2): p. 93-101.
15. Ouellette, M. and B. Papadopoulou, *Coordinated gene expression by post-transcriptional regulons in African trypanosomes.* J Biol, 2009. **8**(11): p. 100.
16. Gunzl, A., *The pre-mRNA splicing machinery of trypanosomes: complex or simplified?* Eukaryot Cell, 2010. **9**(8): p. 1159-70.
17. Kramer, S. and M. Carrington, *Trans-acting proteins regulating mRNA maturation, stability and translation in trypanosomatids.* Trends Parasitol, 2011. **27**(1): p. 23-30.
18. Kramer, S., *Developmental regulation of gene expression in the absence of transcriptional control: the case of kinetoplastids.* Mol Biochem Parasitol, 2012. **181**(2): p. 61-72.
19. Siegel, T.N., et al., *Gene expression in Trypanosoma brucei: lessons from high-throughput RNA sequencing.* Trends Parasitol, 2011. **27**(10): p. 434-41.
20. Berriman, M., et al., *The genome of the African trypanosome Trypanosoma brucei.* Science, 2005. **309**(5733): p. 416-22.
21. Hutchinson, O.C., et al., *VSG structure: similar N-terminal domains can form functional VSGs with different types of C-terminal domain.* Mol Biochem Parasitol, 2003. **130**(2): p. 127-131.
22. Rudenko, G., *Epigenetics and transcriptional control in African trypanosomes.* Essays in biochemistry, 2010. **48**(1): p. 201-19.
23. Schwede, A., S. Kramer, and M. Carrington, *How do trypanosomes change gene expression in response to the environment?* Protoplasma, 2012. **249**(2): p. 223-38.
24. Turner, C.M.R., *The rate of antigenic variation in fly-transmitted and syringe-passaged infections of Trypanosoma brucei.* FEMS Microbiol Lett, 1997. **153**(1): p. 227-231.
25. Rudenko, G., *African trypanosomes: the genome and adaptations for immune evasion.* Essays in biochemistry, 2011. **51**: p. 47-62.
26. Reuner, B., et al., *Cell density triggers slender to stumpy differentiation of Trypanosoma brucei bloodstream forms in culture.* Mol Biochem Parasitol, 1997. **90**(1): p. 269-80.
27. Vassella, E., et al., *Differentiation of African trypanosomes is controlled by a density sensing mechanism which signals cell cycle arrest via the cAMP pathway.* J Cell Sci, 1997. **110 (Pt 21)**: p. 2661-71.
28. Hill, K.L., *Biology and mechanism of trypanosome cell motility.* Eukaryot Cell, 2003. **2**(2): p. 200-8.

29. Kelly, S., et al., *Genome organization is a major component of gene expression control in response to stress and during the cell division cycle in trypanosomes.* Open Biol, 2012. **2**(4): p. 120033.
30. Matthews, K.R., J.R. Ellis, and A. Paterou, *Molecular regulation of the life cycle of African trypanosomes.* Trends Parasitol, 2004. **20**(1): p. 40-7.
31. MacGregor, P. and K.R. Matthews, *Identification of the regulatory elements controlling the transmission stage-specific gene expression of PAD1 in Trypanosoma brucei.* Nucleic Acids Res, 2012. **40**(16): p. 7705-17.
32. MacGregor, P., et al., *Transmission stages dominate trypanosome within-host dynamics during chronic infections.* Cell Host Microbe, 2011. **9**(4): p. 310-8.
33. Fevre, E.M., et al., *The burden of human African trypanosomiasis.* PLoS neglected tropical diseases, 2008. **2**(12): p. e333.
34. Pays, E., et al., *The trypanolytic factor of human serum.* Nature reviews. Microbiology, 2006. **4**(6): p. 477-86.
35. Vanhollebeke, B. and E. Pays, *The trypanolytic factor of human serum: many ways to enter the parasite, a single way to kill.* Molecular microbiology, 2010. **76**(4): p. 806-14.
36. Priotto, G., et al., *Nifurtimox-eflornithine combination therapy for second-stage African Trypanosoma brucei gambiense trypanosomiasis: a multicentre, randomised, phase III, non-inferiority trial.* Lancet, 2009. **374**(9683): p. 56-64.
37. Mortelmans, J., *Socio-economic problems related to animal trypanosomiasis in Africa.* Soc Sci Med, 1984. **19**(10): p. 1105-7.
38. Kristjanson, P.M., et al., *Measuring the costs of African animal trypanosomosis, the potential benefits of control and returns to research.* Agricultural Systems, 1999. **59**(1): p. 79-98.
39. Torr, S.J., J.W. Hargrove, and G.A. Vale, *Towards a rational policy for dealing with tsetse.* Trends Parasitol, 2005. **21**(11): p. 537-41.
40. Shaw, A.P., *Assessing the economics of animal trypanosomosis in Africa--history and current perspectives.* Onderstepoort J Vet Res, 2009. **76**(1): p. 27-32.
41. Welburn, S.C. and I. Maudlin, *Priorities for the elimination of sleeping sickness.* Adv Parasitol, 2012. **79**: p. 299-337.
42. La Greca, F. and S. Magez, *Vaccination against trypanosomiasis: can it be done or is the trypanosome truly the ultimate immune destroyer and escape artist?* Hum Vaccin, 2011. **7**(11): p. 1225-33.

43. Halliwell, B. and C.E. Cross, *Oxygen-derived species: their relation to human disease and environmental stress.* Environ Health Perspect, 1994. **102 Suppl 10**: p. 5-12.
44. Circu, M.L. and T.Y. Aw, *Reactive oxygen species, cellular redox systems, and apoptosis.* Free Radic Biol Med, 2010. **48**(6): p. 749-62.
45. Meister, A. and S.S. Tate, *Glutathione and related gamma-glutamyl compounds: biosynthesis and utilization.* Annual review of biochemistry, 1976. **45**: p. 559-604.
46. Lu, S.C., *Regulation of glutathione synthesis.* Molecular aspects of medicine, 2009. **30**(1-2): p. 42-59.
47. Circu, M.L. and T.Y. Aw, *Glutathione and apoptosis.* Free Radic Res, 2008. **42**(8): p. 689-706.
48. Meister, A. and M.E. Anderson, *Glutathione.* Annual review of biochemistry, 1983. **52**: p. 711-60.
49. Chakravarthi, S., C.E. Jessop, and N.J. Bulleid, *The role of glutathione in disulphide bond formation and endoplasmic-reticulum-generated oxidative stress.* EMBO reports, 2006. **7**(3): p. 271-5.
50. Jessop, C.E. and N.J. Bulleid, *Glutathione directly reduces an oxidoreductase in the endoplasmic reticulum of mammalian cells.* J Biol Chem, 2004. **279**(53): p. 55341-7.
51. Frand, A.R. and C.A. Kaiser, *Two pairs of conserved cysteines are required for the oxidative activity of Ero1p in protein disulfide bond formation in the endoplasmic reticulum.* Mol Biol Cell, 2000. **11**(9): p. 2833-43.
52. Chen, J., et al., *Enhanced mitochondrial gene transcript, ATP, bcl-2 protein levels, and altered glutathione distribution in ethinyl estradiol-treated cultured female rat hepatocytes.* Toxicol Sci, 2003. **75**(2): p. 271-8.
53. Oktyabrsky, O.N. and G.V. Smirnova, *Redox regulation of cellular functions.* Biochemistry (Moscow), 2007. **72**(2): p. 132-145.
54. Lillig, C.H. and A. Holmgren, *Thioredoxin and related molecules--from biology to health and disease.* Antioxidants & redox signaling, 2007. **9**(1): p. 25-47.
55. Molina-Navarro, M.M., et al., *Prokaryotic and eukaryotic monothiol glutaredoxins are able to perform the functions of Grx5 in the biogenesis of Fe/S clusters in yeast mitochondria.* FEBS letters, 2006. **580**(9): p. 2273-80.
56. Wingert, R.A., et al., *Deficiency of glutaredoxin 5 reveals Fe-S clusters are required for vertebrate haem synthesis.* Nature, 2005. **436**(7053): p. 1035-39.

57. Holmgren, A., *Thioredoxin. 6. The amino acid sequence of the protein from escherichia coli B.* Eur J Biochem, 1968. **6**(4): p. 475-84.
58. Holmgren, A., *Thioredoxin structure and mechanism: conformational changes on oxidation of the active-site sulfhydryls to a disulfide.* Structure, 1995. **3**(3): p. 239-43.
59. Yang, Y., et al., *Reactivity of the human thioltransferase (glutaredoxin) C7S, C25S, C78S, C82S mutant and NMR solution structure of its glutathionyl mixed disulfide intermediate reflect catalytic specificity.* Biochemistry, 1998. **37**(49): p. 17145-56.
60. Holmgren, A., *Glutathione-dependent enzyme reactions of the phage T4 ribonucleotide reductase system.* J Biol Chem, 1978. **253**(20): p. 7424-30.
61. Holmgren, A., *Glutathione-dependent synthesis of deoxyribonucleotides. Purification and characterization of glutaredoxin from Escherichia coli.* J Biol Chem, 1979. **254**(9): p. 3664-71.
62. Holmgren, A., *Glutathione-dependent synthesis of deoxyribonucleotides. Characterization of the enzymatic mechanism of Escherichia coli glutaredoxin.* J Biol Chem, 1979. **254**(9): p. 3672-8.
63. Shelton, M.D., P.B. Chock, and J.J. Mieyal, *Glutaredoxin: role in reversible protein s-glutathionylation and regulation of redox signal transduction and protein translocation.* Antioxidants & redox signaling, 2005. **7**(3-4): p. 348-66.
64. Nakamura, H., K. Nakamura, and J. Yodoi, *Redox regulation of cellular activation.* Annu Rev Immunol, 1997. **15**: p. 351-69.
65. Watson, W.H. and D.P. Jones, *Oxidation of nuclear thioredoxin during oxidative stress.* FEBS letters, 2003. **543**(1-3): p. 144-7.
66. Hansen, J.M., Y.M. Go, and D.P. Jones, *Nuclear and mitochondrial compartmentation of oxidative stress and redox signaling.* Annu Rev Pharmacol Toxicol, 2006. **46**: p. 215-34.
67. Brigelius-Flohe, R., *Glutathione peroxidases and redox-regulated transcription factors.* Biol Chem, 2006. **387**(10-11): p. 1329-35.
68. Rhee, S.G., H.Z. Chae, and K. Kim, *Peroxiredoxins: a historical overview and speculative preview of novel mechanisms and emerging concepts in cell signaling.* Free Radic Biol Med, 2005. **38**(12): p. 1543-52.
69. Wood, Z.A., et al., *Structure, mechanism and regulation of peroxiredoxins.* Trends Biochem Sci, 2003. **28**(1): p. 32-40.
70. Aebi, H., *Catalase in vitro.* Methods Enzymol, 1984. **105**: p. 121-6.
71. Fairlamb, A.H., et al., *Trypanothione: a novel bis(glutathionyl)spermidine cofactor for glutathione reductase in trypanosomatids.* Science, 1985. **227**(4693): p. 1485-7.

72. Fairlamb, A.H. and A. Cerami, *Metabolism and functions of trypanothione in the Kinetoplastida.* Annu Rev Microbiol, 1992. **46**: p. 695-729.
73. Shames, S.L., et al., *Purification and characterization of trypanothione reductase from Crithidia fasciculata, a newly discovered member of the family of disulfide-containing flavoprotein reductases.* Biochemistry, 1986. **25**(12): p. 3519-26.
74. Ariyanayagam, M.R., et al., *Phenotypic analysis of trypanothione synthetase knockdown in the African trypanosome.* Biochem J, 2005. **391**(Pt 2): p. 425-32.
75. Dormeyer, M., et al., *Trypanothione-dependent synthesis of deoxyribonucleotides by Trypanosoma brucei ribonucleotide reductase.* J Biol Chem, 2001. **276**(14): p. 10602-6.
76. Nogoceke, E., et al., *A unique cascade of oxidoreductases catalyses trypanothione-mediated peroxide metabolism in Crithidia fasciculata.* Biol Chem, 1997. **378**(8): p. 827-36.
77. Hillebrand, H., A. Schmidt, and R.L. Krauth-Siegel, *A second class of peroxidases linked to the trypanothione metabolism.* J Biol Chem, 2003. **278**(9): p. 6809-15.
78. El-Sayed, N.M., et al., *The genome sequence of Trypanosoma cruzi, etiologic agent of Chagas disease.* Science, 2005. **309**(5733): p. 409-15.
79. Ivens, A.C., et al., *The genome of the kinetoplastid parasite, Leishmania major.* Science, 2005. **309**(5733): p. 436-42.
80. Krauth-Siegel, R.L. and M.A. Comini, *Redox control in trypanosomatids, parasitic protozoa with trypanothione-based thiol metabolism.* Biochimica et biophysica acta, 2008. **1780**(11): p. 1236-48.
81. Bacchi, C.J., et al., *Polyamine metabolism: a potential therapeutic target in trypanosomes.* Science, 1980. **210**(4467): p. 332-4.
82. Pepin, J., et al., *Difluoromethylornithine for arseno-resistant Trypanosoma brucei gambiense sleeping sickness.* Lancet, 1987. **2**(8573): p. 1431-3.
83. Weldrick, D.P., et al., *The effect of buthionine sulfoximine on the growth of Leishmania donovani in culture.* FEMS Microbiol Lett, 1999. **173**(1): p. 139-46.
84. Kapoor, P., M. Sachdev, and R. Madhubala, *Inhibition of glutathione synthesis as a chemotherapeutic strategy for leishmaniasis.* Tropical medicine & international health : TM & IH, 2000. **5**(6): p. 438-42.
85. Faundez, M., et al., *Buthionine sulfoximine increases the toxicity of nifurtimox and benznidazole to Trypanosoma cruzi.* Antimicrob Agents Chemother, 2005. **49**(1): p. 126-30.

86. Torrie, L.S., et al., *Chemical validation of trypanothione synthetase: a potential drug target for human trypanosomiasis.* J Biol Chem, 2009. **284**(52): p. 36137-45.
87. Wyllie, S., et al., *Dissecting the essentiality of the bifunctional trypanothione synthetase-amidase in Trypanosoma brucei using chemical and genetic methods.* Molecular microbiology, 2009. **74**(3): p. 529-40.
88. Olin-Sandoval, V., R. Moreno-Sanchez, and E. Saavedra, *Targeting trypanothione metabolism in trypanosomatid human parasites.* Curr Drug Targets, 2010. **11**(12): p. 1614-30.
89. Olin-Sandoval, V., et al., *Drug target validation of the trypanothione pathway enzymes through metabolic modelling.* The FEBS journal, 2012. **279**(10): p. 1811-33.
90. Lueder, D.V. and M.A. Phillips, *Characterization of Trypanosoma brucei gamma-glutamylcysteine synthetase, an essential enzyme in the biosynthesis of trypanothione (diglutathionylspermidine).* J Biol Chem, 1996. **271**(29): p. 17485-90.
91. Brekken, D.L. and M.A. Phillips, *Trypanosoma brucei gamma-glutamylcysteine synthetase. Characterization of the kinetic mechanism and the role of Cys-319 in cystamine inactivation.* J Biol Chem, 1998. **273**(41): p. 26317-22.
92. Huynh, T.T., et al., *Gene knockdown of gamma-glutamylcysteine synthetase by RNAi in the parasitic protozoa Trypanosoma brucei demonstrates that it is an essential enzyme.* J Biol Chem, 2003. **278**(41): p. 39794-800.
93. Fyfe, P.K., et al., *Leishmania trypanothione synthetase-amidase structure reveals a basis for regulation of conflicting synthetic and hydrolytic activities.* J Biol Chem, 2008. **283**(25): p. 17672-80.
94. Smith, K., et al., *Purification of glutathionylspermidine and trypanothione synthetases from Crithidia fasciculata.* Protein Sci, 1992. **1**(7): p. 874-83.
95. Oza, S.L., et al., *A single enzyme catalyses formation of Trypanothione from glutathione and spermidine in Trypanosoma cruzi.* J Biol Chem, 2002. **277**(39): p. 35853-61.
96. Comini, M., et al., *Trypanothione synthesis in crithidia revisited.* J Biol Chem, 2005. **280**(8): p. 6850-60.
97. Oza, S.L., et al., *Properties of trypanothione synthetase from Trypanosoma brucei.* Mol Biochem Parasitol, 2003. **131**(1): p. 25-33.
98. Oza, S.L., et al., *Trypanothione biosynthesis in Leishmania major.* Mol Biochem Parasitol, 2005. **139**(1): p. 107-16.

99. Oza, S.L., M.R. Ariyanayagam, and A.H. Fairlamb, *Characterization of recombinant glutathionylspermidine synthetase/amidase from Crithidia fasciculata.* Biochem J, 2002. **364**(Pt 3): p. 679-86.
100. Koenig, K., et al., *Convenient isolation and kinetic mechanism of glutathionylspermidine synthetase from Crithidia fasciculata.* J Biol Chem, 1997. **272**(18): p. 11908-15.
101. Amssoms, K., et al., *Glutathione-like tripeptides as inhibitors of glutathionylspermidine synthetase. Part 1: Substitution of the glycine carboxylic acid group.* Bioorg Med Chem Lett, 2002. **12**(18): p. 2553-6.
102. Xiao, Y., D.E. McCloskey, and M.A. Phillips, *RNA interference-mediated silencing of ornithine decarboxylase and spermidine synthase genes in Trypanosoma brucei provides insight into regulation of polyamine biosynthesis.* Eukaryot Cell, 2009. **8**(5): p. 747-55.
103. Willert, E.K. and M.A. Phillips, *Regulated expression of an essential allosteric activator of polyamine biosynthesis in African trypanosomes.* PLoS pathogens, 2008. **4**(10): p. e1000183.
104. Taylor, M.C., et al., *Validation of spermidine synthase as a drug target in African trypanosomes.* Biochem J, 2008. **409**(2): p. 563-9.
105. Arrick, B.A., O.W. Griffith, and A. Cerami, *Inhibition of glutathione synthesis as a chemotherapeutic strategy for trypanosomiasis.* J Exp Med, 1981. **153**(3): p. 720-5.
106. Bacchi, C.J., et al., *In vivo effects of alpha-DL-difluoromethylornithine on the metabolism and morphology of Trypanosoma brucei brucei.* Mol Biochem Parasitol, 1983. **7**(3): p. 209-25.
107. Willert, E. and M.A. Phillips, *Regulation and function of polyamines in African trypanosomes.* Trends Parasitol, 2012. **28**(2): p. 66-72.
108. Frearson, J.A., et al., *Target assessment for antiparasitic drug discovery.* Trends Parasitol, 2007. **23**(12): p. 589-95.
109. Dumas, C., et al., *Disruption of the trypanothione reductase gene of Leishmania decreases its ability to survive oxidative stress in macrophages.* EMBO J, 1997. **16**(10): p. 2590-8.
110. Tovar, J., et al., *Down-regulation of Leishmania donovani trypanothione reductase by heterologous expression of a trans-dominant mutant homologue: effect on parasite intracellular survival.* Proceedings of the National Academy of Sciences of the United States of America, 1998. **95**(9): p. 5311-6.
111. Krieger, S., et al., *Trypanosomes lacking trypanothione reductase are avirulent and show increased sensitivity to oxidative stress.* Molecular microbiology, 2000. **35**(3): p. 542-52.

112. Henderson, G.B., et al., *Substrate specificity of the flavoprotein trypanothione disulfide reductase from Crithidia fasciculata.* Biochemistry, 1987. **26**(11): p. 3023-7.
113. Shames, S.L., et al., *Trypanothione reductase of Trypanosoma congolense: gene isolation, primary sequence determination, and comparison to glutathione reductase.* Biochemistry, 1988. **27**(14): p. 5014-9.
114. Kuriyan, J., et al., *X-ray structure of trypanothione reductase from Crithidia fasciculata at 2.4-A resolution.* Proceedings of the National Academy of Sciences of the United States of America, 1991. **88**(19): p. 8764-8.
115. Hunter, W.N., et al., *Active site of trypanothione reductase. A target for rational drug design.* J Mol Biol, 1992. **227**(1): p. 322-33.
116. Bailey, S., et al., *Substrate interactions between trypanothione reductase and N1-glutathionylspermidine disulphide at 0.28-nm resolution.* Eur J Biochem, 1993. **213**(1): p. 67-75.
117. Zhang, Y., et al., *Trypanosoma cruzi trypanothione reductase. Crystallization, unit cell dimensions and structure solution.* J Mol Biol, 1993. **232**(4): p. 1217-20.
118. Lantwin, C.B., et al., *The structure of Trypanosoma cruzi trypanothione reductase in the oxidized and NADPH reduced state.* Proteins, 1994. **18**(2): p. 161-73.
119. Bond, C.S., et al., *Crystal structure of Trypanosoma cruzi trypanothione reductase in complex with trypanothione, and the structure-based discovery of new natural product inhibitors.* Structure, 1999. **7**(1): p. 81-9.
120. Henderson, G.B., et al., *Engineering the substrate specificity of glutathione reductase toward that of trypanothione reduction.* Proceedings of the National Academy of Sciences of the United States of America, 1991. **88**(19): p. 8769-73.
121. el-Waer, A., et al., *Synthesis of N-benzyloxycarbonyl-L-cysteinylglycine 3-dimethylaminopropylamide disulfide: a cheap and convenient new assay for trypanothione reductase.* Anal Biochem, 1991. **198**(1): p. 212-6.
122. Benson, T.J., et al., *Rationally designed selective inhibitors of trypanothione reductase. Phenothiazines and related tricyclics as lead structures.* Biochem J, 1992. **286 (Pt 1)**: p. 9-11.
123. Chan, C., et al., *Phenothiazine inhibitors of trypanothione reductase as potential antitrypanosomal and antileishmanial drugs.* J Med Chem, 1998. **41**(2): p. 148-56.

124. Spinks, D., et al., *Investigation of trypanothione reductase as a drug target in Trypanosoma brucei.* ChemMedChem, 2009. **4**(12): p. 2060-9.
125. Ludemann, H., et al., *Trypanosoma brucei tryparedoxin, a thioredoxin-like protein in African trypanosomes.* FEBS letters, 1998. **431**(3): p. 381-5.
126. Montemartini, M., et al., *Sequence, heterologous expression and functional characterization of a novel tryparedoxin from Crithidia fasciculata.* Biol Chem, 1998. **379**(8-9): p. 1137-42.
127. Montemartini, M., et al., *Sequence analysis of the tryparedoxin peroxidase gene from Crithidia fasciculata and its functional expression in Escherichia coli.* J Biol Chem, 1998. **273**(9): p. 4864-71.
128. Gommel, D.U., et al., *Catalytic characteristics of tryparedoxin.* Eur J Biochem, 1997. **248**(3): p. 913-8.
129. Schmidt, H. and R.L. Krauth-Siegel, *Functional and physicochemical characterization of the thioredoxin system in Trypanosoma brucei.* J Biol Chem, 2003. **278**(47): p. 46329-36.
130. Alphey, M.S., et al., *The high resolution crystal structure of recombinant Crithidia fasciculata tryparedoxin-I.* J Biol Chem, 1999. **274**(36): p. 25613-22.
131. Hofmann, B., et al., *Structures of tryparedoxins revealing interaction with trypanothione.* Biol Chem, 2001. **382**(3): p. 459-71.
132. Melchers, J., et al., *Glutathionylation of trypanosomal thiol redox proteins.* J Biol Chem, 2007. **282**(12): p. 8678-94.
133. Comini, M.A., R.L. Krauth-Siegel, and L. Flohe, *Depletion of the thioredoxin homologue tryparedoxin impairs antioxidative defence in African trypanosomes.* Biochem J, 2007. **402**(1): p. 43-9.
134. Reckenfelderbaumer, N. and R.L. Krauth-Siegel, *Catalytic properties, thiol pK value, and redox potential of Trypanosoma brucei tryparedoxin.* J Biol Chem, 2002. **277**(20): p. 17548-55.
135. Tetaud, E., et al., *Molecular characterisation of mitochondrial and cytosolic trypanothione-dependent tryparedoxin peroxidases in Trypanosoma brucei.* Mol Biochem Parasitol, 2001. **116**(2): p. 171-83.
136. Castro, H., et al., *Two linked genes of Leishmania infantum encode tryparedoxins localised to cytosol and mitochondrion.* Mol Biochem Parasitol, 2004. **136**(2): p. 137-47.
137. Motyka, S.A., et al., *Overexpression of a cytochrome b5 reductase-like protein causes kinetoplast DNA loss in Trypanosoma brucei.* J Biol Chem, 2006. **281**(27): p. 18499-506.

138. Romao, S., et al., *The cytosolic tryparedoxin of Leishmania infantum is essential for parasite survival.* International journal for parasitology, 2009. **39**(6): p. 703-11.
139. Hsu, J.Y., et al., *Divergence of trypanothione-dependent tryparedoxin cascade into cytosolic and mitochondrial pathways in arsenite-resistant variants of Leishmania amazonensis.* Mol Biochem Parasitol, 2008. **157**(2): p. 193-204.
140. Wilkinson, S.R., et al., *RNA interference identifies two hydroperoxide metabolizing enzymes that are essential to the bloodstream form of the african trypanosome.* J Biol Chem, 2003. **278**(34): p. 31640-6.
141. Castro, H., et al., *Mitochondrial redox metabolism in trypanosomatids is independent of tryparedoxin activity.* PLoS One, 2010. **5**(9): p. e12607.
142. Reckenfelderbaumer, N., et al., *Identification and functional characterization of thioredoxin from Trypanosoma brucei brucei.* J Biol Chem, 2000. **275**(11): p. 7547-52.
143. Schmidt, A., C.E. Clayton, and R.L. Krauth-Siegel, *Silencing of the thioredoxin gene in Trypanosoma brucei brucei.* Mol Biochem Parasitol, 2002. **125**(1-2): p. 207-10.
144. Ceylan, S., et al., *The dithiol glutaredoxins of african trypanosomes have distinct roles and are closely linked to the unique trypanothione metabolism.* J Biol Chem, 2010. **285**(45): p. 35224-37.
145. Comini, M.A., et al., *Monothiol glutaredoxin-1 is an essential iron-sulfur protein in the mitochondrion of African trypanosomes.* J Biol Chem, 2008. **283**(41): p. 27785-98.
146. Filser, M., et al., *Cloning, functional analysis, and mitochondrial localization of Trypanosoma brucei monothiol glutaredoxin-1.* Biol Chem, 2008. **389**(1): p. 21-32.
147. Lopez, J.A., et al., *Evidence for a trypanothione-dependent peroxidase system in Trypanosoma cruzi.* Free Radic Biol Med, 2000. **28**(5): p. 767-72.
148. Wilkinson, S.R., et al., *Distinct mitochondrial and cytosolic enzymes mediate trypanothione-dependent peroxide metabolism in Trypanosoma cruzi.* J Biol Chem, 2000. **275**(11): p. 8220-5.
149. Piacenza, L., et al., *Peroxiredoxins play a major role in protecting Trypanosoma cruzi against macrophage- and endogenously-derived peroxynitrite.* Biochem J, 2008. **410**(2): p. 359-68.
150. Schlecker, T., et al., *Substrate specificity, localization, and essential role of the glutathione peroxidase-type tryparedoxin peroxidases in Trypanosoma brucei.* J Biol Chem, 2005. **280**(15): p. 14385-94.

151. Fueller, F., et al., *High throughput screening against the peroxidase cascade of African trypanosomes identifies antiparasitic compounds that inactivate tryparedoxin.* J Biol Chem, 2012. **287**(12): p. 8792-802.
152. Ullu, E., C. Tschudi, and T. Chakraborty, *RNA interference in protozoan parasites.* Cell Microbiol, 2004. **6**(6): p. 509-19.
153. Hirumi, H. and K. Hirumi, *Continuous cultivation of Trypanosoma brucei blood stream forms in a medium containing a low concentration of serum protein without feeder cell layers.* The Journal of parasitology, 1989. **75**(6): p. 985-9.
154. Wang, Z., et al., *Inhibition of Trypanosoma brucei gene expression by RNA interference using an integratable vector with opposing T7 promoters.* J Biol Chem, 2000. **275**(51): p. 40174-9.
155. Shapiro, A.L., E. Vinuela, and J.V. Maizel, Jr., *Molecular weight estimation of polypeptide chains by electrophoresis in SDS-polyacrylamide gels.* Biochemical and biophysical research communications, 1967. **28**(5): p. 815-20.
156. Fairlamb, A.H., et al., *In vivo effects of difluoromethylornithine on trypanothione and polyamine levels in bloodstream forms of Trypanosoma brucei.* Molecular and biochemical parasitology, 1987. **24**(2): p. 185-91.
157. Luo, J.L., et al., *Novel kinetics of mammalian glutathione synthetase: characterization of gamma-glutamyl substrate cooperative binding.* Biochemical and biophysical research communications, 2000. **275**(2): p. 577-81.
158. Dinescu, A., et al., *Function of conserved residues of human glutathione synthetase: implications for the ATP-grasp enzymes.* J Biol Chem, 2004. **279**(21): p. 22412-21.
159. Dinescu, A., M.E. Anderson, and T.R. Cundari, *Catalytic loop motion in human glutathione synthetase: A molecular modeling approach.* Biochemical and biophysical research communications, 2007. **353**(2): p. 450-6.
160. Herrera, K., et al., *Reaction mechanism of glutathione synthetase from Arabidopsis thaliana: site-directed mutagenesis of active site residues.* J Biol Chem, 2007. **282**(23): p. 17157-65.
161. Dinescu, A., et al., *The role of the glycine triad in human glutathione synthetase.* Biochemical and biophysical research communications, 2010. **400**(4): p. 511-6.
162. Fyfe, P.K., M.S. Alphey, and W.N. Hunter, *Structure of Trypanosoma brucei glutathione synthetase: domain and loop alterations in the*

catalytic cycle of a highly conserved enzyme. Mol Biochem Parasitol, 2010. **170**(2): p. 93-9.
163. Henderson, G.B., et al., *Biosynthesis of the trypanosomatid metabolite trypanothione: purification and characterization of trypanothione synthetase from Crithidia fasciculata.* Biochemistry, 1990. **29**(16): p. 3924-9.
164. Kornberg, A. and W.E. Pricer, Jr., *Enzymatic phosphorylation of adenosine and 2,6-diaminopurine riboside.* J Biol Chem, 1951. **193**(2): p. 481-95.
165. Jez, J.M. and R.E. Cahoon, *Kinetic mechanism of glutathione synthetase from Arabidopsis thaliana.* J Biol Chem, 2004. **279**(41): p. 42726-31.
166. Osterman, A.L., et al., *Lysine-69 plays a key role in catalysis by ornithine decarboxylase through acceleration of the Schiff base formation, decarboxylation, and product release steps.* Biochemistry, 1999. **38**(36): p. 11814-26.
167. Willert, E.K., R. Fitzpatrick, and M.A. Phillips, *Allosteric regulation of an essential trypanosome polyamine biosynthetic enzyme by a catalytically dead homolog.* Proceedings of the National Academy of Sciences of the United States of America, 2007. **104**(20): p. 8275-80.
168. Marblestone, J.G., et al., *Comparison of SUMO fusion technology with traditional gene fusion systems: enhanced expression and solubility with SUMO.* Protein Sci, 2006. **15**(1): p. 182-9.
169. Butt, T.R., et al., *SUMO fusion technology for difficult-to-express proteins.* Protein Expr Purif, 2005. **43**(1): p. 1-9.
170. Xiao, Y., et al., *Product feedback regulation implicated in translational control of the Trypanosoma brucei S-adenosylmethionine decarboxylase regulatory subunit prozyme.* Molecular microbiology, 2013. **88**(5): p. 846-61.
171. Kuettel, S., et al., *The de novo and salvage pathways of GDP-mannose biosynthesis are both sufficient for the growth of bloodstream-form Trypanosoma brucei.* Molecular microbiology, 2012. **84**(2): p. 340-51.
172. Roper, J.R., et al., *Galactose metabolism is essential for the African sleeping sickness parasite Trypanosoma brucei.* Proceedings of the National Academy of Sciences of the United States of America, 2002. **99**(9): p. 5884-9.
173. Estevez, A.M., et al., *Knockout of the glutamate dehydrogenase gene in bloodstream Trypanosoma brucei in culture has no effect on editing of mitochondrial mRNAs.* Mol Biochem Parasitol, 1999. **100**(1): p. 5-17.

174. Schnaufer, A., et al., *An RNA ligase essential for RNA editing and survival of the bloodstream form of Trypanosoma brucei.* Science, 2001. **291**(5511): p. 2159-62.
175. Wirtz, E., et al., *A tightly regulated inducible expression system for conditional gene knock-outs and dominant-negative genetics in Trypanosoma brucei.* Mol Biochem Parasitol, 1999. **99**(1): p. 89-101.
176. Roberts, S.C., et al., *Genetic analysis of spermidine synthase from Leishmania donovani.* Mol Biochem Parasitol, 2001. **115**(2): p. 217-26.
177. Hirumi, H. and K. Hirumi, *Continuous cultivation of Trypanosoma brucei blood stream forms in a medium containing a low concentration of serum protein without feeder cell layers.* J Parasitol, 1989. **75**(6): p. 985-9.
178. Shahi, S.K., R.L. Krauth-Siegel, and C.E. Clayton, *Overexpression of the putative thiol conjugate transporter TbMRPA causes melarsoprol resistance in Trypanosoma brucei.* Molecular microbiology, 2002. **43**(5): p. 1129-38.
179. Worthen, C., B.C. Jensen, and M. Parsons, *Diverse effects on mitochondrial and nuclear functions elicited by drugs and genetic knockdowns in bloodstream stage Trypanosoma brucei.* PLoS neglected tropical diseases, 2010. **4**(5): p. e678.
180. Cruz, A., C.M. Coburn, and S.M. Beverley, *Double targeted gene replacement for creating null mutants.* Proceedings of the National Academy of Sciences of the United States of America, 1991. **88**(16): p. 7170-4.
181. Cruz, A.K., R. Titus, and S.M. Beverley, *Plasticity in chromosome number and testing of essential genes in Leishmania by targeting.* Proceedings of the National Academy of Sciences of the United States of America, 1993. **90**(4): p. 1599-603.
182. Bourbouloux, A., et al., *Hgt1p, a high affinity glutathione transporter from the yeast Saccharomyces cerevisiae.* J Biol Chem, 2000. **275**(18): p. 13259-65.
183. Matthews, K.R., *The developmental cell biology of Trypanosoma brucei.* J Cell Sci, 2005. **118**(Pt 2): p. 283-90.
184. Velez, N., C.A. Brautigam, and M.A. Phillips, *Trypanosoma brucei S-adenosylmethionine decarboxylase N terminus is essential for allosteric activation by the regulatory subunit prozyme.* J Biol Chem, 2013. **288**(7): p. 5232-40.
185. Haider, N., et al., *The spermidine synthase of the malaria parasite Plasmodium falciparum: molecular and biochemical characterisation of*

the polyamine synthesis enzyme. Mol Biochem Parasitol, 2005. **142**(2): p. 224-36.
186. Wu, H., et al., *Structure and mechanism of spermidine synthases.* Biochemistry, 2007. **46**(28): p. 8331-9.
187. Ikeguchi, Y., M.C. Bewley, and A.E. Pegg, *Aminopropyltransferases: function, structure and genetics.* J Biochem, 2006. **139**(1): p. 1-9.
188. Zhang, H. and H.J. Forman, *Glutathione synthesis and its role in redox signaling.* Semin Cell Dev Biol, 2012. **23**(7): p. 722-8.
189. Burhans, W.C. and N.H. Heintz, *The cell cycle is a redox cycle: linking phase-specific targets to cell fate.* Free Radic Biol Med, 2009. **47**(9): p. 1282-93.
190. Jones, D.P. and Y.M. Go, *Redox compartmentalization and cellular stress.* Diabetes Obes Metab, 2010. **12 Suppl 2**: p. 116-25.
191. Diaz Vivancos, P., et al., *A nuclear glutathione cycle within the cell cycle.* Biochem J, 2010. **431**(2): p. 169-78.
192. Forman, H.J., H. Zhang, and A. Rinna, *Glutathione: overview of its protective roles, measurement, and biosynthesis.* Molecular aspects of medicine, 2009. **30**(1-2): p. 1-12.
193. Huang, C.S., M.E. Anderson, and A. Meister, *Amino acid sequence and function of the light subunit of rat kidney gamma-glutamylcysteine synthetase.* J Biol Chem, 1993. **268**(27): p. 20578-83.
194. Gipp, J.J., C. Chang, and R.T. Mulcahy, *Cloning and nucleotide sequence of a full-length cDNA for human liver gamma-glutamylcysteine synthetase.* Biochemical and biophysical research communications, 1992. **185**(1): p. 29-35.
195. Zhang, H. and H.J. Forman, *Redox regulation of gamma-glutamyl transpeptidase.* Am J Respir Cell Mol Biol, 2009. **41**(5): p. 509-15.
196. Casero, R.A. and A.E. Pegg, *Polyamine catabolism and disease.* Biochem J, 2009. **421**(3): p. 323-38.
197. Pegg, A.E., *Mammalian polyamine metabolism and function.* IUBMB Life, 2009. **61**(9): p. 880-94.
198. Pegg, A.E., *S-Adenosylmethionine decarboxylase.* Essays in biochemistry, 2009. **46**: p. 25-45.
199. Pegg, A.E. and R.A. Casero, Jr., *Current status of the polyamine research field.* Methods Mol Biol, 2011. **720**: p. 3-35.
200. Pegg, A.E., *Regulation of ornithine decarboxylase.* J Biol Chem, 2006. **281**(21): p. 14529-32.
201. Persson, L., *Polyamine homoeostasis.* Essays in biochemistry, 2009. **46**: p. 11-24.

202. Nowotarski, S.L., S. Origanti, and L.M. Shantz, *Posttranscriptional regulation of ornithine decarboxylase.* Methods Mol Biol, 2011. **720**: p. 279-92.
203. Kahana, C., *Regulation of cellular polyamine levels and cellular proliferation by antizyme and antizyme inhibitor.* Essays in biochemistry, 2009. **46**: p. 47-61.
204. Mangold, U., et al., *Antizyme, a mediator of ubiquitin-independent proteasomal degradation and its inhibitor localize to centrosomes and modulate centriole amplification.* Oncogene, 2008. **27**(5): p. 604-13.
205. Hanfrey, C., et al., *Abrogation of upstream open reading frame-mediated translational control of a plant S-adenosylmethionine decarboxylase results in polyamine disruption and growth perturbations.* J Biol Chem, 2002. **277**(46): p. 44131-9.
206. Mize, G.J. and D.R. Morris, *A mammalian sequence-dependent upstream open reading frame mediates polyamine-regulated translation in yeast.* RNA, 2001. **7**(3): p. 374-81.
207. Law, G.L., et al., *Polyamine regulation of ribosome pausing at the upstream open reading frame of S-adenosylmethionine decarboxylase.* J Biol Chem, 2001. **276**(41): p. 38036-43.
208. Ruan, H., et al., *The upstream open reading frame of the mRNA encoding S-adenosylmethionine decarboxylase is a polyamine-responsive translational control element.* J Biol Chem, 1996. **271**(47): p. 29576-82.
209. Phillips, M.A., P. Coffino, and C.C. Wang, *Cloning and sequencing of the ornithine decarboxylase gene from Trypanosoma brucei. Implications for enzyme turnover and selective difluoromethylornithine inhibition.* J Biol Chem, 1987. **262**(18): p. 8721-7.